

**Synthesis Gas Conversion to Aliphatic Alcohols: Study of MoS<sub>2</sub>  
catalytic systems**

BY

**Faisal Baksh**

B.S. Chemical Engineering, University of the Punjab, 2004

Submitted to the graduate degree program in Chemical Engineering and the  
Graduate Faculty of the University of Kansas School of Engineering  
in partial fulfillment of the requirements for the degree of  
Master of Science

Chairperson: \_\_\_\_\_  
Raghunath V. Chaudhari

Committee members\* \_\_\_\_\_  
Bala Subramaniam

\_\_\_\_\_  
Susan Williams

Date defended: 03/10/2010

The Thesis Committee for Faisal Baksh certifies  
that this is the approved version of the following thesis:

**Synthesis Gas Conversion to Aliphatic Alcohols: Study of MoS<sub>2</sub>  
catalytic systems**

Committee:

\_\_\_\_\_  
Chairperson\* Raghunath V. Chaudhari

\_\_\_\_\_  
Bala Subramaniam

\_\_\_\_\_  
Susan Williams

Date approved: 04/13/2010

## **Dedicated to**

Those who ask questions and search for answers, and then they keep asking and they keep looking

“The first step to knowledge is to know that we are ignorant” – Socrates

## **Acknowledgments**

I wish to offer my sincere gratitude to my advisor, Dr. R.V.Chaudhari, for his guidance, help and patience in many different aspects related to my research. I appreciate the stimulating discussions, the suggestions and directions, the availability for questions 24/7 and most of all, the encouragement to innovate and think out of the box. And in the end, the help in penning down this thesis on paper.

I am also grateful to my committee members, Dr. Bala and Dr. Williams for their extremely helpful inputs and suggestions.

Thanks to Dr. Fenghui Nui and Dr. Debdut Roy, without whom I wonder how I would have started my experiments. Your efforts are much appreciated. Thanks to Dr. Victor Day for the XRD analyses; David Moore and Heather Shinogle for assistance with the SEM and TEM machines.

Thanks to many other colleagues and friends who made it possible. Special thanks to Ly, Mahboob, Ali, Soleak, Victor, Yuanchun, Sylvia and Massi who made time fly by and accommodated my research needs along with me. To friends who were not here, Rashid, Saeed, Qammar, Saqlain, but encouraged me and made me realize that I would ‘pull it off’. To Claudia, who made me realize the presenter was as important as the researcher and helped me with words.

I am grateful to my parents, my sisters, and my cousins for their love and support.

## ABSTRACT

The recent energy debate and demand for renewable fuels has intensified research activities for conversion of biomass derived feedstocks to fuels and fuel additives. Synthesis of ethanol and higher aliphatic alcohols from syngas ( $\text{CO} + \text{H}_2$ ) is therefore receiving renewed interest. An important objective of this thesis was to develop commercially competitive catalysts and understand the fundamental issues affecting their performance.

Molybdenum Sulfide ( $\text{MoS}_2$ ) class of catalysts were synthesized by sulfidation of ammonium thiomolybdate and acetate salts of co-promoters. Several catalyst formulations were prepared by calcination, followed by doping with alkali promoters. Solid state modifications were made in some cases to dilute the active  $\text{MoS}_2$  material in supported catalysts. By modifying synthesis procedures, homogeneous and narrow size distribution of the sulfide material was obtained. Size control  $<20$  nm was also achieved for the  $\text{MoS}_2$  agglomerates by a novel chelation synthesis technique, which was particularly useful in enhancing alcohol yields. The catalyst performance was studied in a fixed bed reactor, operating in a range of 280-350°C, 69-92 bar and typical gas space velocities of 3000-10000 L/g.cat/hr.

Analytical equipment with the capability to perform online gas phase analysis of oxygenates along with permanent gases was setup. This led to the quantitative determination of reactants/products concentrations in a time-on-stream run and detection of oscillations in concentration profiles of oxygenates. Such an oscillatory behavior has not been reported before and it could be important for safe operation and understanding the scale up parameters of the process. Alcohol active catalysts were thoroughly tested for steady state activity and evaluated for parametric effects on conversion and selectivity. Depending upon the composition, a catalyst showed varying sensitivity to operating conditions. Temperature, space velocity and  $\text{CO}:\text{H}_2$  ratio in the syngas possessed the greatest capability in altering the product portfolio and overall reaction rates.

Use of co-promoters like Cu, led to increased alcohol selectivity of >85%, whereas promoters like Rh significantly improved the yield of alcohols (alcohol yields > 500 g/kg.cat/hr). Such high yields and selectivities are indicative of a major advancement over the existing MoS<sub>2</sub> based catalyst systems. By changing the support type and modifying support basicity, selectivity for alcohols as well as overall alcohol yield could be improved by 3 times at temperatures > 300°C. Modification of aluminosilicate supports by interchanging framework cations has not been reported for higher alcohol synthesis and offers a very simple technique for enhancing performance of supported catalysts. Use of zeolites as supports offers increased C<sub>2+</sub>/C<sub>1</sub> alcohol ratios from nominal value of 2 to 4. Active catalysts were characterized by SEM, TEM, EDS and XRD, which revealed that the final catalyst morphology greatly affects the alcohol synthesis performance of the catalyst.

# Synthesis Gas Conversion to Aliphatic Alcohols: Study of MoS<sub>2</sub> catalytic systems

1	Introduction and Literature review .....	15
1.1	Higher Alcohols .....	15
1.2	Synthesis Gas - a prominent building block .....	19
1.3	Synthesis Gas reactions of Fischer-Tropsch type .....	21
1.4	Types of Catalytic systems for alcohol synthesis .....	24
1.4.1	Homogeneous Catalysts: .....	24
1.4.2	Heterogeneous Catalysts .....	25
1.4.2.1	Noble Metal Catalysts: .....	26
1.4.2.2	Modified Methanol synthesis Catalysts .....	28
1.4.2.3	Modified Fischer-Tropsch catalysts .....	29
1.4.2.4	Molybdenum based catalysts .....	31
1.5	HAS Reaction Mechanism .....	33
1.6	Selection of MoS <sub>2</sub> catalytic system: Advantages & Issues .....	36
1.7	Scope and Objective .....	39
1.8	REFERENCES .....	41
2	Experimental Setup: Catalyst synthesis & evaluation .....	46
2.1	Reactor Unit .....	46
2.1.1	Modifications to original reactor set-up .....	48
2.1.1.1	Activated Carbon filter .....	49
2.1.1.2	Analysis of Volatile Components .....	49
2.1.1.3	Analysis at reactor exit .....	51
2.1.1.4	Exit Flowrate Measurement .....	51
2.1.1.5	Bubble flowmeter .....	53
2.1.1.6	Separate Exit Sampling .....	53
2.1.1.7	Heat Tracing .....	54
2.1.1.8	Filter .....	54
2.1.2	Calibration curves for Mass Flow Controllers .....	54
2.2	Chromatography .....	55

2.2.1	Liquid Sampling .....	55
2.2.2	Gas Sampling .....	56
2.2.2.1	Sampling technique and issues .....	57
2.2.3	Calibration methodology and units.....	58
2.3	Fixed Bed Reactor Assembly and Loading.....	59
2.3.1	Dimensions and Thermocouple location .....	59
2.3.2	Catalyst loading technique.....	60
2.3.3	Salvaging used catalyst.....	63
2.4	Catalyst synthesis.....	64
2.4.1	Pre-sulfided form.....	64
2.4.1.1	Synthesis and decomposition of Precursor ATM.....	65
2.4.1.2	pH controlled ATM synthesis.....	66
2.4.1.3	Chelated synthesis of ATM.....	67
2.4.1.4	Base modified supports.....	67
2.4.1.5	Calcination Procedure.....	68
2.4.2	Hydrogenation + Sulfidation.....	69
2.5	Catalyst Performance Evaluation: Material Balance .....	70
2.6	GLOSSARY .....	72
2.7	References .....	73
3	Synthesis, characterization and evaluation of MoS <sub>2</sub> based catalysts .....	75
3.1	Introduction.....	75
3.2	Catalyst preparation .....	77
3.3	Results, Characterization and Discussion .....	80
3.3.1	Effect of Metal Loading.....	84
3.3.2	Altering support basicity.....	93
3.3.3	Effect of cobalt as co-promoter.....	101
3.3.4	Effect of Rhodium as co-promoter .....	111
3.3.5	Effect of Copper as co-promoter .....	118
3.3.6	Effect of Alkali promoter .....	121
3.3.7	Effect of operating conditions .....	125
3.3.7.1	Pressure.....	125
3.3.7.2	Temperature.....	126
3.3.7.3	Syngas ratio.....	129



3.3.7.4	Gas Hourly Space velocity (GHSV).....	131
3.3.7.5	Methanol recycle.....	132
3.4	GLOSSARY.....	135
3.5	REFERENCES.....	136
4	Conclusions and Recommendations.....	140
4.1	Conclusions.....	140
4.2	Future path.....	142
5	Appendix.....	145

## LIST OF FIGURES

Figure 1-1- Chemicals from syngas .....	20
Figure 1-2 Observed and postulated species in F-T synthesis .....	21
Figure 1-3 Alcohol synthesis mechanism over modified methanol catalyst .....	34
Figure 1-4 Reaction scheme for HAS over Rh based catalysts .....	34
Figure 1-5 Reaction scheme over MoS <sub>2</sub> based catalysts.....	35
Figure 1-6 Structures of MoS <sub>2</sub> . yellow represents sulfur, blue molybdenum. Note how a MoS <sub>2</sub> stack consists of Mo sandwiched in between sulfur layers. Stacking represents piling up of stacks on top of one another. Molybdenum, the active metal, is only exposed at the edges; it is inaccessible from the top or bottom (basal planes) .....	38
Figure 2-1 Flowsheet description of catalytic testing unit .....	46
Figure 2-2 Actual view of the fixed bed system.....	47
Figure 2-3 Reactor Setup with modifications highlighted, as described in section 2.1.1 .....	48
Figure 2-4 vapor pressure trends for linear C <sub>1-3</sub> alcohols and water .....	50
Figure 2-5 working principle of a mass flow meter .....	52
Figure 2-6 Calibration curve used for carbon monoxide's MFC .....	54
Figure 2-7 Preparation of samples for gas phase calibration of volatile / liquid components .....	59
Figure 2-8 cross-sectional view of reactor with inlet and outlet. Location of thermocouples relative to bottom end of thermowell .....	61
Figure 2-9 Cross sectional view of inverted fixed bed reactor assembly, with catalyst loaded.....	62
Figure 2-10 Calcination unit based on a tube furnace .....	69
Figure 3-1 General scheme of catalysts prepared and tested according to project goals.....	76
Figure 3-2 Type-I isotherm for CP.9.1, indicating pore size distribution .....	79
Figure 3-3 Onstream time required at reaction startup to achieve steady state performance. MoS <sub>2</sub> -K <sub>2</sub> CO <sub>3</sub> catalyst, 40 wt% loading on clay. 330°C, 68 bar, CO:H <sub>2</sub> =2.0, 6000L/kg.cat/hr.....	81

Figure 3-4 Transient state with varying concentrations as measured by GC. Run 23 <sup>rd</sup> _I, Rh-MoS <sub>2</sub> catalyst, 335°C, 90 bar, CO:H <sub>2</sub> =0.5 and 6,000 L/kg.cat/hr.....	82
Figure 3-5 Variation in selectivity of total alcohols, alkanes and other oxygenates at different metal loadings at similar operating conditions: 300°C, 1300 psi, CO:H <sub>2</sub> = 2, GHSV = 6000 ml/g.cat/hr. ....	87
Figure 3-6 Effect of temperature on total alcohol selectivity (left) and yields (right) at varying metal loadings.....	87
Figure 3-7 SEM of CP5.1, showing homogeneous size distribution. <b>A</b> and <b>B</b> represent locations for EDAX analysis.....	89
Figure 3-8 TEM of CP5.1, showing how semi-spherical MoS <sub>2</sub> are bundled together. ....	90
Figure 3-9 SEM of CT.16 (CP5.1+ Bentonite).....	91
Figure 3-10 CT.16 SEM-zoom in on a chunk of K-MoS <sub>2</sub> precursor in bentonite .....	91
Figure 3-11 SEM of used catalyst CT.16U.....	92
Figure 3-12 SEM+EDs of CT.16U, homogeneity in chemical composition.....	92
Figure 3-13 Effect of temperature on conversion and alcohol selectivity for catalysts + support with varying basicity.....	96
Figure 3-14 Effect of temperature on product yields on catalysts + support with varying basicity ..	97
Figure 3-15 SEM of CT.22(CP.5.1+KY zeolite) .....	98
Figure 3-16 SEM of used catalyst, CT.22U.....	99
Figure 3-17 XRD comparison of CP.5.1, CT.22 and CT.22U. Patterns indicate that zeolite structure remains intact after the reaction.....	100
Figure 3-18 Comparison between reported alcohol synthesis catalysts of CoMoS type.....	106
Figure 3-19 SEM image of used catalyst CT.29U. The smaller particles are believed to be CoMoS mixed phase supported on MoS <sub>2</sub> layers.....	107

Figure 3-20 TEM of CP.8.1. Smaller CoMoS particles display strong diffraction patterns at edges, characteristic of crystalline material.....	108
Figure 3-21 Fig 4.15. FTIR spectra of CP.8.1 (without alkali) and 29 <sup>th</sup> _U (CP.8.1. with alkali and post reaction).....	110
Figure 3-22 Performance comparison of between different Rh-Mo based systems.....	115
Figure 3-23 TEM of CP.6.2, indicating nanosized MoS <sub>2</sub> particles. Darker areas show MoS <sub>2</sub> layers stacked on top of one another.....	116
Figure 3-24 SEM of CP.6.2 (Rh- MoS <sub>2</sub> particles). A MoS <sub>2</sub> high rise is visible.....	117
Figure 3-25 CO <sub>2</sub> inclusive selectivities of different catalysts tested. Shaded regions depict normal ranges reported in literature. Similar operating conditions of 330°C, 90 bar, 3000 h <sup>-1</sup> , CO/H <sub>2</sub> =1 .....	118
Figure 3-26 Effect of potassium loading on product yields over CuCoMoS catalyst. Similar operating conditions @ 350°C, 88 atm, CO:H <sub>2</sub> = 1 and GHSV=3,000 L/kg.cat/hr.....	122
Figure 3-27 Effect of potassium loading on catalytic performance of CuCoMoS . Similar operating conditions @ 350°C, 88 atm, CO:H <sub>2</sub> = 1 and GHSV=3,000 L/kg.cat/hr.....	123
Figure 3-28 Effect of temperature on product yields, MoS <sub>2</sub> +K <sub>2</sub> CO <sub>3</sub> /K-Y zeolite; ~ 90bar, CO:H <sub>2</sub> =2, 6000 L/kg.cat/hr.....	126
Figure 3-29 Effect of temperature on catalyst performance, MoS <sub>2</sub> +K <sub>2</sub> CO <sub>3</sub> /K-Y zeolite; ~ 90bar, CO:H <sub>2</sub> =2, 6000 L/kg.cat/hr.....	127
Figure 3-30 Effect of temperature on product yields, MoS <sub>2</sub> +K <sub>2</sub> CO <sub>3</sub> /K-Y zeolite; ~ 90bar, CO:H <sub>2</sub> =2, 6000 L/kg.cat/hr.....	127
Figure 3-31 Arrhenius plot of reaction rate dependence on temperature.....	129
Figure 3-32 Effect of CO:H <sub>2</sub> ratio on catalyst performance, MoS <sub>2</sub> +K <sub>2</sub> CO <sub>3</sub> /K-Y zeolite; 350°C, ~ 90bar, 6000 L/kg.cat/hr.....	130
Figure 3-33 Comparison of alcohol yield over different catalyst as a function of CO:H <sub>2</sub> . Conditions: 330-350°C, ~ 90bar, 6000 L/kg.cat/hr .....	131

Figure 3-34 Effect of GHSV on catalyst performance,  $\text{MoS}_2+\text{K}_2\text{CO}_3/\text{K-Y zeolite}$ ;  $350^\circ\text{C}$ ,  $\sim 90\text{bar}$ ,

$\text{CO:H}_2=2$  ..... 132

Figure 3-35 Effect of GHSV on product yields,  $\text{CoMoS}+\text{K}_2\text{CO}_3$ ;  $330^\circ\text{C}$ ,  $\sim 90\text{bar}$ ,  $\text{CO:H}_2=1$  ..... 132

## LIST OF TABLES

Table 1-1 Use of Alcohols.....	15
Table 1-2 Commercial development of HAS technology .....	19
Table 1-3 Comparison of higher alcohol activity for modified methanol catalysts .....	29
Table 1-4 MoS <sub>2</sub> -Based Catalysts and their performance.....	32
Table 2-1 Configuration of GC used for offline liquid analysis.....	55
Table 2-2 GC method used for gas sampling .....	57
Table 3-1 Catalysts prepared with reference to synthesis technique.....	77
Table 3-2 Nomenclature for catalyst tested- includes final composition of catalyst before loading .....	78
Table 3-3 BET surface areas of catalyst samples tested .....	79
Table 3-4 Alcohol yield selection based on averaged values, that match the liquid product collected. ....	83
Table 3-5 Effect of metal loading on performance of K <sub>2</sub> CO <sub>3</sub> -MoS <sub>2</sub> catalyst (K:Mo = 0.6:1).....	85
Table 3-6 Effect of support basicity on performance of K <sub>2</sub> CO <sub>3</sub> -MoS <sub>2</sub> catalyst(K:Mo = 0.6:1).....	94
Table 3-7 Performance evaluation of CoMoS type catalysts. K <sub>2</sub> CO <sub>3</sub> loading at 10 wt%. .....	103
Table 3-8 Effect of additional alkali salt doping post-calcination: product selectivity shifts from alkanes to alcohols.....	105
Table 3-9 Performance of Rh-MoS <sub>2</sub> catalyst. Rh:Mo=0.015:1; K:Mo=0.5:1; 60%loading on KYzeolite .....	112
Table 3-10 Performance of CuCoMoS catalyst. Cu:Mo=0.2:1; Co:Mo=0.4:1; 8wt% K <sub>2</sub> CO <sub>3</sub> .....	119
Table 3-11 Effects of syngas ratio on catalyst performance.....	130
Table 3-12 Increase in C <sub>2+</sub> alcohols over Ct.22 catalyst upon cofeeding methanol with syngas.....	133

## APPENDIX

Appendix 1- Calibration curve for methanol – Shimadzu GC software EZStart.....	145
Appendix 2 - Calibration curve for ethanol – Shimadzu GC software EZStart.....	146
Appendix 3 – Sample chromatogram from online gas sampling GC. The software is adjusted such that it automatically picks up the peaks (already calibrated) and displays the calculated concentration.....	147
Appendix 4 – Calculation performed for gas phase calibration of oxygenated compounds.....	148
Appendix 5 – Sample GC output report.....	150
Appendix 6 – Data acquisition panel for reactor. Reactor pressure and temperature are graphed online	151
Appendix 7 – Sample calculation for quantifying catalyst performance. Inputs are concentrations (GC output-Appendix-5), reactor operating conditions and flowrates .....	152
Appendix 8- Report template displaying operating variables and performance parameters of importance for a particular catalyst.....	153

# 1 INTRODUCTION AND LITERATURE REVIEW

## 1.1 HIGHER ALCOHOLS

Alcohols as products serve a wide variety of purposes in our society. They are widely accepted due to their properties as solvents, germicide, fuels and especially as intermediates in the synthesis of chemicals and specialty products including foods and pharmaceuticals<sup>[1-2]</sup>. Historically, higher aliphatic alcohols or just higher alcohols have referred to alcohols with carbon chains up to 6 – 8. The higher homologues, C<sub>12+</sub> alcohols, are derived from plant sources e.g. coconut/palm/corn oils etc. Those in the range of C<sub>8-12</sub>, are valuable intermediates for detergents and plasticizers, and are known as ‘Plasticizer range alcohols’<sup>[2]</sup>.

Methanol	Intermediate for MTBE (Methyl Tert-Butyl Ether), biodiesel, (DME) DiMethyl Ether, acetic acid, formaldehyde (40% methanol consumption) and from there into products as diverse as plastics, plywood, paints, explosives, and permanent press textiles.  As a disinfectant and a fuel.
Ethanol	Antiseptic, antidote, transportation fuel, alcoholic beverage (since early times)  Chemical intermediate for ethyl halides, ethyl esters, diethyl ether, acetic acid, butadiene, and ethyl amines.
Propanol	Propane halides, propionic acid, propyl acetate, propionaldehyde, etc.
Iso-propanol	Exceptional solvent, Fuel additive, electric board & equipment cleaner, sterilizer.
Butanol	Fuel (most suitable alternative to gasoline), solvent in coatings and thinners, perfumes, butoxides

*Table 1-1 Use of Alcohols*



Generally, alcohols can be used as intermediates according to the classic organic transformations that are symbolic of alcohols. These include, but are not limited to, dehydration (mostly diethyl ether), esterification, alkoxide deprotonation (transition metal alkoxides used as coatings and catalysts), alkyl halides, oxidation (aldehydes and carboxylic acid from primary; ketones from secondary)<sup>[2]</sup>.

Ethanol and other higher alcohols have developed a significant interest centered in their use for producing clean renewable fuels, e.g. MTBE, DME, gasoline, fuel cells <sup>[1, 3]</sup>. Table 1-1 reviews some of the applications of these C<sub>1-4</sub> alcohols. In recent years, an urgent need has emerged for replacing petroleum derived fuels with alternative fuels or additives. This change is attributed to several reasons, which include:

- National stability by replacing dependency on import of oil
- Extreme variations in crude oil prices
- Sustainable and greener environment by using renewable fuels and technologies
- Reduced emissions and better air quality

Biofuels, along with solar energy, have received significant attention and the biggest chunk of government funding according to the advanced Energy Initiative <sup>[4]</sup>. Amongst biofuels, ‘cellulosic ethanol’ has received special emphasis. Recently, noble winner Crutzen <sup>[5]</sup> published findings that N<sub>2</sub>O emissions associated with corn-ethanol generation can cause a net negative impact on global warming. Grassy or woody plants, or biomass, on the other hand have more favorable climate impact because of decreased nitrogen demand. The Energy Independence and Security Act of 2007 <sup>[6]</sup> mandates use of 20.5 billion gallons in US gasoline supply in 2015, increasing to 36 billion gallons by 2022. ‘Corn ethanol’ will be capped at 15 billion gallons, leaving ‘cellulosic ethanol’ to fulfill the gap in ethanol demand. Use of E10 (10% ethanol and 90% gasoline) has also been mandated in some US states, and it is finding increasing use all over US. Earlier, Energy Policy Act of 2005 <sup>[7]</sup> mandated use of 6.1 billion gallons of biofuels by 2009 and 7.5 by 2012. Ethanol production was already at 9 billion gallons in 2009 in USA, indicating that use of biofuels has quickly caught on. With the average US gasoline consumption at 138

billion gallons in 2008, Exxon CEO commented that US has passed its peak gasoline consumption, due to blending of biofuels and advances in electric cars <sup>[8]</sup>.

In the 90s, oxygenate blending in gasoline was mandated according to the reformulated gasoline (RFG) imitative of Clean Air Act (CAA) of 1990. This was essential to limit CO and VOC emissions from automobile tailpipes, which are hazardous to health and environment <sup>[9]</sup>. Methyl tert-butyl ether (MTBE) was one of the most widely used and studied oxygenate. Gasoline blends containing MTBE up to 15% by volume were developed and used. However, problems like ground and surface water contamination, fume inhalation during pumping and its adverse effects on human health have sought its decrease in usage <sup>[10]</sup>. The resulting gap in oxygenate demand has been fulfilled by ethanol and ethanol production is seeing a growth at a rate of 30% per annum. Higher alcohols are also excellent additives for gasoline. 1-butanol is considered by many to be the most suitable alcohol replacement for gasoline. Plans for conversion of existing bioethanol facilities to biobutanol are already being drawn up.

Early on, methanol-gasoline blends were extensively tested <sup>[11-12]</sup> as methanol has the highest oxygen content amongst the alcohols (0.5 mass fraction) <sup>[13]</sup>. Their use was later banned by EPA as it had phase separation and corrosion problems, which negatively affected the engine. Higher alcohols are preferred over methanol as a gasoline additive. Addition of higher alcohols, instead of methanol, can provide advantages such as water tolerance in phase separation, reduced fuel volatility and increased net calorific value <sup>[11, 14]</sup>. Several patents were issued for catalysts and higher alcohol blends which could be used with gasoline engines <sup>[15-16]</sup>. EPA waivers were also obtained for blending limits of mixed alcohols in gasoline <sup>[11]</sup>, e.g. Octamix, Ecalene (see Table 1-2). Other blends were successfully marketed in other countries, e.g. Superfuel E in Italy during 1980s <sup>[12]</sup>.

Because, ethanol has a lower energy density when compared to gasoline (24.0 vs. 34.2 MJ/L), it is widely speculated that ethanol-gasoline mix results in decreased engine performance. E.g. Gasohol (ethanol 10%-gasoline 90% - 33.2 MJ/L) has 3.2% lower energy content than gasoline and therefore should result in lower miles per gallon (mpg). However, it is well known that, in addition to improving emissions, the oxygenate content improves engine efficiency due to its contribution to 'octane rating'.

Engine testing has confirmed that ethanol-gasoline mixtures provide better brake horsepower, decreased fuel consumption and decreased emissions [17-18]. In fact, the optimum blending ratio was 20% (v/v) ethanol in gasoline. Higher alcohols also have similar beneficial effects; break specific fuel consumption was significantly lower for mixed alcohol-gasoline mixtures when compared with neat gasoline. CO and hydrocarbon emissions were lower. However, when the oxygen content (not to be confused with oxygenate content) was increased considerably, from 2% to 5%, NO<sub>x</sub> emissions increased [13].

Neat-alcohol fuels have higher quantities of lower alcohols, like methanol and ethanol. Engines designed for methanol are more powerful than similar sized gasoline engines. Race cars run on methanol based fuels [12]. One of the biggest issues is with cold start and vapor locking, as methanol has lower vapor pressure and high heat of vaporization. However, this aspect has been researched and solutions have been proposed [19].

That mixed alcohols are useful as fuel additives and can provide an alternative to fuels obtained from crude oil was known early on. Several companies tried to commercialize their higher alcohol synthesis technologies. Research was withheld at the level of demonstration units as crude oil prices stabilized [3, 12]. Table 1-2 lists the advances achieved by several companies in higher alcohol synthesis (HAS).

Process	Description	Scale	Product characteristics
<b>IFP Idemitsu</b>	- Syngas from natural gas reforming; Cu-Co-based modified FT synthesis catalysts; methanol distillation; extractive distillation with diethylene glycol (DEG); 260-320 °C; 60-130 bar	2.4 ton/d	produced C <sub>1-7</sub> linear alcohols; higher alcohols between 20 and 70%
<b>SEHT Superfuel E</b>	- Partial oxidation of natural gas to syngas; Cu-Zn-based modified methanol synthesis catalyst; distillation of methanol and ethanol; 350-400 °C; 120-180 bar	400 ton/d	crude alcohol mixture contained 20% water; final water content <0.1%; blended
<b>Lurgi-Octamix</b>	Steam and autothermal natural gas reforming; Cu-Zn-based modified methanol synthesis catalyst; stabilizer column; 270-300 °C; 69-103 bar	2 ton/d	mixed alcohols containing 1-2% water

<b>Dow</b>	K-Co-MoS <sub>2</sub> catalyst, syngas with H <sub>2</sub> S converted to higher alcohols; 290-310 °C; 103–138 bar	Bench scale	300 g/kg.cat/hr; 80% alcohol selectivity, 75% C <sub>2+</sub> alcohols amongst liquids
<b>PEFI-Ecalene</b>	Nanosized K-MoS <sub>2</sub> catalysts. Slurry reactor; syngas with sulfur in slurry; 200-300 °C; 35–207 bar	scale up to 1.5 ton/d	greater alcohol yields of >400 g/kg.cat/hr
<b>MixAlco</b>	fermentation of municipal solid waste into chemicals such as acids, esters, ketones, etc. followed by catalytic hydrogenation of acids;	0.045 ton/d	2-propanol as major alcohol component;

*Table 1-2 Commercial development of HAS technology<sup>[3, 12]</sup>*

Significant research was done on conversion of methanol to gasoline over ZSM-5 catalysts. The technology for Methanol-To-Gasoline (MTG) was commercialized by ExxonMobil. It was also demonstrated that mixed alcohols undergo a similar dehydration process over ZSM-5 and with yields and fractions better than those achieved from methanol alone<sup>[20]</sup>. Yet another indirect use of ethanol in renewable technology is in fuel cells. Ethanol can be reformed over typical Ni catalyst to give hydrogen with performance comparable to methanol and DME<sup>[21-22]</sup>. Recently, direct ethanol fuel cell technology has also surfaced. Ethanol is less toxic than methanol and has a higher energy density<sup>[23-24]</sup>. Ethanol is also a substitute to methanol during the trans-esterification step involved in production of bio-diesel or FAME.

## 1.2 SYNTHESIS GAS - A PROMINENT BUILDING BLOCK

Synthesis gas is essentially a mixture of CO and H<sub>2</sub>, and other gases like CO<sub>2</sub>, N<sub>2</sub>, alkanes etc. It is known under different names in different eras and places depending upon its use and manufacture, e.g. town gas, water gas, producer gas. It is a starting material of choice for most of the world's gigantic chemical industries, e.g. ammonia, H<sub>2</sub>, methanol. These chemicals are the backbone for a more diverse spectrum of industrial chemicals<sup>[12, 25]</sup>. The depth in its utilization is complemented by the routes through which it can be manufactured<sup>[26-27]</sup>.

### 1. Coal Gasification

2. Natural Gas (or liquids) reforming
3. Biomass Gasification

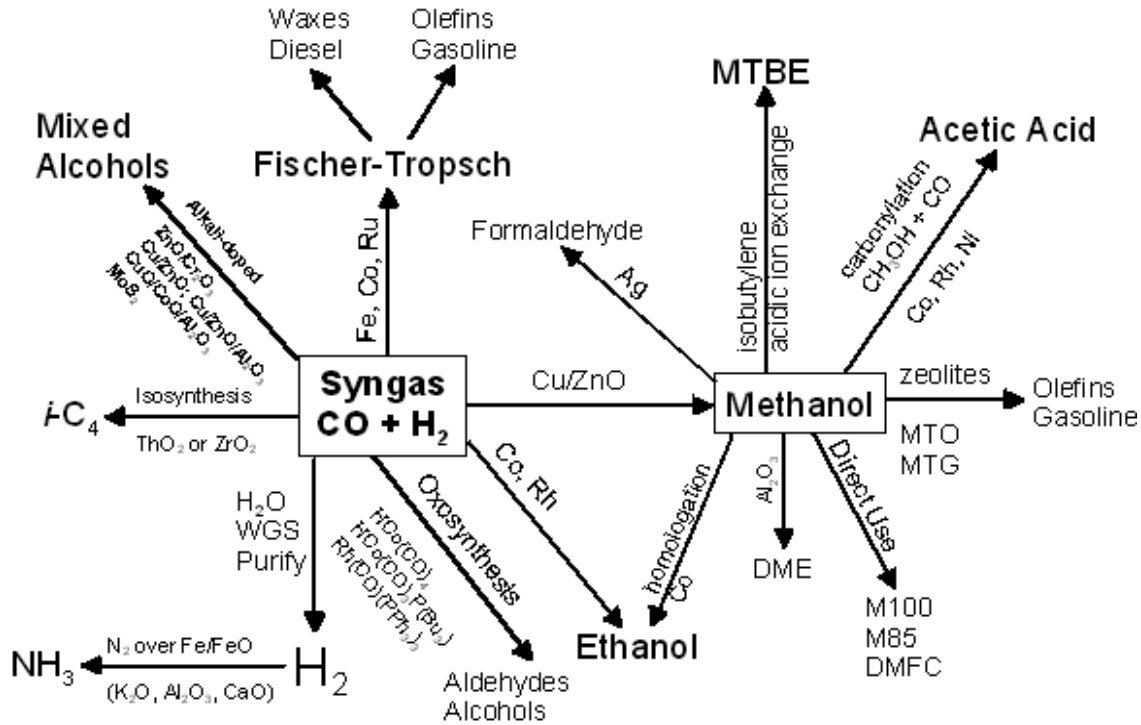


Figure 1-1- Chemicals from syngas <sup>[11]</sup>

As its synthesis is not dependent on petroleum feedstocks, expanding the product base into areas of products manufactured from petroleum offers a great incentive: Energy Security. Fuels manufactured from syngas via the Fisher-Tropsch became an established technology in South Africa and helped that nation free its oil addiction <sup>[28-29]</sup>. China has also planned similar projects of coal conversion to chemicals, the most recent example, employing ExxonMobils MTG technology <sup>[30]</sup>. Conversion of biomass to syngas followed by further chemical conversions is certainly a preferred route for fuels and chemicals production. Lignin, a difficult component of biomass with respect to conversion to useful products, can be effectively converted into syngas <sup>[11, 31]</sup>.

### 1.3 SYNTHESIS GAS REACTIONS OF FISCHER-TROPSCH TYPE

In Fischer-Tropsch (F-T) synthesis, **alkanes** and **olefins** are considered the major products with **oxygenates** being the side products. In F-T synthesis for higher alcohols, the selectivity to alcohols is increased by restricting the hydrogenation capability of the catalyst. As explained by Hindermann et al.<sup>[32]</sup>, there are different intermediates stabilized on the metal surface and polymerization (C-C bond formation) of these surface intermediates gives different compounds. The relative concentration of these intermediates will vary as a function of metal, promoters, support and operating conditions. Thus, these relative concentrations of intermediates together with reactor configuration will dictate which products are formed. It is for this reason that the exact F-T mechanism still eludes us even after 100 years of its discovery. Hindermann boiled it down as, *“it is unlikely that a unified mechanism for Fischer-Tropsch reactions exist”*.

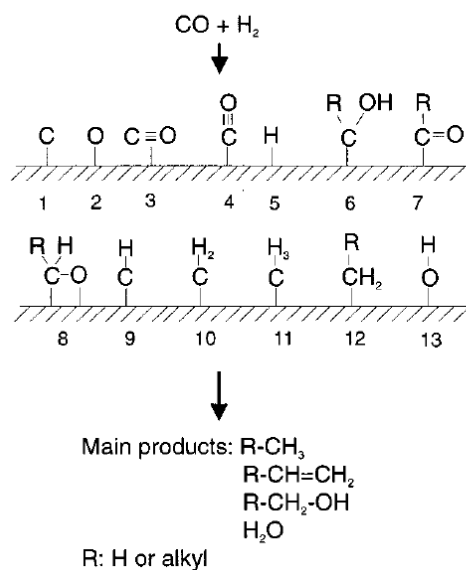


Figure 1-2 Observed and postulated species in F-T synthesis<sup>[34]</sup>

The following mechanisms have been proposed and validated (the **types** referred to are surface species formed from CO and H<sub>2</sub>, as described in Figure 1-2) :

1. **Surface carbide mechanism:**<sup>[33-34]</sup>

Insertion of methylene species (-CH<sub>2</sub>-) in a growing chain of **type 12** (Figure 1-2).

2. **Hydroxycarbene mechanism**<sup>[35-37]</sup>



Reaction between hydroxycarbene ( ) intermediates, to form species like **type 6** (Figure 1-2), followed by further hydrogenation to give alkanes or oxygenates.

3. **CO insertion mechanism**<sup>[38-39]</sup>

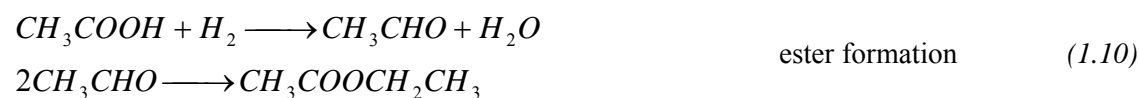
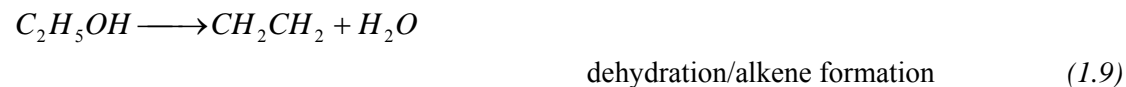
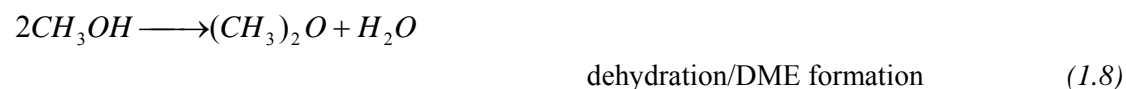
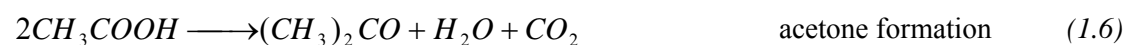
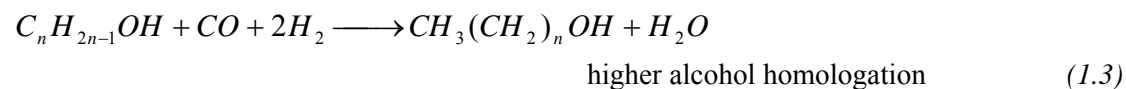
The insertion of 'CO' from metal carbonyl intermediates into a metal-alkyl bond can give rise to a number of acyl intermediates of **type 7** (Figure 1-2). Further reactions can form aldehydes, acids, alcohols and branched alkanes or oxygenates.

4. **Secondary and parallel reactions**

Hydrogenation and isomerization of reinserted olefins seems to be one of the most prominent secondary reactions<sup>[34]</sup>. Dry's model combines two mechanisms, i.e. both CH<sub>2</sub> and CO are active surface intermediates<sup>[40]</sup>. Sachtler<sup>[41]</sup> adds that chain growth occurs via non-oxygenated surface intermediates and a parallel mechanism of CO insertion gives oxygenates.

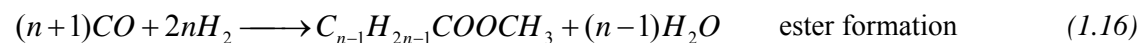
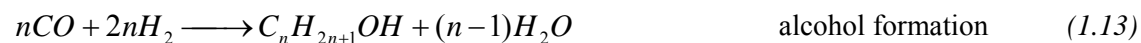
Based on thermodynamic data, Weitkamp proposed primary and secondary products for CO hydrogenation reactions<sup>[42]</sup>. Although, the operating conditions of FT synthesis are such that equilibrium is not reached, thermodynamic analysis does throw light on what products are more probable. E.g. high pressures required for higher alcohol synthesis (HAS) would prohibit ketone formation (chemical equilibria -volume expansion Eq-1.6). Indeed, ketones are not typically observed over most HAS catalysts.

For alcohol synthesis, following reactions are considered to be important. Note that reactions occurring over modified methanol catalysts are not discussed here, as they do not necessarily fall under the domain of FT reactions



These reactions are by no means a comprehensive guide of the HAS kinetics. These can at best, be considered a general guideline by which FT type of alcohol synthesis takes place. For MoS<sub>2</sub> based catalysts, the mechanism has been investigated as proposed in Section 1.5. To summarize the reactions based on the products obtained over MoS<sub>2</sub> based catalysts, the following set of reactions are generalized [43].





#### 1.4 TYPES OF CATALYTIC SYSTEMS FOR ALCOHOL SYNTHESIS

The choice of catalysts depends on the type and quality of products desired, which further dictates the selection of the reactor systems, operating conditions and separation/purification equipment. Thus, the overall process scheme will depend upon the catalyst being used. Generally, catalysts for higher alcohols synthesis (HAS) are differentiated as follows:

- Homogeneous catalysts
- Heterogeneous catalysts:
  - *Noble metal catalysts*
  - *Modified methanol synthesis catalysts*
  - *Modified Fischer-Tropsch catalyst*
  - *Molybdenum based catalysts*

Description of each type is as follows:

##### 1.4.1 HOMOGENEOUS CATALYSTS:

Solutions of Co, Ru or Rh complexes have been reported as catalysts for direct conversion of syngas to C<sub>2</sub> oxygenates and as homologation catalysts capable of converting methanol to higher alcohols. Clearly, the most interesting aspect is the homologation chemistry, where higher selectivity towards ethanol can be obtained<sup>[3]</sup>. Indeed significant research activity was noted in the 1980s, on the

homologation of methanol to ethanol. Mn and Fe complexes are also reported along with the aforementioned noble metal catalysts and many researchers reported ethanol selectivity in excess of 80% [3]. At Argonne Labs [44], dimanganese deca-carbonyl catalyst used at 200°C, CO:H<sub>2</sub>=3:1 and 300 bar pressure was reported to give 85% yield of liquid products, 90% of which was ethanol. Use of *N-methylpiperidine* as a basic promoter produces CO<sub>2</sub> instead of H<sub>2</sub>O, hence simplifying the final separation processes for ethanol. Another catalyst system consisting of iron carbonyl with 1-methyl-2-pyrrolidinone at similar operating conditions was claimed to be an effective catalyst, which produced a similar ‘dry ethanol’ product [44]. Union Carbide [45] reported a bi-metallic Rh-Ru-diphosphine-MeI catalyst system, operating at 140°C, CO:H<sub>2</sub>=1:2 and 69 bar with 80% selectivity to ethanol. According to a Japanese patent [108], Ethanol can be produced with 96% selectivity and 22% MeOH conversion over a mixed catalyst system consisting of CoS-Cu-Bu<sub>3</sub>P<sub>2</sub>-N-methylpyrrolidone at 250°C, CO:H<sub>2</sub>=1:1 and 197 bar.

If the target alcohol is only ethanol, an interesting 2-step approach could be production of methanol, for which well established technology is already available, and then ethanol in a separate step with even a different catalyst. The product mixture obtained from methanol plant, containing some unreacted syngas, can be fed into the homologation reactor. A detailed economic analysis has not been performed for such a process scheme, but it is expected that the more severe operating conditions, separation requirements and catalyst cost of the homogeneous chemistry would be major issues in developing a commercially feasible process.

#### **1.4.2 HETEROGENEOUS CATALYSTS**

Heterogeneous catalysis is a cornerstone of the petro-chemical industry. Owing to its robustness and ease of use in fixed bed reactors, a heterogeneous catalytic system would offer an easy scale-up for biomass based chemical processes. For example, the bio-diesel industry is actively exploring the development of a solid-catalyst for the transesterification process, which would provide environmental benefits by reduced use of alkalis and acids [46]. Most of the research activity in syngas to alcohols has

centered on the development of heterogeneous catalysts as it is known that alcohols can be prepared over a variety of catalysts and the scales of operations envisaged are very large. The heterogeneous HAS catalysts can be divided into the following four types:

#### 1.4.2.1 Noble Metal Catalysts:

Supported Rh, Re, Ru and Pt, Pd to a lesser extent, have been reported for the direct conversion of syngas to C<sub>2</sub> oxygenates. Significant results were obtained by Union Carbide in 1975 for SiO<sub>2</sub> supported Rh catalysts, along with metals like Fe, Mn, Th as promoters. Alcohol yields were nonetheless very low. With further research and understanding, Rh was recognized as one of the most promising metal component in catalysts for enhancing the formation of ethanol; its cost however, became the biggest limiting factor. Rhodium could perform <sup>[1]</sup>:

- Associative/Dissociative adsorption of CO
- Hydrogenation to form methyl species (CH<sub>3</sub>•)
- CO insertion into methyl species to form acetyl (CH<sub>3</sub>CO•) and further hydrogenation to form ethanol

The results on catalyst performance significantly varied with loadings, promoters, supports and dispersion characteristics. Rh/SiO<sub>2</sub> is known to favor adsorption of CO non-dissociatively, whereas with Al<sub>2</sub>O<sub>3</sub> or TiO<sub>2</sub> as supports, CO is adsorbed dissociatively <sup>[47]</sup>. The role of Fe as a promoter is not clearly understood. Some debate that the promoter provides interaction sites for O that is part of the CO adsorbed on Rh <sup>[1]</sup>, i.e. promote dissociation of CO. Others <sup>[48]</sup> suggest the promoter's role is stabilization of acetyl (CH<sub>3</sub>CHO•) species, thereby enhancing hydrogenation to ethanol instead of desorption to acetaldehyde. Davis recently quantified the effect of Fe as promoter <sup>[48]</sup>: 2% Rh/SiO<sub>2</sub> showed no activity for ethanol. However, 2%Rh/5%Fe/SiO<sub>2</sub> exhibited dramatic increase in ethanol selectivity to 22%. It is also recognized that the ability to insert CO is important for oxygenate selectivity <sup>[53]</sup>. Hayes et.al. <sup>[50]</sup> found an optimum catalyst composition of 2%Rh/10%Fe/Al<sub>2</sub>O<sub>3</sub>, that gave an ethanol selectivity of 50% at a CO conversion of 3.6%. Increased ethanol selectivity was attributed to enhanced Rh-Fe interaction, which in

turn was enhanced by the FeO-support interaction due to higher surface hydroxyl groups of alumina. Davis <sup>[48]</sup> optimized catalyst at 2%Rh/5%Fe/TiO<sub>2</sub> getting a CO conversion of 6% and ethanol selectivity of 37%, with alkanes at 41% being the undesirable products. Catalyst testing was carried out at 270°C, CO:H<sub>2</sub>=1:1 and ~21 bar. Mn has also been used as a promoter with Rh and probably, is one of the most investigated promoters <sup>[3]</sup>. However, the results were not as promising as the iron promoter with respect to ethanol selectivity and conversion <sup>[51]</sup>.

Gronchi et al. <sup>[49]</sup> studied effects of various supports; La<sub>2</sub>O<sub>3</sub>, ZrO<sub>2</sub>, V<sub>2</sub>O<sub>3</sub> and found that V<sub>2</sub>O<sub>3</sub> was the best as it provided a high dispersion of Rh. At 230°C and atmospheric pressure using a 1%Rh/V<sub>2</sub>O<sub>3</sub> catalyst, 37% selectivity to ethanol was achieved at a CO conversion of 4.5%, other major by-products being alkanes. With a 0.5% Rh loading on La<sub>2</sub>O<sub>3</sub>, operating at 220°C and atmospheric pressure, Ichikawa et. al <sup>[52]</sup> obtained some significant results: ethanol selectivity 61% (total oxygenate selectivity of 81%), CO conversion 36% and low selectivities towards alkanes. Indeed lanthana was found to be more active for ethanol amongst the others tested by the group. They inferred: Rh supported on I-IIA group oxide supports, MgO, BaO, CaO, produced methanol predominantly amongst oxygenates; on III-IVB groups, La<sub>2</sub>O<sub>3</sub>, Ce<sub>2</sub>O<sub>3</sub>, TiO<sub>2</sub>, ZrO<sub>2</sub>, ThO<sub>2</sub>, ethanol was formed selectively; whereas with other supports like Al<sub>2</sub>O<sub>3</sub> and SiO<sub>2</sub>, hydrocarbons were preferred products. Thus, the product spectrum could be linked to the surface acidity/basicity of the supports.

Ichikawa <sup>[53]</sup> further investigated the idea of positive effect of basic nature of the support for intrazeolite catalysts, where Co-Ru were anchored within the zeolite framework. Higher oxygenate selectivity was found to increase with zeolite basicity, e.g. NaX performed better than NaY <sup>[47]</sup> Elsewhere<sup>[54]</sup> they reported a Rh-Ti-Fe-Ir/SiO<sub>2</sub> catalyst with ethanol selectivity of 50% at a 12.5% CO conversion with operating conditions of 260°C, CO:H<sub>2</sub>=1:1 and 51 bar. The catalyst was optimized with beneficial effect of each promoter being incorporated.

At Pacific Northwest labs, novel reactor technology was applied to test a Rh promoted catalyst by Hu et.al.<sup>[55]</sup>. A catalyst consisting of Rh (6%)/Mn (1.5%)/SiO<sub>2</sub> gave an ethanol selectivity of 61% and CO

conversion of 25% in a microchannel reactor. Increase in temperature from 265 to 300 °C led to increased conversion (41%), more methane (34 to 48%) with a decrease in ethanol selectivity to 45%. Decrease in H<sub>2</sub>/CO ratio led to a decrease in the syngas conversion and ethanol selectivity.

#### 1.4.2.2 Modified Methanol synthesis Catalysts

These are catalysts composed of essential combinations of Cu/Zn/Cr with other elements like Mg/Mn/Pd/Zr/Co added to enhance the productivity or improve selectivity of certain products. The addition of Cu allows operation at lower temperatures and also improves the overall alcohol selectivity<sup>[56]</sup>. Without the addition of alkali promoters, however, higher alcohols are not obtained in significant quantities. Industrially, Cu/Zn/Al<sub>2</sub>O<sub>3</sub> type catalysts are known to be excellent for selective production of methanol from syngas. The presence of alkali was first noticed as a nuisance as it led to byproducts, i.e. C<sub>2+</sub> oxygenates. The first systematic experiments used Cs as the alkali promoter over Cr<sub>2</sub>O<sub>3</sub>/Mn catalyst<sup>[57]</sup>. With low temperature methanol catalysts, Smith et al.<sup>[58]</sup> noticed the effect of alkali impurities, carried on from the catalyst synthesis, in methanol synthesis. The composition of higher alcohols obtained over these catalysts is unique. After methanol, isobutanol is usually the dominant product OR isobutanol is the dominant higher alcohol. This is due to the reaction mechanism over the catalyst, which is quite different from FT synthesis (see section 1.5). Higher alcohols are formed by condensation reactions. However, this disparity in higher alcohol composition and the ability to alter the alcohol composition gave this catalyst family a significant advantage in the 80s: MTBE synthesis from methanol and isobutanol/isobutene. MTBE was the preferred oxygenate for gasoline blending under the 1990 CAA. However, isobutene, the raw material, is obtained from petroleum sources and the abrupt demand for MTBE constrained isobutene supplies<sup>[59]</sup>. As isobutene can easily and efficiently be obtained by the dehydration of isobutanol, these catalysts became attractive. Minimal water production would allow direct reaction of the alcohol products over a suitable zeolite catalyst<sup>[60]</sup>. By varying the reaction conditions and catalyst composition, Epling et al.<sup>[61]</sup> were successful in not only limiting alcohols other than methanol and isobutanol, but also obtained significantly higher quantities of isobutanol compared to methanol.

	Catalyst <sup>e</sup>	T (°C)	p (MPa)	CO/H <sub>2</sub> ratio	GHSV (h <sup>-1</sup> )	STY Isobutanol <sup>a</sup>	STY Alcohols <sup>a</sup>
Tronconi	Zn/Cr/Cs	405	8.5	1	8000	84	218
Klier	Cu/Zn/Cr/Cs Zn/Cr/Cs	325/405	7.6	1.3	18375 <sup>b</sup>	139 <sup>c</sup>	480 <sup>c,d</sup>
Sofianos	Cu/Zn/Cr/Zr/ Mn/K	325	10.0	1	8000	77 <sup>c</sup>	528 <sup>c</sup>
Apestequia	Cu/Mg/Ce/K	320	5.0	1	1832	7	80
Stiles	Cu/Zn/Mn/ Co/Cr/K/Cs	410	17.0	0.5	40000	325	1610
Keim	Zr/Zn/Mn/Pd/K	415	25.0	1	17540	446	1292

<sup>a</sup> g l<sup>-1</sup> h<sup>-1</sup>.

<sup>b</sup> Nlkg<sup>-1</sup> h<sup>-1</sup>.

<sup>c</sup> g kg<sup>-1</sup> h<sup>-1</sup>.

Table 1-3 Comparison of higher alcohol activity for modified methanol catalysts<sup>[59]</sup>

Table 1-3 shows that the testing conditions for this catalyst family are widely different and hence, drawing conclusions is a bit difficult task. Alkane selectivity between these catalysts was between 10-30% but increase in pressure has a very strong effect on increasing isobutanol selectivity. An interesting improvement made to the system was by Klier et.al.<sup>[62]</sup>, where they utilized a dual bed configuration consisting of a methanol synthesis catalyst Cs/Cu/ZnO/Cr<sub>2</sub>O<sub>3</sub> operating at lower temperature followed by Cs/ZnO/Cr<sub>2</sub>O<sub>3</sub> catalyst operating at higher temperature. Overall yields did not necessarily improve, but yields of higher alcohols, especially isobutanol, increased. Infact, some of the methanol decomposed to CO and H<sub>2</sub> over the second bed. Later, they experimented with two tandem beds of Cs/Cu/ZnO/Cr<sub>2</sub>O<sub>3</sub> operating at different temperatures<sup>[63]</sup>. One at lower temperature producing lower oxygenates and the latter affecting the chain growth. A modified reaction kinetic network was used to model the reactor which was used as a predictive tool for optimization. The mass ratio between the two beds was optimized to maximize isobutanol yields. At similar operating conditions isobutanol was increased from 138 to 202 g/kg.cat/hr. Iglesia et. al.<sup>[64]</sup> reported catalysts supported on magnesia and ceria, which are active at lower pressure and temperature (310 °C and 45 bar) for higher alcohols. Methanol production takes place on Cu sites and is near equilibrium. Chain growth happened at Cu-base sites.

### 1.4.2.3 Modified Fischer-Tropsch catalysts

Normal FT catalysts are based on Co, Fe, Ru supported on Al<sub>2</sub>O<sub>3</sub> or SiO<sub>2</sub>. Only Co catalysts exhibit a strong selectivity towards ethanol (and HAs) and successful FT catalyst compositions have Co as the main phase. The most noticeable candidates are CoCu based catalysts with K, Cs, Ba, La as

promoters<sup>[3]</sup>. Many patents have been filed by IFP based on their research on these types of catalysts<sup>[65-66]</sup>. According to IFP patents, alcohol space time yields (STY) of upto 600 g/kg.cat/h are possible. However, elsewhere, yields in the range of 100-200 g/kg.cat/hr are reported for these catalysts<sup>[14]</sup>. Although active, these catalysts yield a significant amount of hydrocarbons with alcohol selectivity ranging between 40-60%.

A significant amount of work has been done using catalysts with Cu-Co combinations. However, selectivity as high as reported in IFP patents has not been reproduced. It has been reported that preparation and activation techniques affect the alcohol selectivity to a great extent<sup>[67]</sup>. Shieffer<sup>[68]</sup> correlated higher alcohol activity with copper dispersion and also noticed that catalysts prepared with starting salts that have high water solubility gave better results. Mahdavi optimized the catalyst composition and operating conditions of a CuCoZn/Al<sub>2</sub>O<sub>3</sub> system<sup>[69]</sup> and found that at 285 °C, 70 bar, GHSV of 3410 h<sup>-1</sup>, alcohol selectivity of 90% and yields of 100 g/kg.cat/hr can be achieved. At lower operating pressure of 40 bar, temperature of 290°C and GHSV of 3,000 h<sup>-1</sup>, Boz<sup>[70]</sup> obtained alcohol productivity of ~78 g/kg.cat/hr. Kinnemann<sup>[71]</sup> prepared a coprecipitated CuFeMo based catalyst which gave alcohol yield of 125 g/kg.cat/hr with 50% selectivity. The CO conversion was 23% at conditions of 280°C, 85 bar and 3000 L/kg/hr. Catalysts based on other FT elements have been reported to provide better results w.r.t alcohols. Sun et. al. reported a CuFeMn/ZrO<sub>2</sub> catalyst with alcohol productivity of 250 g/kg.cat/hr at milder operating conditions of 260°C and 60 bar.

At PNNL<sup>[72]</sup>, research was done on a number of different catalysts. FT based catalysts of the type K/Fe/Cu/Al<sub>2</sub>O<sub>3</sub> produced interesting results. The catalyst produced significant quantities of higher hydrocarbon liquids and therefore the catalyst was tested at higher flowrates. Alcohols were produced in significant quantities as by-products. FT-MeOH-Pd catalyst prepared was a 1:1:1 mix of FT catalyst (K/Fe/Cu/Al<sub>2</sub>O<sub>3</sub>), modified methanol (K/Cu/Zn/Al<sub>2</sub>O<sub>3</sub>) and a Pd/Al<sub>2</sub>O<sub>3</sub> catalyst. At 350 °C, GHSV = 25000 h<sup>-1</sup> and 89 bar, a CO conversion of 50% produced a product mix consisting of 12% alcohols, 15% methane and 77% higher hydrocarbons. Alcohol yield corresponded to 278 g/ml.cat/hr.

#### 1.4.2.4 Molybdenum based catalysts

Mo based catalysts are known for their CO hydrogenation capabilities, amongst various other uses. For HAS, there are three basic alternatives of the Mo catalysts, based on their chemical and physical forms:

- Mo-oxide
- MoS<sub>2</sub>
- Mo<sub>2</sub>C based (or nitride)

All these forms need alkali doping to steer the products to alcohols instead of alkanes, and in all cases, as alcohol selectivity increases, overall conversion decreases. Howe <sup>[73-74]</sup> noticed an interesting phenomenon with Mo as a CO hydrogenation catalyst or when added to other FT catalysts: the product profile of alkanes is limited to C<sub>1-5</sub> range. Subsequently, Mo based FT catalysts were investigated for production of LPG gas substitute. Zhang et. al. <sup>[79]</sup> prepared ultrafine unsulfided CoMoK catalysts by a sol-gel technique which showed a significant alcohol activity. At 300°C, 60 bar, GHSV 10,000 h<sup>-1</sup>, alcohol yields of 620 g/kg.cat/hr were obtained with a C<sub>2+</sub>/C<sub>1</sub> alcohol ration of 1.1 (indicating higher alcohol activity in addition to methanol). However, total alcohol selectivity was 49%, significantly lower than the 70% benchmark for MoS<sub>2</sub> catalysts. A Texaco patent also reported alcohol yields of 270-500 g/kg.cat/hr on a MoCoK/Al<sub>2</sub>O<sub>3</sub> catalyst, but alcohol selectivity was 44%. Research done by Fujimoto <sup>[75]</sup>, Inoue <sup>[76-77]</sup> and Tatsumi <sup>[78-80]</sup> also gave similar results: C<sub>1-5</sub> alcohols could be obtained at ~300g/kg.cat/hr at selectivities < 50%. Murchison <sup>[81]</sup> pointed out that sulfides of Mo were more selective and active for alcohol synthesis than the oxides. Alcohol selectivity improved from 40 to 80%, when Mo/Act.C was replaced by MoS<sub>2</sub>/Act.C catalyst. Sulfiding of transition metal catalysts is known to retard their hydrogenation capabilities <sup>[14]</sup>. Thus, reduction in alkane formation with minimal effect on alcohol formation seems to be the benefit of sulfided catalysts.

Patterson <sup>[82]</sup> reported use of molybdenum carbides for CO hydrogenation. By increasing pressures, product distribution could be altered to alcohols. Sun et. al. <sup>[83]</sup> added Co or Ni to the Mo<sub>2</sub>C and



obtained greater activity for higher alcohols than the unpromoted Mo-carbide. At 300 °C, 80 bar, GHSV 2,000 h<sup>-1</sup>, they obtained alcohol yields of 324 g/ml.cat/hr consisting of 65% of C<sub>2+</sub> alcohols. Overall alcohol selectivity was 48%.

The sulfur variants of Mo catalysts offer the added advantage of sulfur resistance making these catalysts operable with coal derived synthesis gas without extensive sulfur cleaning. In fact, Stevens reported the benefit of 50 ppm H<sub>2</sub>S in feed gas as a means of altering and improving higher alcohol selectivity<sup>[84]</sup>.

Addition of Group VII elements like Co, Ni in MoS<sub>2</sub> catalysts improves alcohol activity. Cobalt is particularly useful in affecting the CH<sub>3</sub>OH → C<sub>2</sub>H<sub>5</sub>OH homologation chemistry. The beneficial effect of these promoters has been confirmed by many researchers<sup>[81, 85-86]</sup>. Rh has been used as a promoter providing interesting results<sup>[87-88]</sup>. Rh can alter the orientation of the MoS<sub>2</sub> phase in addition to providing additional CO hydrogenation capacity. Performance enhancement in alcohol synthesis as a result of Ni addition into the MoS<sub>2</sub> system is also well documented<sup>[78, 89-90]</sup>.

catalyst	experimental conditions				carbon selectivity (%) <sup>b</sup>					alc STY (mg/(g cat h))		
	temp (°C)	press (psig)	GHSV (h <sup>-1</sup> )	H <sub>2</sub> /CO	X <sub>CO</sub> <sup>a</sup> (%)	HC	CO <sub>2</sub>	C <sub>1</sub> -OH	C <sub>2</sub> -OH	C <sub>3+</sub> -OH	EtOH	Σ <sub>alcohol</sub>
MoS <sub>2</sub> (Dow Chemical)	295	1050	1300	1.0	29.2	14.5	NA	22.7	40.7	17.4	NA	NA
KRhMoS <sub>2</sub> /Al <sub>2</sub> O <sub>3</sub>	327	1450	4800	2.0	11.1	41.0 <sup>c</sup>	NA	11.0	19.0	29.0	NA	174 <sup>d</sup>
KRhMoS <sub>2</sub> /Al <sub>2</sub> O <sub>3</sub>	327	1450	14400	2.0	5.5	17.0 <sup>c</sup>	NA	26.0	28.0	28.0	NA	389 <sup>d</sup>
KCoMoS <sub>2</sub> /C-1 <sup>f</sup>	330	725	4800	2.0	14.5	72.6 <sup>d</sup>	NA	11.1	10.6	5.6	NA	108 <sup>d</sup>
KCoMoS <sub>2</sub> /C-4 <sup>e</sup>	330	725	4800	2.0	11.7	58.1 <sup>d</sup>	NA	18.7	13.2	8.0	NA	150 <sup>d</sup>
KCoMoS <sub>2</sub> /C-16 <sup>h</sup>	330	725	4800	2.0	8.7	60.7 <sup>c</sup>	NA	19.6	16.1	5.6	NA	96 <sup>d</sup>
K <sub>2</sub> CO <sub>3</sub> CoMoS <sub>2</sub>	270	2100	2546	1.1	10.4	12.7	1.70	48.2	29.6	7.8	NA	250
LaKNiMoS <sub>2</sub>	320	1160	2500	1.0	33.5	34.0 <sup>c</sup>	NA	7.5	18.5	40.0	NA	170 <sup>d</sup>
K <sub>2</sub> CO <sub>3</sub> NiMoS <sub>2</sub>	320	1160	2500	1.0	55.6	52.6	NA	6.2	15.4	25.8	NA	153 <sup>e</sup>
K <sub>2</sub> CO <sub>3</sub> NiMoS <sub>2</sub>	280	1160	2500	1.0	20.6	36.6	NA	10.8	27.2	25.4	NA	102
Cs <sub>2</sub> CO <sub>3</sub> CoMoS <sub>2</sub> /clay	320	2000	4000	1.1	28.7	31.3	NA	10.8	30.3	22.0	NA	NA
K <sub>2</sub> CO <sub>3</sub> CoMoS <sub>2</sub> /clay	320	2000	4000	1.1	31.9	36.0	NA	13.5	23.1	21.6	NA	NA

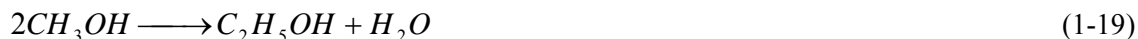
Table 1-4 MoS<sub>2</sub>-Based Catalysts and their performance<sup>[3]</sup>

A peculiar advantage of these catalysts is that they can achieve high selectivity to ethanol. CO<sub>2</sub> free selectivity for ethanol of 30% is often reported. Optimization of the overall process and reactor technology can improve the selectivity further. Santiesteban<sup>[91]</sup> observed that methanol injection increased higher alcohols and theoretically, all methanol could be converted to higher alcohols by methanol recycle. In the PEFI Ecalene process<sup>[92]</sup>, use of a CSTR reactor and a nanosized MoS<sub>2</sub> catalyst

allows ethanol selectivity greater than 45% and alcohol yields of 400-500 g/kg.cat/hr. Dow Chemical and Union Carbide have reported alcohol selectivity of 75-90%. By manipulating catalyst compositions and operating conditions, ethanol production can be fine-tuned. Various researchers have shown effects of promoters ranging from Co, Ce, K, La, Rh, Ni. For cobalt, the optimum ratio has also been researched. A Co/Mo=0.5 appears consistently <sup>[86, 93]</sup>. Below this ratio, Co is accommodated into a CoMoS phase which is proven to be the active phase for HDS reactions <sup>[94-95]</sup> and also for HAS <sup>[86, 96]</sup>. Above this ratio, the Co<sub>8</sub>S<sub>9</sub> segregates out and is inactive for HAS.

## 1.5 HAS REACTION MECHANISM

Early on in 1930s, some insight was offered into the mechanism for alcohol synthesis catalysts by Frolich and Cryder <sup>[97]</sup>. Catalysts used were Zn-Mn-Cr (modified methanol type), with K being added from the Cr precursor, potassium chromate. They noticed lower ethanol yields as compared to other higher alcohols and proposed a condensation mechanism for alcohol formation instead of one based on aldehydes as intermediates to alcohols. Owing to the composite nature of their catalyst, they did not rule out other mechanisms, in fact even acknowledged Fischer-Tropsch reactions to take place concurrently, but to a minor degree.



In early 1980s, researchers at Lehigh University pointed out the use of low temperature methanol catalysts, modified with an alkali as a suitable catalyst for higher alcohols. Based on product distribution, three major pathways for carbon growth were postulated:

- Linear growth: Insertion of CO or C<sub>1</sub> intermediate

- Aldol condensation: Aldehydic intermediate(H-OC\*) + oxygenated intermediate
- Ester formation: Condensation of two aldehydes OR aldehydic intermediate + methoxide(CH<sub>3</sub>O\*)

Amongst the product distribution, 2-methyl linear alcohols were dominant. Again ethanol was found in lower concentrations than C<sub>1</sub> and C<sub>3+</sub> alcohols. The condensation reaction was considered to be much faster than the linear chain growth and their kinetic model agreed well with the product distribution.

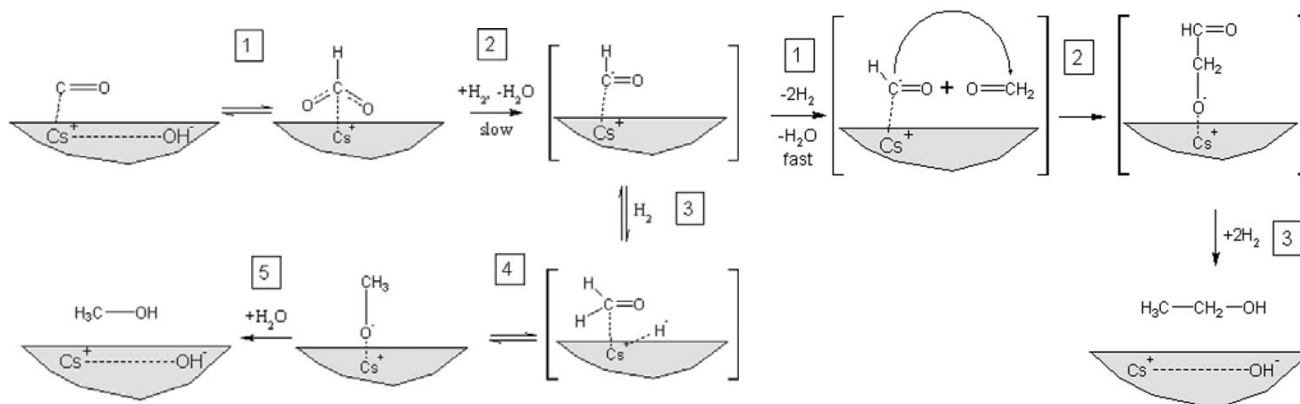


Figure 1-3 Alcohol synthesis mechanism over modified methanol catalyst [1]

The reaction mechanism for ethanol over noble catalysts like **Rh-based catalysts** is less disputed. CO adsorbs on the different sites on the catalyst, followed by CH<sub>2</sub> insertion which upon subsequent hydrogenation gives ethanol.

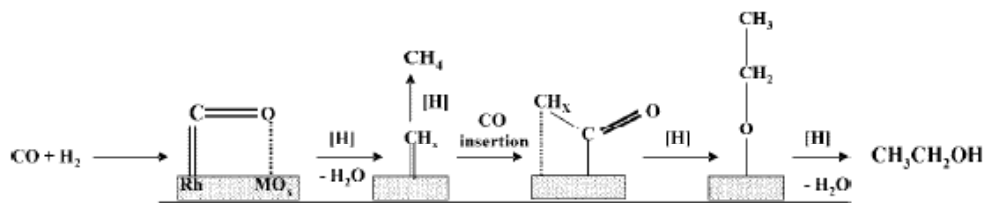


Figure 1-4 Reaction scheme for HAS over Rh based catalysts [3]

At Lehigh work was also done on **MoS<sub>2</sub> based catalysts**, possibly after the disclosure of Dow and Union Carbide patents in the early 1980s. As the sulfide based catalysts have only been used recently, not many detailed mechanistic studies have been performed.

Smith et. al. [98] discussed the mechanism for product formation over alkali-MoS<sub>2</sub> catalysts. Santiesteban [91] conducted labeling studies to gain insight and conclude Smith's formulated mechanism. The mechanism is depicted in Figure 1-5.

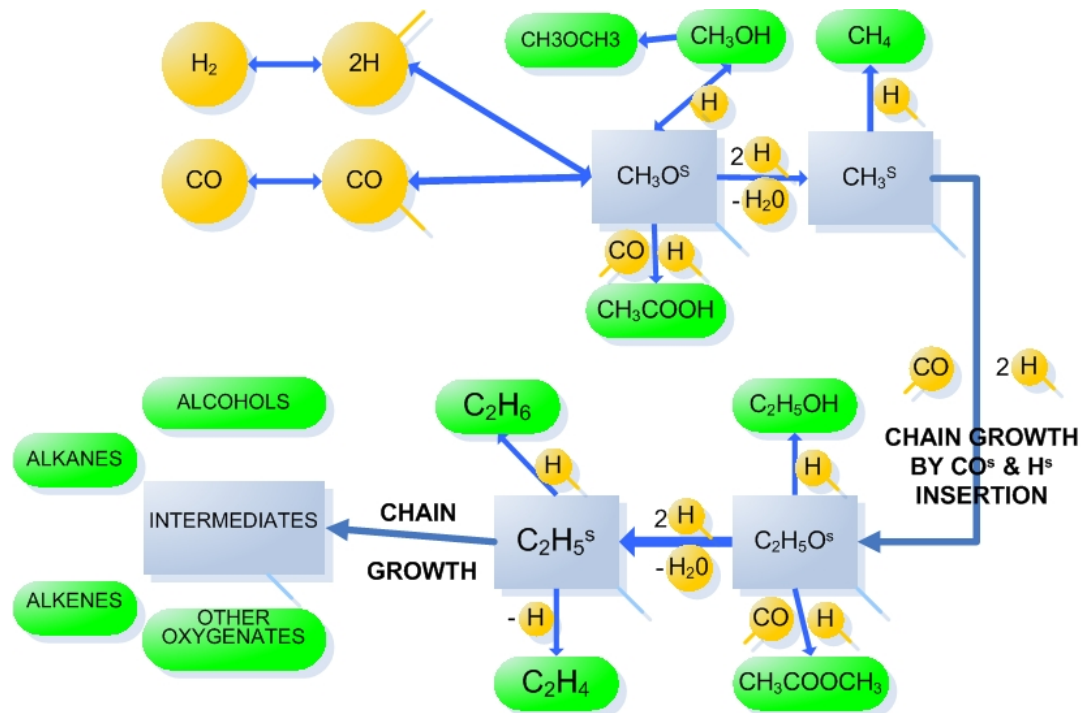


Figure 1-5 Reaction scheme over MoS<sub>2</sub> based catalysts

Santiesteban experiments consisted of injecting <sup>13</sup>C labeled methanol into the reactor and monitoring the carbon enrichment via NMR and GC/MS analysis. It was noted that:

- Double <sup>13</sup>C were not found in higher alcohols (no condensation)
- Equivalent amounts of <sup>13</sup>CH<sub>3</sub>CH<sub>3</sub>CH<sub>2</sub>OH and CH<sub>3</sub><sup>13</sup>CH<sub>3</sub>CH<sub>2</sub>OH
- Ethanol <sup>13</sup>C enrichment > Propanol <sup>13</sup>C enrichment
- Preferential methyl <sup>13</sup>C enrichment of methyl esters
- No methanol decomposition to CO and H<sub>2</sub>
- Alkane enrichment

These findings confirm the mechanism suggested before; that higher alcohols (alkanes and oxygenates) are formed by linear chain growth and that products of similar carbon number have similar intermediates.

Kinetic models were developed by Park<sup>[43]</sup> and Gunturu<sup>[99]</sup>, both of which primarily followed the model proposed by Smith. Gunturu's model was able to predict recycle effects of methanol. It was incorporated into NREL's detailed simulation/economic analysis of ethanol production from biomass gasification<sup>[100]</sup>. Improvements made by Park were:

- inclusion of water gas shift reaction
- temperature dependent kinetic and equilibrium parameters

The kinetic models developed over MoS<sub>2</sub> catalysts have shown good agreement with experimental results. However, certain authors claim that all methane is not derived from the formyl and acyl intermediates and that it is simply a result of the methanation reaction<sup>[32, 101]</sup>. Others even say that alcohol and alkane formation takes place on separate sites<sup>[88, 102]</sup> and this is strengthened by the fact that alkane and alcohols have different ASF growth ratios ' $\alpha$ ', which would not be so if they were from the same intermediate. The Anderson-Schulz-Flory (ASF) distribution is the statistical distribution curve for Fischer-Tropsch products, and  $\alpha$  is the chain growth probability factor.

## 1.6 SELECTION OF MoS<sub>2</sub> CATALYTIC SYSTEM: ADVANTAGES & ISSUES

The most promising series of catalysts for HAS are the modified methanol and the molybdenum based catalysts<sup>[3, 14, 56, 101]</sup>. They do not have the complications associated with catalyst synthesis and reproducibility (CuCo types), lack of selectivity towards alcohols (FT types) or the excessive price of starting materials (noble metals group). With a focus on ethanol and linear alcohols, it became clear that molybdenum based catalysts would have to be utilized, as ethanol and other linear alcohols are not

obtained in appreciable quantities over the modified methanol catalysts. Some of the specific advantages that MoS<sub>2</sub> based catalysts offer are:

1. Their resistance to sulfur contamination can make them well suited for syngas derived from coal, in addition to that derived from other sources. In fact sulfur inclusion in the feed leads to increase in formation of higher alcohols <sup>[84, 96]</sup>.
2. Linear alcohols are formed. With variation of catalyst composition and operating conditions, it is possible to maximize a specific range of alcohols, e.g. ethanol or n-butanol can be targeted.
3. Catalyst is stable for long durations. Deactivation due to coke formation is relatively less severe even at high CO/H<sub>2</sub> ratios in the syngas <sup>[3]</sup>.
4. Moderate amounts of CO<sub>2</sub> are tolerated. Increased amounts of CO<sub>2</sub> in syngas do not necessarily poison/inhibit the catalyst, but production of higher alcohols decreases <sup>[103]</sup>.
5. Amongst the molybdenum group of catalysts, MoS<sub>2</sub> offers better alcohol selectivity.
6. HAS is highly exothermic and many groups have suggested use of slurry reactors to increase CO conversion. Whereas modified methanol catalysts have not shown improvement w.r.t higher alcohols when used in a slurry phase <sup>[59, 104]</sup>, MoS<sub>2</sub> catalysts in CSTR mode have performed better than when operated in fixed bed <sup>[92]</sup>.
7. Use of supercritical fluids to enhance fixed bed operation also fared better for higher alcohols <sup>[101]</sup>.
8. Performance of MoS<sub>2</sub> has been linked with its structure and morphology <sup>[95]</sup>. In this regard, one can borrow improvements in synthesis techniques from HDS catalysts and other MoS<sub>2</sub> application areas like, semiconductors, tribology.

One of the biggest issues with Mo based catalysts, and other HAS catalysts in general, is the lack of understanding of what affects and promotes higher alcohols as opposed to alkanes and other oxygenates. Although the reaction pathways have been identified and are somewhat consented upon, it is still unclear what properties and interactions of the metal drives the reaction in a particular direction.

Some of the known issues with MoS<sub>2</sub> based catalysts are:

1. Exact mechanism of alkali promotion: Does it modify the surface configuration, electronic properties, metal stability and dispersion, intermediate stabilization, acidity or a combination of these?
2. Which structural characteristics of MoS<sub>2</sub> affect its activity and selectivity towards higher alcohols? For HAS, a semi-crystalline MoS<sub>2</sub> material performs better than either amorphous or crystalline <sup>[105-106]</sup>, but why? The edge sites and the basal sites offer different catalytic potentials. Thus control of size and degree of stacking is also considered important in achieving selectivity to specific products <sup>[95]</sup>.

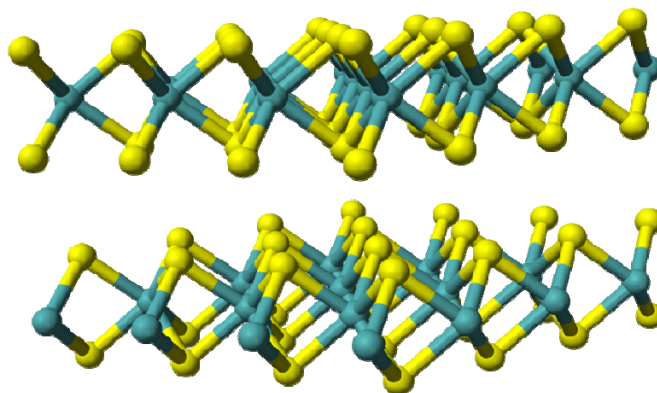


*Figure 1-6 Structures of MoS<sub>2</sub>. yellow represents sulfur, blue molybdenum. Note how a MoS<sub>2</sub> stack consists of Mo sandwiched in between sulfur layers. Stacking represents piling up of stacks on top of one another. Molybdenum, the active metal, is only exposed at the edges; it is inaccessible from the top or bottom (basal planes)*

3. Loss of sulfur from the catalyst during operation is known and can be a serious problem. Sulfur contamination of products could be a serious issue if desulphurization is not planned for the products <sup>[14, 96]</sup>. Loss of sulfur can also alter the electronic (and catalytic) properties of the catalyst as MoS<sub>2</sub> is a semiconductor material.
4. Woo reported that when MoS<sub>2</sub>, doped with K<sub>2</sub>CO<sub>3</sub> as a promoter, is exposed to air for extended periods, loss of alcohol selectivity results <sup>[107]</sup>. Although, it can be corrected with further fresh doping, it represents a problem in shelf-life of the catalyst.

5. MoS<sub>2</sub> is a structured material and is stable under syngas reaction environments at temperatures >300°C without a support. A support would still offer the advantage of improving dispersion and lowering catalyst costs, but, supports affect alcohol selectivity. Therefore, a balance needs to be struck between support type and metal loading for an optimized catalyst.

## 1.7 SCOPE AND OBJECTIVE

The scope of this research work was to synthesize, test and improve HAS catalysts with a focus on aliphatic alcohols. Research activities are underway to develop an efficient process that can convert petroleum alternates to syngas and then catalytically combine them to form higher alcohols. A major bottleneck is identified to be the HAS catalyst. Any breakthrough in reactor + catalyst technology will greatly enhance the overall process economics.

The methodology adapted in this work is to quickly screen for effects of support, promoters and novel synthesis techniques for HAS catalysts. It is hoped that through this screening, key issues in tuning catalytic activity and selectivity can be identified to guide further efforts in catalyst/process development for syngas to higher alcohols. It would also be worthwhile to study optimization of reactor operation and kinetics of reactions involved for a catalyst that has the potential for commercialization. Parameters and characteristics, like calcination techniques and alkali-metal ratios, for which ample research and optimization has already been done and published, are therefore, not studied here. Specific research goals were:

- **Metal loading:** Pinpoint optimum loading ratios for use of MoS<sub>2</sub> with supports
- **Support characteristics:** Neutral supports like Activated Carbon are documented to perform better for alcohol synthesis as opposed to acidic supports like Al<sub>2</sub>O<sub>3</sub>. Alter acidity/basicity characteristics of a particular support to see if alcohol selectivities are affected.
- **Co-promoters:** Co and Ni are well researched promoters for HAS. Evaluate if other FT active elements have comparable effects in enhancing HA activity.



- **Operating conditions:** Enhance catalyst performance for HAS by varying all operating conditions, including effect of product recycle.
- **Characterization:** With the aid of BET surface area measurement, XRD, SEM and TEM coupled EDS measurements, evaluate which surface and structural characteristics affect HAS performance.

To achieve these goals, well defined synthesis, evaluation and characterization capabilities needed to be set up. Following capabilities were required:

- **Reactor Setup:** Setup a new Parr fixed bed reactor system.
- **Gas Chromatography:** Setup of a GC for online gas analysis and another for liquid analysis, so that reaction products can be quantified.
- **Material Balancing:** Calibration of GC and mass flow controllers and a streamlined evaluation system that accounts for 85% of the mass conversion.
- **Catalyst synthesis:** Standardize synthesis procedure for sulfide based materials including final calcination in tube furnace in inert atmosphere.

## 1.8 REFERENCES

1. Spivey, J.J. and A. Egbebi, *Heterogeneous catalytic synthesis of ethanol from biomass-derived syngas*. Chemical Society Reviews, 2007. **36**(9): p. 1514-1528.
2. Kirk-Othmer, *Encyclopedia of Chemical Technology*. 1991, Wiley-Interscience.
3. Subramani, V. and S.K. Gangwal, *A review of recent literature to search for an efficient catalytic process for the conversion of syngas to ethanol*. Energy & Fuels, 2008. **22**(2): p. 814-839.
4. Bush, G. *Advanced Energy Initiative*. 2006; Available from: <http://georgewbush-whitehouse.archives.gov/stateoftheunion/2006/energy/index.html#section2>.
5. Crutzen, P.J., et al., *N<sub>2</sub>O release from agro-biofuel production negates global warming reduction by replacing fossil fuels*. Atmos. Chem. Phys., 2008. **8**(2): p. 389-395.
6. Congress, U. *Energy Independence and Security Act of 2007*. 2007; Available from: [http://en.wikipedia.org/wiki/Energy\\_Independence\\_and\\_Security\\_Act\\_of\\_2007](http://en.wikipedia.org/wiki/Energy_Independence_and_Security_Act_of_2007).
7. Congress, U. *Energy Policy Act of 2005*. 2005; Available from: [http://en.wikipedia.org/wiki/Energy\\_Policy\\_Act\\_of\\_2005](http://en.wikipedia.org/wiki/Energy_Policy_Act_of_2005).
8. Tillerson, R. *Exxon CEO: We've Passed The Peak Of US Gasoline Consumption*. 2009; Available from: <http://www.businessinsider.com/2007-was-the-ultimate-peak-for-us-gas-consumption-2009-10>.
9. WRI, *Pilot-Scale Demonstration of Pefi's Oxygenated Transportation Fuels Production Technology*. 2005. p. Medium: ED.
10. Ahmed, F.E., *Toxicology and human health effects following exposure to oxygenated or reformulated gasoline*. Toxicology Letters, 2001. **123**(2-3): p. 89-113.
11. Spath, P.L. and D.C. Dayton, *Preliminary Screening —Technical and Economic Assessment of Synthesis Gas to Fuels and Chemicals with Emphasis on the Potential for Biomass-Derived Syngas*. 2003, National Renewable Energy Laboratory.
12. Mills, G.A., *Status and future opportunities for conversion of synthesis gas to liquid fuels*. Fuel, 1994. **73**(8): p. 1243-1279.
13. DOE, *The economical production of alcohol fuels from coal-derived synthesis gas*, OSTI ID: 14013 Mar 1999. 1999. 448 pages.
14. Forzatti, P., E. Tronconi, and I. Pasquon, *Higher alcohol synthesis*. Catalysis Reviews-Science and Engineering, 1991. **33**(1-2): p. 109-168.
15. Kozlowski, *Motor fuel*, US patent. 3901664, 1975.
16. Mazanec, *Alcohol compositions for blending with gasoline*, US patent. 4705532, 1987.
17. Ameri, M., B. Ghobadlan, and I. Baratian, *Technical comparison of a CHP using various blends of gasohol in an IC engine*. Renewable Energy, 2008. **33**(7): p. 1469-1474.
18. Al-Hasan, M., *Effect of ethanol-unleaded gasoline blends on engine performance and exhaust emission*. Energy Conversion and Management, 2003. **44**(9): p. 1547-1561.
19. Markel, A.J. and B.K. Bailey, *Modeling and cold start in alcohol-fueled engines*, OSTI ID: 650264 1998.
20. Toghiani, H., et al., *Synthesis Gas to Hydrocarbons over CuO-CoO-Cr<sub>2</sub>O<sub>3</sub>/H<sup>+</sup>-ZSM-5 Bifunctional Catalysts*. The Journal of Physical Chemistry C, 2008. **112**(31): p. 11847-11858.
21. Ohl, J., *Hydrogen energy cycle: An overview*. Journal of Materials Research, 2005. **20**(12): p. 3180-3187.
22. Holladay, J.D., et al., *An overview of hydrogen production technologies*. Catalysis Today, 2009. **139**(4): p. 244-260.
23. Zhou, W.J., et al., *Bi- and tri-metallic Pt-based anode catalysts for direct ethanol fuel cells*. Journal of Power Sources, 2004. **131**(1-2): p. 217-223.
24. Antolini, E., *Catalysts for direct ethanol fuel cells*. Journal of Power Sources, 2007. **170**(1): p. 1-12.

25. Pruet, R.L., *Synthesis gas - a raw-material for industrial-chemicals*. Science, 1981. **211**(4477): p. 11-16.
26. Pena, M.A., J.P. Gómez, and J.L.G. Fierro, *New catalytic routes for syngas and hydrogen production*. Applied Catalysis A: General, 1996. **144**(1-2): p. 7-57.
27. Wilhelm, D.J., et al., *Syngas production for gas-to-liquids applications: technologies, issues and outlook*. Fuel Processing Technology, 2001. **71**(1-3): p. 139-148.
28. Dry, M.E. and H.B.D. Erasmus, *Update of the Sasol synfuels process*. Annual Review of Energy, 1987. **12**: p. 1-21.
29. De Klerk, A., *PETR 29-Refining of Fischer-Tropsch syncrude: Lessons from the past*. Abstracts of Papers of the American Chemical Society, 2008. **236**: p. 29-PETR.
30. Jones, S. and Y. Zhu, *Techno-economic Analysis for the Conversion of Lignocellulosic Biomass to Gasoline via the Methanol-to-Gasoline (MTG) Process*. 2009, Pacific Northwest National Laboratory, PNNL-18481 .
31. Petrus, L. and M.A. Noordermeer, *Biomass to biofuels, a chemical perspective*. Green Chemistry, 2006. **8**(10): p. 861-867.
32. Hindermann, J.P., G.J. Hutchings, and A. Kiennemann, *Mechanistic aspects of the formation of hydrocarbons and alcohols from CO hydrogenation*. Catalysis Reviews-Science and Engineering, 1993. **35**(1): p. 1-127.
33. Schulz, H. and M. Claeys, *Kinetic modelling of Fischer-Tropsch product distributions*. Applied Catalysis a-General, 1999. **186**(1-2): p. 91-107.
34. Van der Laan, G.P. and A. Beenackers, *Kinetics and selectivity of the Fischer-Tropsch synthesis: A literature review*. Catalysis Reviews-Science and Engineering, 1999. **41**(3-4): p. 255-318.
35. Anderson, R.B., J. Feldman, and H.H. Storch, *Synthesis of alcohols by hydrogenation of carbon monoxide*. Industrial and Engineering Chemistry, 1952. **44**(10): p. 2418-2424.
36. Kummer, J.T. and P.H. Emmett, *Chemisorption of carbon monoxide and the heterogeneity of the surface of iron catalysts*. Journal of the American Chemical Society, 1951. **73**(6): p. 2886-2889.
37. Kummer, J.T., et al., *Mechanism studies of the fischer-tropsch synthesis - the addition of radioactive alcohol*. Journal of the American Chemical Society, 1951. **73**(2): p. 564-569.
38. Schulz, H. and H. Pichler, *Recent results in synthesis of hydrocarbons from CO and H<sub>2</sub>*. Chemie Ingenieur Technik, 1970. **42**(18): p. 1162-&.
39. Brown, S.L. and S.G. Davies, *Reductive polymerization of carbon-monoxide - synthesis of entirely co-derived pentanoic acid*. Journal of the Chemical Society-Chemical Communications, 1986(1): p. 84-85.
40. Dry, M.E., P.M. Loggenberg, and R.G. Copperthwaite, *A surface study of the CO hydrogenation reaction on fused iron catalysts*. Surface and Interface Analysis, 1990. **16**(1-12): p. 347-351.
41. Sachtler, W.M.H. and P. Biloen, *Mechanism of hydrocarbon synthesis over fischer-tropsch catalysts*. Advances in Catalysis, 1981. **30**: p. 165-216.
42. Weitkamp, A.W. and C.G. Frye, *Products of hydrogenation of carbon monoxide - relation of product composition to reaction mechanism*. Industrial and Engineering Chemistry, 1953. **45**(2): p. 363-367.
43. Park, T.Y., I.S. Nam, and Y.G. Kim, *Kinetic analysis of mixed alcohol synthesis from syngas over K/MoS<sub>2</sub> catalyst*. Industrial & Engineering Chemistry Research, 1997. **36**(12): p. 5246-5257.
44. Chen, M.J. and J.W. Rathke, *Homologation of methanol catalyzed by manganese carbonyl in tertiary amine methanol solutions*. Organometallics, 1989. **8**(2): p. 515-520.
45. Moloy, K.G. and R.W. Wegman, *A novel catalyst for the low-pressure, low-temperature homologation of methanol*. Journal of the Chemical Society-Chemical Communications, 1988(12): p. 820-821.
46. Boz, N., N. Degirmenbasi, and D.M. Kalyon, *Conversion of biomass to fuel: Transesterification of vegetable oil to biodiesel using KF loaded nano-[gamma]-Al<sub>2</sub>O<sub>3</sub> as catalyst*. Applied Catalysis B: Environmental, 2009. **89**(3-4): p. 590-596.

47. Trautmann, S. and M. Baerns, *Infrared spectroscopic studies of co adsorption on rhodium supported by SiO<sub>2</sub>, Al<sub>2</sub>O<sub>3</sub>, and TiO<sub>2</sub>*. Journal of Catalysis, 1994. **150**(2): p. 335-344.
48. Haider, M.A., M.R. Gogate, and R.J. Davis, *Fe-promotion of supported Rh catalysts for direct conversion of syngas to ethanol*. Journal of Catalysis, 2009. **261**(1): p. 9-16.
49. Gronchi, P., E. Tempesti, and C. Mazzocchia, *Metal dispersion dependent selectivities for syngas conversion to ethanol on V<sub>2</sub>O<sub>3</sub> supported rhodium*. Applied Catalysis a-General, 1994. **120**(1): p. 115-126.
50. Burch, R. and M.J. Hayes, *The Preparation and Characterisation of Fe-Promoted Al<sub>2</sub>O<sub>3</sub>-Supported Rh Catalysts for the Selective Production of Ethanol from Syngas*. Journal of Catalysis, 1997. **165**(2): p. 249-261.
51. Ojeda, M., et al., *Manganese-promoted Rh/Al<sub>2</sub>O<sub>3</sub> for C<sub>2</sub>-oxygenates synthesis from syngas: Effect of manganese loading*. Applied Catalysis A: General, 2004. **261**(1): p. 47-55.
52. Ichikawa, M., *Catalysis by supported metal crystallites from carbonyl clusters .2. Catalytic ethanol synthesis from CO and H<sub>2</sub> under atmospheric-pressure over supported rhodium crystallites prepared from Rh carbonyl clusters deposited on TiO<sub>2</sub>, ZrO<sub>2</sub>, and La<sub>2</sub>O<sub>3</sub>*. Bulletin of the Chemical Society of Japan, 1978. **51**(8): p. 2273-2277.
53. Shen, J.G.C. and M. Ichikawa, *Intrazeolite anchoring of Co, Ru, and [Ru-Co] carbonyl clusters: Synthesis, characterization, and their catalysis for CO hydrogenation*. Journal of Physical Chemistry B, 1998. **102**(29): p. 5602-5613.
54. Arakawa, H., et al., *Selective synthesis of ethanol over Rh-Ti-Fe-Ir/SiO<sub>2</sub> catalyst at high-pressure syngas conversion*. Chemistry Letters, 1985(7): p. 881-884.
55. Hu, J., et al., *Conversion of biomass-derived syngas to alcohols and C<sub>2</sub> oxygenates using supported Rh catalysts in a microchannel reactor*. Catalysis Today, 2007. **120**(1): p. 90-95.
56. Herman, R.G., *Advances in catalytic synthesis and utilization of higher alcohols*. Catalysis Today, 2000. **55**(3): p. 233-245.
57. Morgan, G.T. and R. Taylor, *Ethyl alcohol: A product of high pressure syntheses*. Nature, 1930. **125**: p. 889-889.
58. Smith, K.J. and R.B. Anderson, *The higher alcohol synthesis over promoted Cu/ZnO catalysts*. Canadian Journal of Chemical Engineering, 1983. **61**(1): p. 40-45.
59. Verkerk, K.A.N., et al., *Recent developments in isobutanol synthesis from synthesis gas*. Applied Catalysis A: General, 1999. **186**(1-2): p. 407-431.
60. Mills, G.A., R.R. Chianelli, and J.E. Lyons, *Catalysts for liquid transportation fuels from petroleum, coal, residual oil, and biomass*. Catalysis Today, 1994. **22**(2): p. 361-396.
61. Epling, W.S., D.M. Minahan, and G.B. Hoflund, *An efficient catalyst for the production of isobutanol and methanol from syngas. VIII: Cs- and Pd-promoted Zn/Cr spinel (excess ZnO)*. Catalysis Letters, 1998. **50**(3-4): p. 199-203.
62. Herman, R.G., et al., *Production of methanol and isobutyl alcohol mixtures over double-bed cesium-promoted Cu/ZnO/Cr<sub>2</sub>O<sub>3</sub> and ZnO/Cr<sub>2</sub>O<sub>3</sub> catalysts*. Industrial & Engineering Chemistry Research, 1996. **35**(5): p. 1534-1542.
63. Herman, R.G., M.M. Burcham, and K. Klier, *Higher alcohol synthesis over double bed Cs-Cu/ZnO/Cr<sub>2</sub>O<sub>3</sub> catalysts: Optimizing the yields of 2-methyl-1-propanol (isobutanol)*. Industrial & Engineering Chemistry Research, 1998. **37**(12): p. 4657-4668.
64. Iglesia, E., et al., *Synthesis of higher alcohols on copper catalysts supported on alkali-promoted basic oxides*. Applied Catalysis A: General, 1998. **169**(2): p. 355-372.
65. Sugier, *Production of Alcohols from Synthesis Gases*, US patent 4346179. 1982.
66. Sugier, *Process for manufacturing alcohols particularly saturated linear alcohols from syntehsis gas*, US patent 4291126, 1981.
67. Chaumette, P., et al., *Evolution of alcohol synthesis catalysts under syngas*. Industrial & Engineering Chemistry Research, 1994. **33**(6): p. 1460-1467.

68. Sheffer, G.R. and T.S. King, *Effect of preparation parameters on the catalytic nature of potassium promoted Cu-Co-Cr higher alcohol catalysts*. Applied Catalysis, 1988. **44**(1-2): p. 153-164.
69. Mahdavi, V., et al., *Synthesis of higher alcohols from syngas over Cu-CO<sub>2</sub>O<sub>3</sub>/ZnO, Al<sub>2</sub>O<sub>3</sub> catalyst*. Applied Catalysis a-General, 2005. **281**(1-2): p. 259-265.
70. Boz, I., *Higher alcohol synthesis over a K-promoted Co<sub>2</sub>O<sub>3</sub>/CuO/ZnO/Al<sub>2</sub>O<sub>3</sub> catalyst*. Catalysis Letters, 2003. **87**(3-4): p. 187-194.
71. Kiennemann, A., et al., *Higher alcohol synthesis on modified iron-based catalysts - copper and molybdenum addition*. Applied Catalysis a-General, 1993. **99**(2): p. 175-194.
72. Gerber, M.A., J.F. White, and D.J. Stevens, *Mixed Alcohol Synthesis Catalyst Screening*, Pacific Northwest National Laboratory, PNNL-16763, 2007
73. Howe, R.F. and Y.S. Yong, *Carbon-monoxide hydrogenation over molybdenum zeolite catalysts*. Journal of Molecular Catalysis, 1986. **38**(3): p. 323-326.
74. Howe, R.F. and A. Kazusaka, *Catalysis on Mo(Co)<sub>6</sub>-derived supported molybdenum catalysts - CO oxidation with N<sub>2</sub>O*. Journal of Catalysis, 1988. **111**(1): p. 50-58.
75. Fujimoto, K. and T. Oba, *Synthesis of C<sub>1</sub>-C<sub>7</sub> alcohols from synthesis gas with supported cobalt catalysts*. Applied Catalysis, 1985. **13**(2): p. 289-293.
76. Inoue, M., et al., *Preparation of Ir-Mo-Na<sub>2</sub>O composite catalysts and their performances for alcohol synthesis from syngas*. Applied Catalysis, 1987. **29**(2): p. 361-374.
77. Inoue, M., et al., *Alcohol synthesis from syngas on group-viii metal-catalysts promoted by Mo-Na<sub>2</sub>O*. Applied Catalysis, 1989. **49**(2): p. 213-217.
78. Tatsumi, T., et al., *Nickel-promoted Mo catalysts for alcohol synthesis from CO-H<sub>2</sub>*. Chemistry Letters, 1986(6): p. 919-920.
79. Tatsumi, T., A. Muramatsu, and H. Tominaga, *Importance of sequence of impregnation in the activity development of alkali-promoted mo catalysts for alcohol synthesis from CO-H<sub>2</sub>*. Journal of Catalysis, 1986. **101**(2): p. 553-556.
80. Tatsumi, T., A. Muramatsu, and H. Tominaga, *Influence of support and potassium on CO hydrogenation catalyzed by molybdenum*. Applied Catalysis, 1986. **27**(1): p. 69-82.
81. Murchison, C.B., et al., *Mixed Alcohols from syngas over moly catalysts*. Proceedings of the 9th International Congress of Catalysis, 1988. **2**: p. 626-633.
82. Patterson, P.M., T.K. Das, and B.H. Davis, *Carbon monoxide hydrogenation over molybdenum and tungsten carbides*. Applied Catalysis A: General, 2003. **251**(2): p. 449-455.
83. Xiang, M.L., et al., *K/Fe/beta-Mo<sub>2</sub>C: A novel catalyst for mixed alcohols synthesis from carbon monoxide hydrogenation*. Catalysis Communications, 2007. **8**(1): p. 88-90.
84. Stevens, R.R., *Alcohols from synthesis gas*, (Dow Chemical Co., USA). US 4752622, 1986.
85. Li, X.G., et al., *Higher alcohols from synthesis gas using carbon-supported doped molybdenum-based catalysts*. Industrial & Engineering Chemistry Research, 1998. **37**(10): p. 3853-3863.
86. Li, Z.R., et al., *Effect of cobalt promoter on Co-Mo-K/C catalysts used for mixed alcohol synthesis*. Applied Catalysis a-General, 2001. **220**(1-2): p. 21-30.
87. Li, Z.R., Y.L. Fu, and M. Jiang, *Structures and performance of Rh-Mo-K/Al<sub>2</sub>O<sub>3</sub> catalysts used for mixed alcohol synthesis from synthesis gas*. Applied Catalysis a-General, 1999. **187**(2): p. 187-198.
88. Storm, D.A., *The production of higher alcohols from syngas using potassium-promoted Co/Mo/Al<sub>2</sub>O<sub>3</sub> and Rh/Co/Mo/Al<sub>2</sub>O<sub>3</sub>*. Topics in Catalysis, 1995. **2**(1-4): p. 91-101.
89. Alyea, E.C., D. He, and J. Wang, *Alcohol synthesis from syngas .I. Performance of alkali-promoted Ni-Mo (MOVS) catalysts*. Applied Catalysis a-General, 1993. **104**(1): p. 77-85.
90. Li, D., et al., *Ni/ADM: a high activity and selectivity to C<sub>2+</sub>OH catalyst for catalytic conversion of synthesis gas to C<sub>1</sub>-C<sub>5</sub> mixed alcohols*. Topics in Catalysis, 2005. **32**(3): p. 233-239.
91. Santiesteban, J.G., *Alcohol synthesis from carbon-monoxide and hydrogen over molybdenum-disulfide based catalysts*, Lehigh University: thesis, 1989

92. WRI, *Pilot Scale demonstration of PEFI's oxygenated transportation fuels production technology*. WRI 05-R007R, 2005.
93. Iranmahboob, J., D.O. Hill, and H. Toghiani, *K<sub>2</sub>CO<sub>3</sub>/Co-MoS<sub>2</sub>/clay catalyst for synthesis of alcohol: influence of potassium and cobalt*. *Applied Catalysis a-General*, 2002. **231**(1-2): p. 99-108.
94. Topsøe, H., et al., *Recent basic research in hydrodesulfurization catalysis*. *Industrial & Engineering Chemistry Fundamentals*, 2002. **25**(1): p. 25-36.
95. Chianelli, R.R., *Fundamental-studies of transition-metal sulfide hydrodesulfurization catalysts*. *Catalysis Reviews-Science and Engineering*, 1984. **26**(3-4): p. 361-393.
96. Christensen, J.M., et al., *Effects of H<sub>2</sub>S and process conditions in the synthesis of mixed alcohols from syngas over alkali promoted cobalt-molybdenum sulfide*. *Applied Catalysis A: General*, 2009. **366**(1): p. 29-43.
97. Frolich, P.K. and D.S. Cryder, *Catalysts for the formation of alcohols from carbon monoxide and hydrogen VI Investigation of the mechanism of formation of alcohols higher than methanol*. *Industrial and Engineering Chemistry*, 1930. **22**: p. 1051-1057.
98. Smith, K.J., R.G. Herman, and K. Klier, *Kinetic modeling of higher alcohol synthesis over alkali-promoted Cu/ZnO and MoS<sub>2</sub> catalysts*. *Chemical Engineering Science*, 1990. **45**(8): p. 2639-2646.
99. Gunturu, A.K., et al., *A kinetic model for the synthesis of high-molecular weight alcohols over a sulfided Co-K-Mo/C catalyst*. *Industrial & Engineering Chemistry Research*, 1998. **37**(6): p. 2107-2115.
100. Phillips, S., et al., *Thermochemical Ethanol via Indirect Gasification and Mixed Alcohol Synthesis of Lignocellulosic Bioma*, NREL/TP-510-41168. 2007.
101. Sun, Y.H., et al., *A short review of heterogeneous catalytic process for mixed alcohols synthesis via syngas*. *Catalysis Today*, 2009. **147**(2): p. 133-138.
102. Muramatsu, A., T. Tatsumi, and H.O. Tominaga, *Active species of molybdenum for alcohol synthesis from CO-H<sub>2</sub>*. *Journal of Physical Chemistry*, 1992. **96**(3): p. 1334-1340.
103. Gang, L., et al., *Synthesis of mixed alcohols from CO<sub>2</sub> contained syngas on supported molybdenum sulfide catalysts*. *Applied Catalysis A: General*, 1997. **150**(2): p. 243-252.
104. Roberts, G.W. and X.L. Sun, *Synthesis of higher alcohols in a slurry reactor with cesium-promoted zinc chromite catalyst in decahydronaphthalene*. *Applied Catalysis a-General*, 2003. **247**(1): p. 133-142.
105. Liu, Z.Y., et al., *Screening of alkali-promoted vapor-phase-synthesized molybdenum sulfide catalysts for the production of alcohols from synthesis gas*. *Industrial & Engineering Chemistry Research*, 1997. **36**(8): p. 3085-3093.
106. Woo, H.C., et al., *Structure and distribution of alkali promoter in K/MoS<sub>2</sub> catalysts and their effects on alcohol synthesis from syngas*. *Journal of Catalysis*, 1993. **142**(2): p. 672-690.
107. Woo, H.C., et al., *Room-temperature oxidation of K<sub>2</sub>CO<sub>3</sub>/MoS<sub>2</sub> catalysts and its effects on alcohol synthesis from CO and H<sub>2</sub>*. *Journal of Catalysis*, 1992. **138**(2): p. 525-535.
108. Koho, K.T., *Ethanol*, 1982, Mitsubishi Chemical, JP patent 57080334

## 2 EXPERIMENTAL SETUP: CATALYST SYNTHESIS & EVALUATION

### 2.1 REACTOR UNIT

The tubular reactor system (Fig 2.1) was purchased from Parr Instrument Co with a provision to be used as a vapor phase fixed bed or a trickle bed reactor system. Reactor system is controlled with modular-based controllers, with two control units: a Parr 4843 and Parr MFC control. The former controls the furnace temperature and provides readouts from a 3-point thermocouple within the reactor and a pressure transducer; the latter is for controlling two Brooks Mass Flow Controllers (MFC), model SLA 5850, one for carbon monoxide (CO) and other for hydrogen (H<sub>2</sub>).

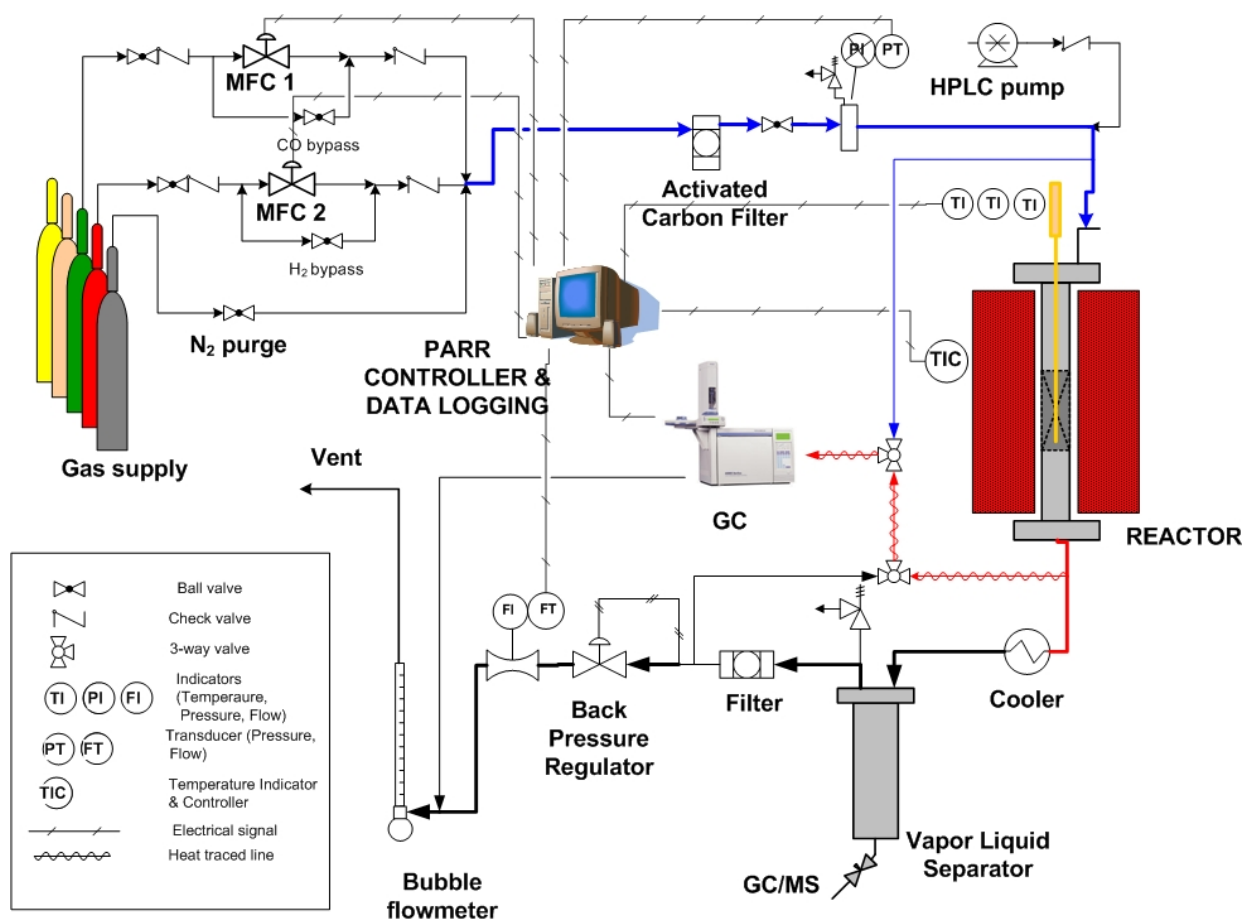


Figure 2-1 Flowsheet description of catalytic testing unit



A SSI injection pump (HPLC) with a head pressure of 2,000 psi and a feed rate range of 0.01-9.99, cm<sup>3</sup>/min, can be used for liquid injection into the reactor feed (to study the influence of recycle of alcohols).

Figure 2-1 Flowsheet description of catalytic testing unit describes a schematic diagram of the fixed bed reactor setup, whereas Figure 2-2 Actual view of the fixed bed system is an actual image of the setup, enclosed in a custom-made fume hood.

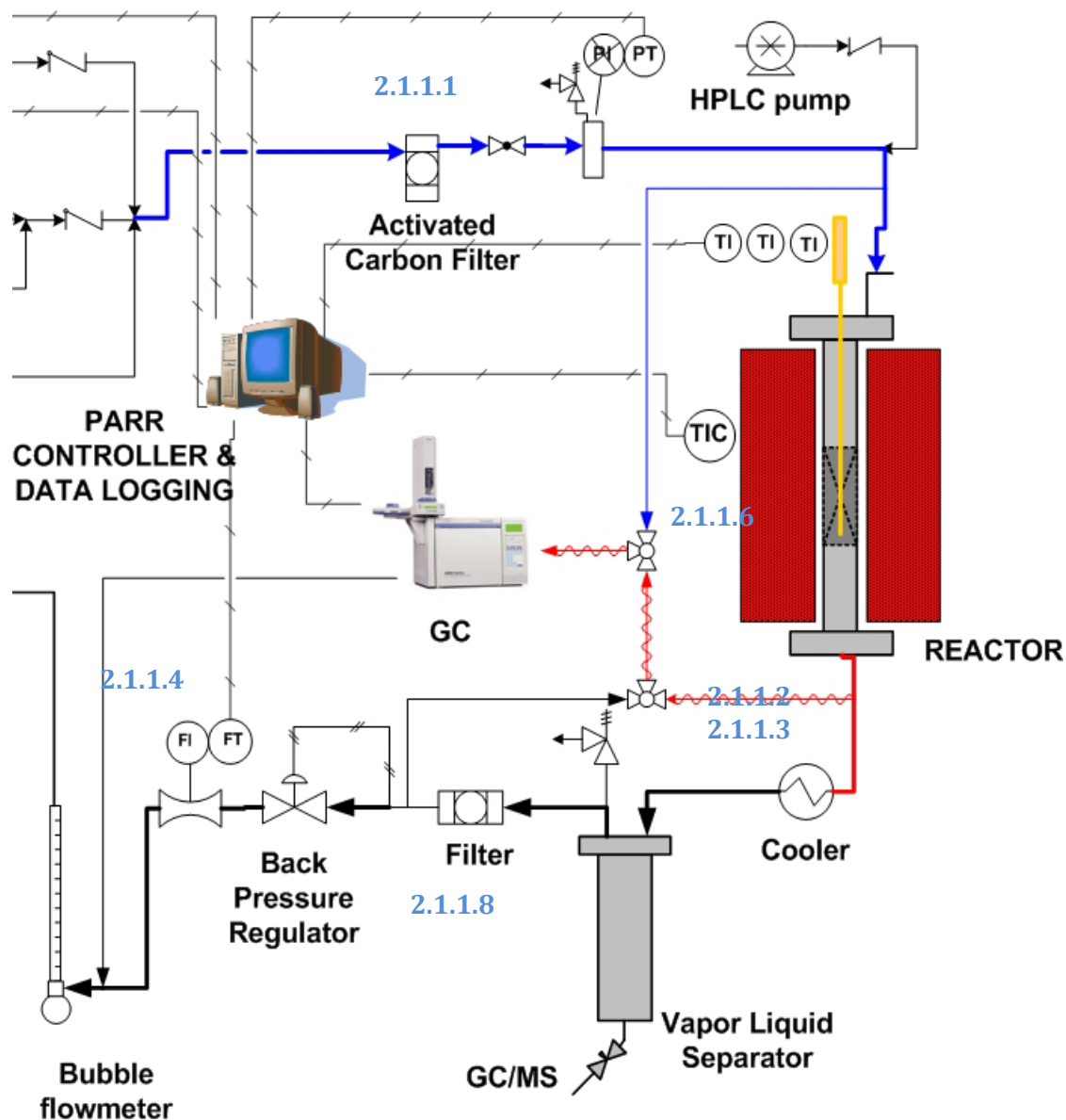


*Figure 2-2 Actual view of the fixed bed system*



## 2.1.1 MODIFICATIONS TO ORIGINAL REACTOR SET-UP

Several modifications were made to the original system to achieve reliable data, especially to account for an overall carbon balance ( $\pm 15\%$ ). Modifications made are highlighted in Figure 2-3 and discussed subsequently.



### 2.1.1.5

Figure 2-3 Reactor Setup with modifications highlighted, as described in section 2.1.1

### 2.1.1.1 Activated Carbon filter

In order to remove trace impurities in the feed gases, carbon filters were installed through which the gas stream can be passed. Carbon monoxide sources are known to contain iron and nickel carbonyls<sup>[1]</sup> which may adversely affect the catalyst performance. Hence it was thought important to remove these impurities by adsorption on an activated carbon filter. A high pressure cartridge based filter (Matheson TriGas 450B) was installed before the reactor inlet.

### 2.1.1.2 Analysis of Volatile Components

The majority of the liquid products over MoS<sub>2</sub> catalysts are expected to be C<sub>1</sub>-C<sub>3</sub> alcohols, which are low boiling compounds (boiling point < 100 °C). This implies that they exhibit a significant vapor pressure (Figure 2-4 ). Thus their separation by condensation at room temperature may not be quantitative.

A sample calculation, based on P<sub>vp</sub> vs. T correlation<sup>[2]</sup>, shows what temperatures are required for successful quantitative separation of methanol from the gaseous stream:

$$\ln\left(\frac{P_{vp}}{P_c}\right) = \frac{1}{(1-T_{vp})} \left[ A \times T_{vp} + (B \times T_{vp})^{1.5} + (C \times T_{vp})^3 + (D \times T_{vp})^6 \right] \quad (2-1)$$

$$\text{where } T_{vp} = 1 - \frac{T}{T_c}$$

$P_c$  = critical pressure, bar

$T_c$  = critical temperature, ° K

$P_{vp}$  = vapor pressure, bar

$T$  = temperature, ° K

$A, B, C, D$  = correlation coefficients

At room temperature (25°C), the vapor pressure of methanol is **0.17 bar**. Based on total alcohol selectivity (CO<sub>2</sub> inclusive) of 60%, this corresponds to a CO conversion of 28%. **Thus at 28% conversion, none of the methanol should be collected in a condenser / separator operating at room temperature.** At -10°C, methanol's P<sub>vp</sub> is **0.02 bar**. At reaction conditions as above, i.e. 28% CO conversion, about **88%** of the methanol can be condensed and separated

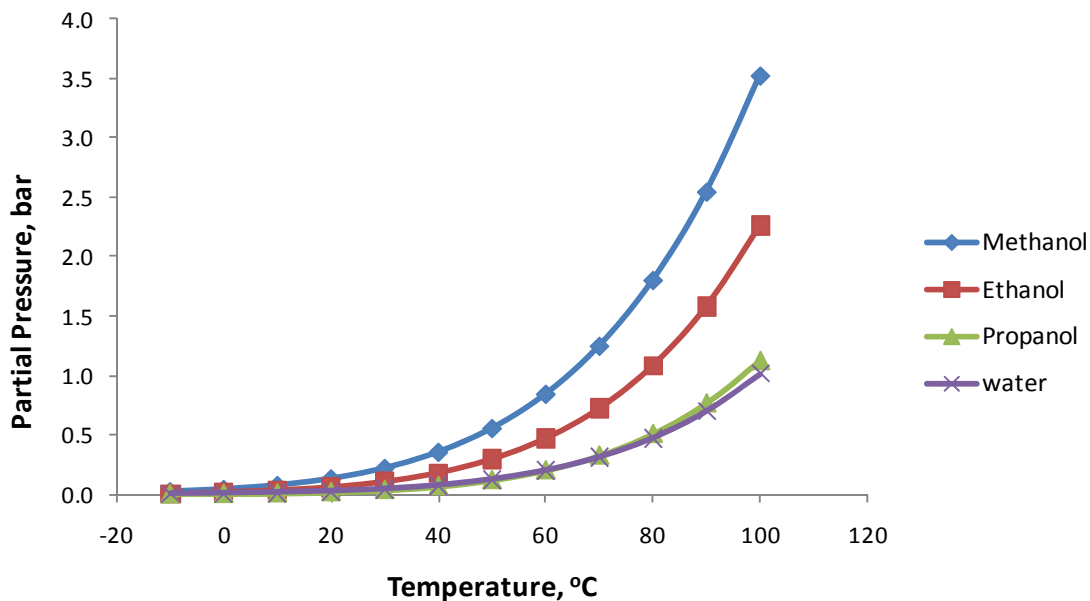


Figure 2-4 vapor pressure trends for linear  $C_{1-3}$  alcohols and water<sup>[3]</sup>

Even at reduced temperatures (-10 °C) successful quantitative separation of alcohols is not achieved. This can partly be due to the inefficiency of the condenser system (heat exchanger).

Another problem is the size of the vapor-liquid separator; its volume is 12 times that of the **empty** reactor volume. Another calculation shows that depending upon the conditions of typical operation (~ 1300 psi, 300 °C), equivalent atmospheric volumes that the system holds will be 45 times the original. Thus, normalized capacity is 27,000 ml compared to the actual volume of 600 ml. With typical gas phase flow rates of 200 ml/min, there would be a delay of 2¼ hrs for the separator exit gases to register the same steady state concentrations that are at the exit of the reactor. Practically, it did take more than 2 hours to achieve the same steady state at the separator exit as was before at the reactor exit.

Such a big reservoir was not needed for liquid products but for a solvent, if the reactor system was operated as a trickle bed reactor. Problem was solved later by filling the separator with inert material to reduce its volume.

These two problems indicated that quantification based on liquid collection would be problematic. It was thought appropriate to analyze all the gases and products in the gas phase, by maintaining the temperature above the condensation temperatures.

### **2.1.1.3 Analysis at reactor exit**

Solution to the above problems required online analysis of the permanent gases, usually done using a Thermal Conductivity Detector (TCD), and the volatile components (Flame Ionization Detector, FID). The advantage of having online gas phase analyses of both permanent gases and volatiles are many and obvious:

- no liquid collection
- no liquid flow rate measurement required for exit stream
- no separate runs in a different GC for liquid phases analyses.

To maintain the products as gases and avoid condensation, the sampling lines were heated to 150 °C using heating tapes and insulating tapes. Configuration of two different columns running simultaneously under a common oven heating program are discussed in **section 2.2.3**

Liquid was still collected and analyzed to detect any new compounds, crosscheck the accuracy of the gas phase GC and confirm the alcohol productivity of the catalyst.

### **2.1.1.4 Exit Flowrate Measurement**

No instrument was provided in the reactor set-up for reactor exit flow rate measurement. Measurement of exit gas phase flow rate is required for accurate evaluation of the material balance. This is because conversion is based on concentration and flow rate measurements and an internal standard is not utilized. The conversions can be more than 10% under certain conditions; a significant volume reduction dictates accounting on molar flow rate basis.

Omega FMA 1820 mass flowmeter was installed downstream of the pressure regulator for measurement of the exit gas flow rate. The analog output (0-4 volts) was connected to a National Instruments compact field point device and the signal was recorded through LabVIEW.

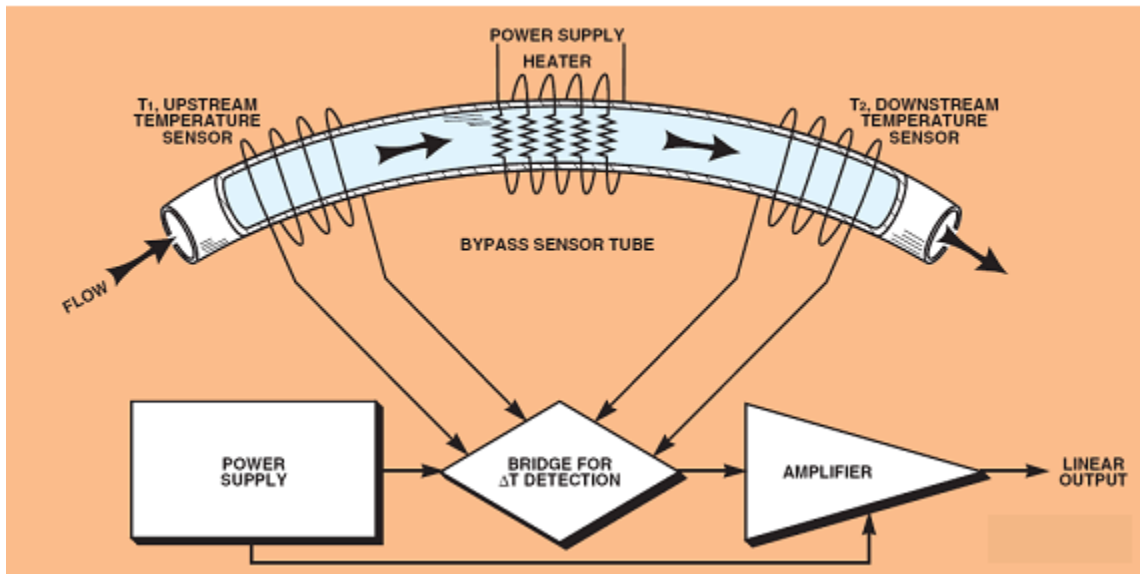


Figure 2-5 working principle of a mass flow meter

The operating principle of mass flow meter is dependent upon the type of gas (specific heat) and not the pressure and temperature. For ease in calculation, a dimensionless K-factor is used to represent the thermodynamic properties of the gas. As the reactor exit gas stream will consist of a mixture of gases, a weighted ‘K factor’ would be needed, which is a function of individual gas phase concentrations. The concentrations would be available as the exit stream is analyzed any way. The working principle of the flow meter is represented in *Figure 2-5* and according to the equations given below:

$$Q_s = \dot{m} / \rho_s \quad (2-2)$$

$$Q_s = \text{volumetric flowrate} \quad \dot{m} = \text{mass flowrate} \quad \rho = \text{gas density}$$

As a flow meter is calibrated to a particular reference gas, use for any other gas needs normalized values, or the K-factor to obtain reliable flow measurement:

$$K = \rho.C_p \quad (2-3)$$

$K$  = correction factor;  $\rho$  = gas density;  $C_p$  = coefficient of specific heat

$$Q_s = Q_r \cdot \frac{K_r}{K} \quad (2-4)$$

$$K \text{ when weighted,} = \sum_{i=1}^{n=\text{no. of gases}} K_i . n_i$$

Literature reports ‘K’ values for known gases <sup>[4]</sup>. However, this technique seldom provided accuracy in the ranges of  $\pm 5\%$ , as claimed by manufacturer literature. Inaccuracies even ranged to the extent of  $\pm 25\%$ , and this much variation can give erroneous mass balance calculations.

#### 2.1.1.5 Bubble flowmeter

As the mass flow meter could not provide accurate readings for the mixture of gases in exit stream, based on the ‘K-factor’ correlation, a soap bubble flow meter was used to calibrate the mass flow meter as well as to record the flow rates directly.

#### 2.1.1.6 Separate Exit Sampling

To alter between the sampling downstream of separator OR reactor exit, a 3-way valve was installed. Another 3-way valve was used to channel sampling to either reactor inlet OR outlet from the reactor. These 2 sets of valves provided following gas sampling options:

- Reactor Inlet
- Reactor Outlet (before condensation/separation)
- Reactor Outlet (after condensation/separation)

Reactor Inlet sampling was necessary because CO and H<sub>2</sub> were mixed online. The inlet concentrations did not always correlate exactly to the volume % mixing rules. The mass balance is sensitive to flow rate and concentrations (to lesser extent), as an internal standard is not used.

### 2.1.1.7 Heat Tracing

Reactor exit sampling line is heat traced to prevent local condensation of volatiles in the lines. Although, the starting temperature of the GC oven is at 100 °C and the switching valves are placed within the GC oven, more reproducible results were obtained with heat traced sampling lines.

### 2.1.1.8 Filter

Since the Back Pressure Regulator (BPR) is sensitive to liquid or solid particles, a grit based filter (15 micron) was installed at it's upstream.

## 2.1.2 CALIBRATION CURVES FOR MASS FLOW CONTROLLERS

As the flow meters were factory calibrated for their respective gases (CO and H<sub>2</sub>), their readings were not far off. The meters were re-calibrated from time to time to ensure accurate measurement. Sample curve for CO in Figure 2-6 shows that the curve is linear, albeit offset from the origin.

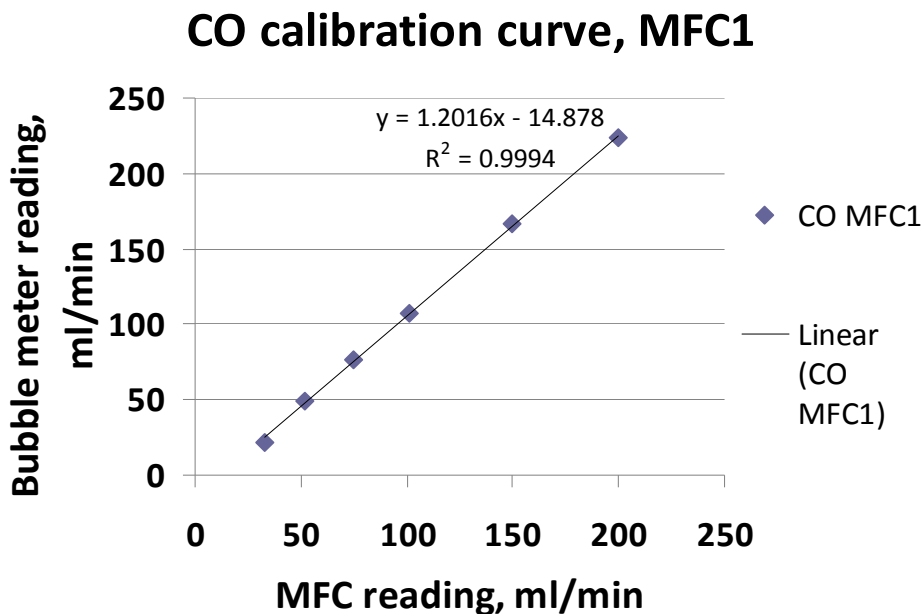


Figure 2-6 Calibration curve used for carbon monoxide's MFC

## 2.2 CHROMATOGRAPHY

### 2.2.1 LIQUID SAMPLING

An Agilent GC 7890 with automatic liquid injection (Agilent 7683B series) was used for quantitative analysis of liquid samples and Agilent Chemstation (B.03.02) software used for control and analysis. Method configuration is as follows:

Parameters	SUPELCOWAX 10
Column	30m * 0.32 mm * 0.25µm film thickness
Oven	35°C (hold for 5 min) ramp 20°C/min to 200°C (hold for 15 min)
Detector	FID
Carrier gas	Helium, 2 ml/min (const. flow mode)
Injection	1µL, split 30:1

*Table 2-1 Configuration of GC used for offline liquid analysis*

The column was powerful in separation of aliphatic alcohols and C<sub>1</sub>-C<sub>5</sub> alcohols were calibrated. For quantitative analysis of these alcohols, 3-point calibrations were performed. Quantification was performed based on volume % as well as molar concentrations. Volume % quantification was particularly useful in conforming accuracy of gas phase analysis of volatiles by online gas sampling GC; the values are found to be in agreement with ± 10% accuracy. A Sample chromatogram is presented in Appendix 3



### 2.2.2 GAS SAMPLING

As discussed in Analysis at reactor exit, the GC analysis was used with two objectives:

- Separation of permanent gases
- Analysis of oxygenates and hydrocarbons

Some of the difficulties in having a GC configuration convenient for both purposes were:

- **Temperature:** Separation of nitrogen from carbon monoxide is critical on most packed columns and typically requires low temperatures, if not cryogenic. On the other hand, as up to C<sub>5</sub> components were to be separated on the FID, a higher temperature is required for elution of higher boiling compounds within a reasonable time limit.
- **Water:** Although the water content at the reactor exit (3-6%) was not high due to the active water gas shift tendency of MoS<sub>2</sub> based catalysts, this would not be true for catalysts of other families. Therefore, both columns should be insensitive to water.
- **C<sub>3</sub>-C<sub>6</sub> hydrocarbons:** Their concentrations are lower and thus a dependable reading could not be obtained on the TCD, as its sensitivity would be too low. On the FID, a polar column would be used (for separation of alcohols), but generally alkanes < C<sub>6</sub> co-elute as a single peak. Thus, a column with intermediate polarity would be needed, which could resolve compounds based on their boiling points

A successful combination was obtained and the method developed is described below in Table 2-2. Notice that a packed column is used with FID detector. Capillary columns are known to have far better resolution power, but their implementation was limited due to lack of a split injector on the GC. A split injector can split the sample to be analyzed, effectively diluting the amount being injected onto the column, to avoid saturation of the column.

Parameters	Column 1	Column 2
Column	60/80 Carboxen 1000 (packing material: carbon molecular sieve) (4.5mx2.1 mm) film thickness 0.50 $\mu\text{m}$	Haysep DB (packing material: Divinylbenzene) (2.5mx3.1mm) film thickness 0.25 $\mu\text{m}$
Oven	100°C (hold for 8 min) - then ramped 30°C/min to 200°C (hold for 14 min)	
Run time	26 min	
Detector	TCD (250°C)	FID (275°C)
Carrier gas	He (50 sccm)	He (35 sccm)

*Table 2-2 GC method used for gas sampling*

Later, a technique was developed whereby the sample loop capacity was reduced from the original and a PLOT-Q (25m \* 0.53mm ID) column was used. This is an intermediate between a packed column and a capillary column and produced better separation than the HaySep DB .

#### **2.2.2.1 Sampling technique and issues**

As shown in Figure 2-1, sampling lines were heated all the way to the GC, the temperature in the GC being always >99 °C. Thus, chances of liquid product condensing within sampling lines were prevented.

A needle valve was used to allow the necessary flow through the GC sampling loop. Within the GC, a 10-way valve provided automatic switching between sampling and analysis. During calibration and analysis, the conditions were kept exactly the same. Two variables in particular could cause significant errors in analysis:

**Flow Rate:** It is recommended to let the sample loop equilibrate with atmospheric pressure before sampling. For online runs, a stream of reactor outlet gas is continuously sampled, thus it's not always convenient to manually stop the flow and let the gas equilibrate. The sampling line is of 1/16" dia and hence, allowing a higher flow rate would buildup backpressure within the loop. This means that the

pressure within the sampling loop would correspondingly increase and be higher than atmospheric. According to the ideal law (Eg 2-5), number of moles is proportional to pressure. As the GC is calibrated for molar concentrations (at atmospheric pressure), any increase in the number of moles due to increase in backpressure will lead to calculation errors. Note that the mole % of each component would not change. If the GC result is calibrated based on area percent, there would not be an error.

**Higher flowrate ~ higher backpressure ~ increased moles in loop ~ erroneous results**

Thus the flow rate is kept at 10-20 ml/min to minimize variation in analysis

**Temperature:** Increasing temperature of the sampling lines was necessary to prevent condensation as mentioned before. It was seen that at lower temperatures, the liquid products produced lower peak areas. The reasoning is unknown, this trend is opposite to theoretical

$$pV = nRT \quad (2-5)$$

It could be argued that lower temperature might allow some condensation and lower the gas phase concentrations, but such pockets were never observed.

### **2.2.3 CALIBRATION METHODOLOGY AND UNITS**

Rigorous calibration was performed for majority of the products of interest to achieve quantitative analysis. Gas phase calibration samples of volatiles/liquids were prepared according to the method depicted in Figure 2-7.

A metered amount of liquid was injected into a known gas flow rate of nitrogen. Sufficient pipe length was provided to ensure mixing and the mixing length was also heated to temperatures of 150 °C, right up to the injection port of the GC. Molar concentrations were calculated and the peak areas were calibrated against these standard concentrations. Multiple readings were taken for a single calibration/standard to ensure reproducibility.

Calibration of gases was more straight-forward. Samples purchased from Suppelco etc. for standard gas mixtures with known compositions were simply injected onto the GC through the gas sampling valve and the known volume % or mole% was correlated against the peak area.

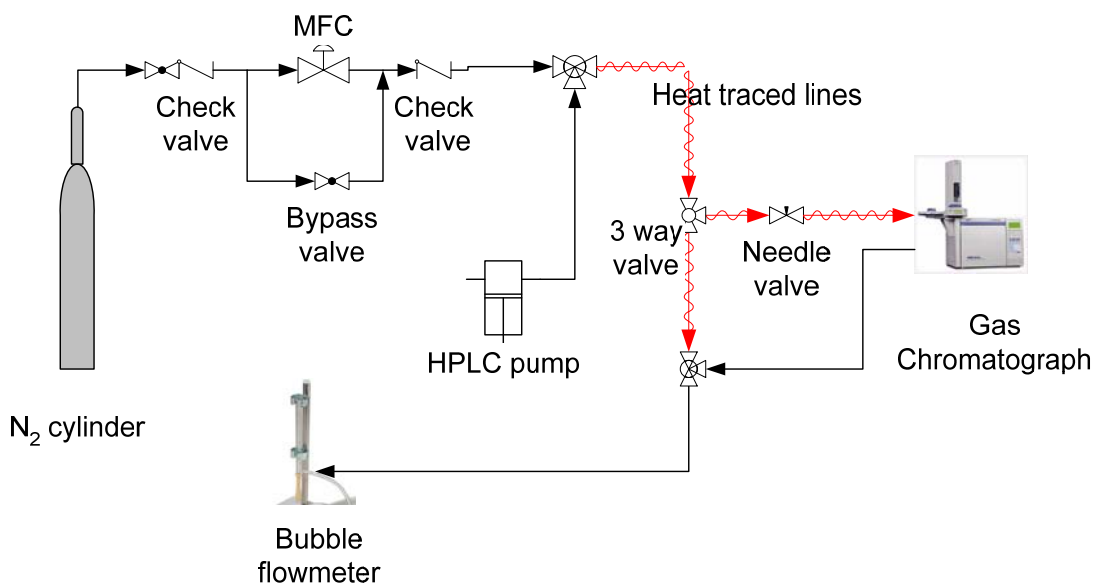


*Figure 2-7 Preparation of samples for gas phase calibration of volatile / liquid components*

For quantification purposes, the calibration table within the GC analysis software (EZStart 7.2) was utilized. Calibration units were mol/m<sup>3</sup> as the mass balance was on a molar basis. A sample Excel sheet is attached as Appendix 4 which shows calculation of these molar standards. Appendix 1 shows the calibration curve and the goodness of fit as determined by the software.

## 2.3 FIXED BED REACTOR ASSEMBLY AND LOADING

A general schematic of the whole reactor system is presented in Figure 2-1 and described in section Reactor Unit.

### 2.3.1 DIMENSIONS AND THERMOCOUPLE LOCATION

The fixed bed unit is shown below in Figure 2-8. The reactor tube consists of welded free machined components. The top and bottom heads are sealed with graphite gaskets, capable of withstanding 500 °C. The heads are secured and compressed by ‘split ring assembly’, typical of Parr Autoclaves. The reactor unit has the following characteristics (maximum limits):

Temperature, °C	500
Pressure, bar	100
Gas Flow Rate , Liter/min	4
Catalyst volume, cm <sup>3</sup>	50
Liquid injection, cm <sup>3</sup> /min	4
Bed height, inch	4
Bed OD, inch	1

Three **fixed** thermocouples are located within a thermowell and can read across the bed height. As typically 3-5 grams of catalyst are loaded un-diluted, only 10-20% of the bed height is occupied by the catalyst. Thus, the catalyst is loaded such that the BOTTOM thermocouple just protrudes from the catalyst bed. Depending upon the amount of catalyst loading and its packed density, the MIDDLE thermocouple may or may not be covered by the catalyst. The locations of the three thermocouples, starting from the bottom tip of the thermowell and moving upwards, are:

BOTTOM :	0.00" (at the tip)
MID:	1.25"
TOP:	2.75"

### **2.3.2 CATALYST LOADING TECHNIQUE**

Before loading, the final catalyst is ground in a mortar and pestle to ensure intimate mixing of the catalytic components in addition to reducing the size of the catalyst. Catalyst was sieved through a US mesh 120 and retained on a 170 mesh. The particle size distribution of the loaded catalyst is thus **0.125 –**



**0.089 mm.** Catalyst was introduced from the bottom of the reactor with the reactor in an inverted position. Volume of the inert silicon carbide packing was adjusted so that the tip of the thermocouple is covered by the catalyst bed; this is the location of the bottom thermocouple. Requirement of inert was calculated simply based on the packed density of the inert itself (constant) and the catalyst being loaded (variable). Thus, knowing how much volume of catalyst is to be loaded, corresponding amount of silicon carbide was weighed and charged to fill the bed volume. Glass wool and stainless steel (SS 314) wire gauzes were used to hold the catalyst bed in place.

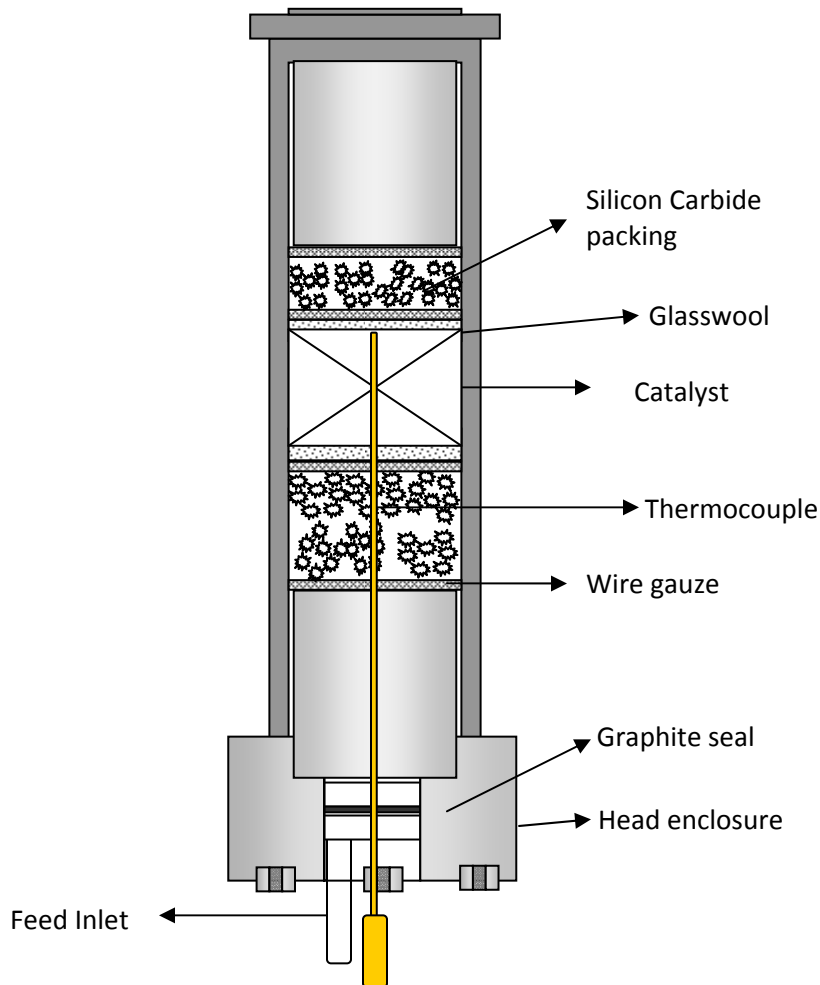


*Figure 2-9 Cross sectional view of inverted fixed bed reactor assembly, with catalyst loaded*

### 2.3.3 SALVAGING USED CATALYST

Both molybdenum and cobalt are pyrophoric in their reduced forms and hence safety precautions were necessary in the handling of used catalyst. It was seen that the catalysts giving high conversions, showed pyrophoric features in open atmosphere after the reaction. Mo and Co are loaded as sulfides, but they can be reduced to the atomic state during reaction conditions. Because hydrogen is one of the reacting components, any hydrogen chemisorbed on the catalyst surface will rapidly oxidize on contact with air and produce hot spots.

At the end of a catalyst testing run, the reactor is de-pressurized slowly and nitrogen is passed through the catalyst bed overnight. Generally, the reactor is not cooled down per se; merely the supply of heat is stopped. This ensures a very slow cool down of the reactor and allows flowing nitrogen to be more effective in removing the adsorbed species (note that generally, physisorbed species are more easily removed at higher temperatures, e.g. Pressure Swing Absorption-PSA). After that, a 1% O<sub>2</sub> in N<sub>2</sub> mix is passed through the reactor, usually at a flow rate corresponding to 50 cc/min for every gram of catalyst for 2-3 hours. Passivation with a 1% O<sub>2</sub>/N<sub>2</sub> mixture is an effective way of retaining catalyst activity.

Catalyst with and without this passivation procedure were re-tested to see if they would regain their initial activity. For the un-passivated catalyst, some surface oxidation and hot spots would occur on exposure to air. When loaded again, reduced and tested, the alcohol activity achieved was lower than the previous activity. For the properly passivated catalyst, the activity was similar to the steady state activity of fresh catalyst when it was loaded.

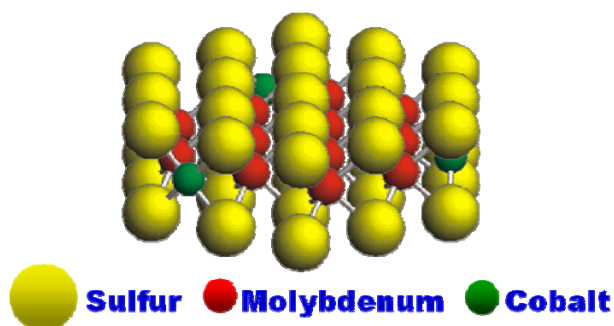
Removal of catalyst is done by first clearing out the inert material (silicon carbide) from the top and the bottom beds. The catalyst is then dislodged and collected. It is weighed and preserved under a N<sub>2</sub> atmosphere. Typically, only 0.1-0.2 g of catalyst is lost if the recovery is performed cautiously.



## 2.4 CATALYST SYNTHESIS

The objective of the present thesis was to investigate the catalytic performance of MoS<sub>2</sub> family of catalysts in syngas conversion to alcohols and understand the role of catalyst synthesis, promoters and co-catalysts as well as the influence of reaction conditions (e.g. CO/H<sub>2</sub> pressure, temperature, recycle methanol in feed ).

Several sulfided catalyst formulations were prepared. Most of the promoters, other than the alkali, K<sub>2</sub>CO<sub>3</sub>, were also in their sulfided forms. MoS<sub>2</sub> itself has a very structured geometry (trigonal prismatic) and the promoters are incorporated within the



MoS<sub>2</sub> matrix <sup>[5]</sup>. Excessive amounts of co-promoter metal are not effective because they will form their own bulk sulfides, which are not effective in HDS <sup>[6]</sup> or HAS <sup>[7]</sup>. For cobalt the optimum co-promoter loading is at Co/Mo < 0.5. Below this ratio, Co is present as a Co-Mo-S phase <sup>[8]</sup>. At higher ratios, Co<sub>9</sub>S<sub>8</sub> can form, which is not active for alcohol synthesis and does promote hydrocarbon formation <sup>[7]</sup>. The ratio can also significantly affect the structure of the final catalyst <sup>[9]</sup>.

Sulfided catalysts can be prepared in two methods, their advantages and disadvantages are discussed accordingly:

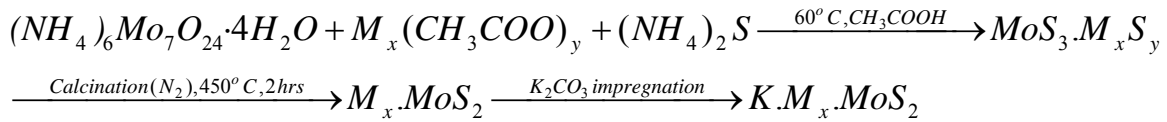
### 2.4.1 PRE-SULFIDED FORM

A sulfiding agent can be used which provides the necessary sulfur to form the sulfide materials insitu during the wet-synthesis process, e.g. H<sub>2</sub>S, (NH<sub>4</sub>)<sub>2</sub>S, DMSO. The resulting amorphous precursor, ammonium thiomolybdate (NH<sub>4</sub>)<sub>2</sub>MoS<sub>4</sub> (ATM) or its variant, is calcined to give the final MoS<sub>2</sub> based material as a precursor for synthesis of most of the catalysts. In our

research, this technique has been used for the synthesis of MoS<sub>2</sub> based materials, the characteristics of which are:

1. A particular advantage is that this procedure gives good yields of sulfides from the precursor salt and ensures complete sulfidation.
2. One of the major disadvantages is if this sulfided precursor is not supported, it will result in a poor dispersion and lower surface area. However, when the sulfide precursor material is deposited onto a support and then calcined, researchers have shown better catalytic activity for HDS when compared to the oxide precursors [9-10].
3. For comparing the effect of supports, it was deemed necessary to have a consistent batch of active materials, so that one can combine the same catalyst with different supports and effect the metal-support interaction by physically mixing the two.
4. Physical handling of liquid sulfiding agents and avoiding use of H<sub>2</sub>S gas in calcinations step also offer significant advantages with respect to safety and environmental concerns.

General outline of the synthesis process is described as follows:



where M= Co, Ni, Cu or Rh

(2-6)

#### 2.4.1.1 Synthesis and decomposition of Precursor ATM

The first step in catalyst synthesis is usually the synthesis of precursor ammonium thiomolybdate (NH<sub>4</sub>)<sub>2</sub>MoS<sub>4</sub> (ATM), which is obtained by reacting ammonium heptamolybdate (NH<sub>4</sub>)<sub>6</sub>Mo<sub>7</sub>O<sub>24</sub>·4H<sub>2</sub>O (AHM) with ammonium sulfide (NH<sub>4</sub>)<sub>2</sub>S at 60°C. Generally, the AHM is dissolved in at least a 100 cm<sup>3</sup> solution.

If only MoS<sub>2</sub> is the desired product, then the above solution can be refluxed further or acidified with acetic acid, to give a brownish-reddish precipitate. If a co-promoted catalyst is required, then the ATM mixture from the above solution is added drop wise along with the other precursor acetate salt (100-200 cm<sup>3</sup>), into a solution containing 30% acetic acid at 60°C. The acetic acid can provide the necessary common ion effect to force the cation out of the solution and form the sulfide. It is assumed that the co-precipitation would help in formation of M-Mo-S species as opposed to independent sulfide species.

The precipitate is vacuum filtered and washed a couple of times. It was observed that some of the cobalt acetate washes out and hence the cobalt is not all sulfided. Iranmahboob<sup>[11]</sup> also reported a similar result. They determined that to obtain a Co/Mo=0.5 ratio, they needed a starting ratio of Co/Mo=1 in the preparation materials.

A typical synthesis procedure involves back-calculation of amount of MoS<sub>2</sub> desired. 28.25 g of AHM was dissolved in 100 cm<sup>3</sup> of water at 60°C. To this mixture, 100 cm<sup>3</sup> of a 44% (NH<sub>4</sub>)<sub>2</sub>S solution was introduced as the sulfiding agent and the reaction was carried out for an hour. 19.92g of cobalt acetate (Co(CH<sub>3</sub>COO)<sub>2</sub>·4H<sub>2</sub>O) was dissolved in a 100 cm<sup>3</sup> solution at 60°C. The cobalt and molybdenum solutions were added drop wise into a 200 cm<sup>3</sup> solution of 30% acetic acid. The solution was agitated for two hours at 60°C. After filtration and overnight drying, 40.81 g of amorphous material was obtained. On calcination, ~ 25g of MoS<sub>2</sub> based material was obtained. The reduction in weight corresponded to the conversion of ATM to MoS<sub>2</sub>: 61.5% weight reduction. The calculation was based on 26g of MoS<sub>2</sub> material.

#### **2.4.1.2 pH controlled ATM synthesis**

When pH of the liquor is changed to acidic, the supersaturation increases and MoS<sub>3</sub> precipitates out. As the nuclei formation is accelerated, the final state of the sulfide is somewhat aggregated and non-homogenous<sup>[12]</sup>. In an alternative procedure, the liquor is aged at a medium

pH range 6.0-6.5 for about 4 hours. All the synthesis steps are similar as presented before in 2.4.1.1. The pH is adjusted by acetic acid and ammonium hydroxide addition. 0.5-1.0g of glycerin is also added to promote a gel like solution and inhibit flocculation. The precipitate is filtered and washed in a similar manner as above.

#### **2.4.1.3 Chelated synthesis of ATM**

Although the pH procedure produced a slightly better (homogeneous size distribution) MoS<sub>2</sub> material; for Co-MoS<sub>2</sub> type catalyst, such homogeneity in shape and size could not be reproduced. There have also been reports and expectations that nano-sized MoS<sub>2</sub> particles would perform better<sup>[13-14]</sup>. Fang reported that *smaller crystallites* promote alcohol formation whereas *larger crystallites* promote alkanes<sup>[15]</sup>. A modified procedure employed the use of a chelating agent for producing Rh-MoS<sub>2</sub> type catalyst. The method is a significant modification to the methods used by Inamura<sup>[16]</sup> and Sugimoto<sup>[17]</sup>, used for synthesis of chelated HDS catalysts and uniform CdS particles, respectively. Typically, a 1:1 molar ratio of M (=Mo and Rh) and EDTA is maintained in a solution at 60°C with a pH maintained at 8.5-9.5 by acetic acid and ammonium hydroxide. Molar concentrations were kept < 0.5 mol/liter and a 1wt% of gelatin was maintained. 20% (NH<sub>4</sub>)<sub>2</sub>S is added drop wise into this batch and the liquor is aged to 5 hrs. The precipitate is washed and dried, following the same procedure as described previously (section 2.4.1.1). The alkali of choice is potassium and it is usually impregnated or physically mixed onto the calcined catalyst. If impregnated, the catalyst is again dried overnight at 100°C.

#### **2.4.1.4 Base modified supports**

Framework cations of aluminosilicate materials like clays and zeolites can be ion-exchanged with more basic cations. Procedure of Joshi<sup>[18]</sup> was adapted for this synthesis. Sodium forms of the supports are refluxed with 5 wt % solution of Cl salt of the alkali, e.g. CsCl or KCl

and the amount used is 15 cm<sup>3</sup> per gram of the support. The support is refluxed at 95°C for 12 hours and then washed thoroughly to remove any Cl<sup>-</sup> ions, filtered and dried overnight.

#### 2.4.1.5 Calcination Procedure

The calcinations procedure is the same for all catalysts prepared, as the aim is to develop MoS<sub>2</sub> from a mixture of ATM and MoS<sub>3</sub>.



A tube furnace is used to provide an inert atmosphere for calcination. The material is loaded in multiple boats that fit the furnace. N<sub>2</sub> is passed through the tube for ½ hour before starting the heating program to ensure an inert environment. 100 ml/min of N<sub>2</sub> flow rate is used for 3-5g of material loaded. The tube furnace is a Carbolite horizontal split tube furnace (model HST/12/300) with a Eurotherm PID temperature controller (model 3216). The tube is of refractory material with dimensions of 12" \* 4" O.D. and a maximum operating temperature of 1200°C. The furnace is ramped at 5°C/min to a temperature upto 450 °C and is left at that temperature for 2 hours. The inert atmosphere is maintained until the furnace has cooled down or at least till 100°C.

The transformation of MoS<sub>3</sub> to MoS<sub>2</sub> occurs with significant evolution of heat at high temperatures and extended duration at this temperature can lead to crystal growth <sup>[19]</sup>. On the other hand, an incomplete calcination would produce an amorphous material with lower surface area. Thus, an optimized procedure described by Chianelli et. al. <sup>[20]</sup> is adopted.

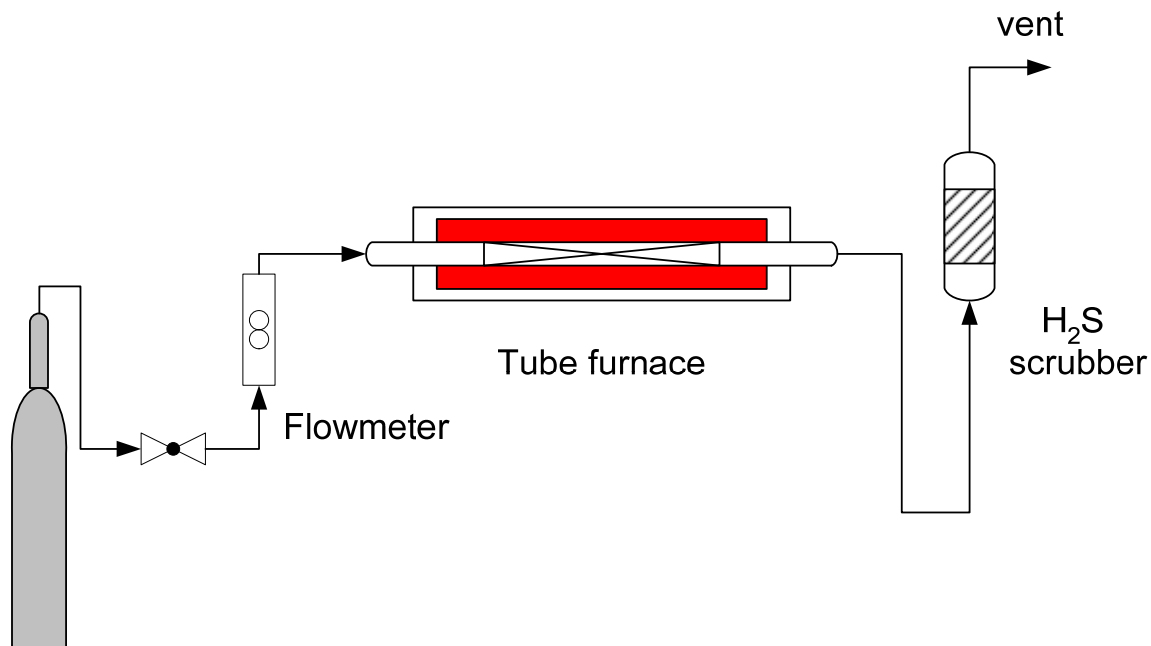


Figure 2-10 Calcination unit based on a tube furnace

#### 2.4.2 HYDROGENATION + SULFIDATION

This is the more conventional method of catalyst preparation, where by the precursors are deposited onto a support and the catalyst is first calcined in air to produce the oxides, which are subsequently converted into the sulfide form <sup>[21]</sup>. The method of addition can be either the simple impregnation techniques or more sophisticated or novel methods that could provide better dispersion of the metal, e.g. sol-gel. Some of the characteristics of this method are:

1. Sulfiding of oxides in a H<sub>2</sub>S/H<sub>2</sub> mixture does not always necessarily produce a completely sulfided catalyst and neither is this a reproducible technique <sup>[22]</sup>.
2. The advantages are that the industry is well versed with this technique and existing procedures/equipment can be utilized if the CoMoS based HAS technology commercializes. In fact, the catalyst synthesis, other than alkali addition, would be exactly similar to existing HDS catalysts as the catalyst components are the same.

3. This synthesis technique also ensures enough catalyst-support interaction, providing stability and dispersion and effective use of support surface area.

## 2.5 CATALYST PERFORMANCE EVALUATION: MATERIAL BALANCE

In evaluation of the catalyst performance, the material balance analysis is crucial to obtain quality data. In this work all the material balance calculations are based on molar flow rates. The conversion is based on carbon balance over the system, which is calculated in two different ways:

$$Conversion_{CO} = \frac{CO_{MF,IN} - CO_{MF,OUT}}{CO_{MF,IN}} = \frac{X_{CO,IN} \cdot F_{IN} - X_{CO,OUT} \cdot F_{OUT}}{X_{CO,IN} \cdot F_{IN}} \quad \text{Eq 2-8}$$

$CO$  = molar flowrate of Carbon Monoxide, mol/min

$X$  = molar concentration, mol/m<sup>3</sup>

$F$  = flowrate, m<sup>3</sup>/min

$$Conversion_{prod} = \frac{\sum n_i \cdot X_i \cdot F_{OUT}}{X_{CO,IN} \cdot F_{IN}} \quad \text{Eq 2-9}$$

Conversion<sub>prod</sub> is based on an accountability of the products seen and effectively checks the resolution power of the GC. Conversion<sub>co</sub> is based on the amount of the CO transformed into products. Other than water, all products are carbon based. However, as majority of the water is removed as CO<sub>2</sub> (strong WGS activity of the catalyst), Conversion<sub>co</sub> provides adequate accountability for the whole system (CO and H<sub>2</sub>).

The accuracy of the mass balance is based on the difference between the two conversions and only results that fall within the ±15% accuracy bracket are presented. Concentrations are recorded by the GC and as described above, the output report is generated in units of mol/m<sup>3</sup>. The exit flow rate is recorded online and is also periodically recorded with a soap bubble flow meter.

The exit flow rate measurement is utilized in both conversion calculations and its accuracy is important to obtain an accurate mass balance.

Selectivity is predominantly reported as CO<sub>2</sub> free selectivity, unless otherwise specified

$$Selectivity_i = \frac{n_i \cdot M_i}{\sum n_i \cdot M_i} \cdot 100 \quad \text{Eq 2-10}$$

$n_i$  = carbon number of 'i' component

$M_i$  = molar flowrate of 'i' component

CO<sub>2</sub> inclusive selectivity is defined as

$$Selectivity_{i,CO_2} = \frac{n_i \cdot M_i}{(\sum n_i \cdot M_i + M_{CO_2})} \cdot 100 \quad \text{Eq 2-11}$$

Yields refer to the productivity of a particular product, reported as '**g/kg catalyst/hr**'. This quantity has become a yardstick for measuring the performance of alcohol synthesis catalysts, especially of MoS<sub>2</sub> types. In the remainder of this text, yield and productivity are used interchangeably. **Appendix 7** depicts a typical exercise for calculating CO conversion, product selectivities and yields for a particular operating condition.

C<sub>2+</sub>/C<sub>1</sub> actually refers to the yield/productivity of all C<sub>2+</sub> alcohols relative to methanol. As current HAS catalysts cannot rival the selectivity or productivity of commercial methanol catalysts, and as higher alcohols are more value-added chemicals, this C<sub>2+</sub>/C<sub>1</sub> ratio can be of particular interest. Also, note that over these catalysts, alcohol chain growth is argued to be rate-determining step <sup>[23]</sup>, thus a higher C<sub>2+</sub>/C<sub>1</sub> ratio can also an appreciable trait amongst these catalysts.

Typically, a catalyst is tested for >40 hours of on-stream operation, over which the operating conditions are varied. A typical report format is attached in Appendix 8.



## 2.6 GLOSSARY

DMSO-Dimethyl sulfoxide

HDS – HydroDe Sulfurization

WGS – Water Gas Shift

FID – Flame Ionization detector

TCD – Thermal Conductivity Detector

GC – Gas Chromatograph

MFC – Mass Flow Controller

## 2.7 REFERENCES

1. Stiles, A.B., et al., *Catalytic conversion of synthesis gas to methanol and other oxygenated products*. Industrial & Engineering Chemistry Research, 1991. **30**(5): p. 811-821.
2. Robert C. Reid, J.M.P., Bruce E. Poling, *The Properties of Gases and Liquids*. 4th ed. 1987: McGraw-Hill Companies.
3. Yaws, C.L. and H.C. Yang, *To estimate vapor pressure easily*, in *Hydrocarbon Processing*. 1989.
4. Omega, *Complete Flow and Level Measurement Handbook and Encyclopedia*. Vol. 29. 1995: Omega press.
5. Chianelli, R.R., *Fundamental-studies of transition-metal sulfide hydrodesulfurization catalysts*. Catalysis Reviews-Science and Engineering, 1984. **26**(3-4): p. 361-393.
6. Prins, R., V.H.J. Debeer, and G.A. Somorjai, *Structure and function of the catalyst and the promoter in co-mo hydrodesulfurization catalysts*. Catalysis Reviews-Science and Engineering, 1989. **31**(1-2): p. 1-41.
7. Li, Z.R., et al., *Effect of cobalt promoter on Co-Mo-K/C catalysts used for mixed alcohol synthesis*. Applied Catalysis a-General, 2001. **220**(1-2): p. 21-30.
8. Topsoe, H., et al., *Recent basic research in hydrodesulfurization catalysis*. Industrial & Engineering Chemistry Fundamentals, 2002. **25**(1): p. 25-36.
9. Inamura, K. and R. Prins, *The role of Co in unsupported Co-Mo sulfides in the hydrodesulfurization of thiophene*. Journal of Catalysis, 1994. **147**(2): p. 515-524.
10. Sundaramurthy, V., A.K. Dalai, and J. Adjaye, *Tetraalkylthiomolybdates-derived Co(Ni)Mo/gamma-Al<sub>2</sub>O<sub>3</sub> sulfide catalysts for gas oil hydrotreating*. Journal of Molecular Catalysis a-Chemical, 2008. **294**(1-2): p. 20-26.
11. Iranmahboob, J., D.O. Hill, and H. Toghiani, *K<sub>2</sub>CO<sub>3</sub>/Co-MoS<sub>2</sub>/clay catalyst for synthesis of alcohol: influence of potassium and cobalt*. Applied Catalysis a-General, 2002. **231**(1-2): p. 99-108.
12. Haruta, M., et al., *Preparation and properties of colloidal spherical particles of molybdenum and cobalt sulfides*. Journal of Colloid and Interface Science, 1984. **101**(1): p. 59-71.
13. Koizumi, N., et al., *Development of sulfur tolerant catalysts for the synthesis of high quality transportation fuels*. Catalysis Today, 2004. **89**(4): p. 465-478.
14. Subramani, V. and S.K. Gangwal, *A review of recent literature to search for an efficient catalytic process for the conversion of syngas to ethanol*. Energy & Fuels, 2008. **22**(2): p. 814-839.
15. Sun, Y.H., et al., *A short review of heterogeneous catalytic process for mixed alcohols synthesis via syngas*. Catalysis Today, 2009. **147**(2): p. 133-138.
16. Inamura, K., et al., *Preparation of active HDS catalysts by controlling the dispersion of active species*. Applied Surface Science, 1997. **121**: p. 468-475.
17. Sugimoto, T., S.H. Chen, and A. Muramatsu, *Synthesis of uniform particles of CdS, ZnS, PbS and CuS from concentrated solutions of the metal chelates*. Colloids and Surfaces a-Physicochemical and Engineering Aspects, 1998. **135**(1-3): p. 207-226.
18. Joshi, U.D., et al., *Effect of nonframework cations and crystallinity on the basicity of NaX zeolites*. Applied Catalysis a-General, 2003. **239**(1-2): p. 209-220.
19. Alonso, G., et al., *Synthesis of tetraalkylammonium thiometallate precursors and their concurrent in situ activation during hydrodesulfurization of dibenzothiophene*. Applied Catalysis a-General, 2004. **263**(1): p. 109-117.

20. Chianelli, R.R., G. Berhault, and B. Torres, *Unsupported transition metal sulfide catalysts: 100 years of science and application*. *Catalysis Today*, 2009. **147**(3-4): p. 275-286.
21. Topsoe, H. and B.S. Clausen, *Importance of Co-Mo-S type structures in hydrodesulfurization*. *Catalysis Reviews-Science and Engineering*, 1984. **26**(3-4): p. 395-420.
22. Wilkinson, K., M.D. Merchan, and P.T. Vasudevan, *Characterization of supported tungsten sulfide catalysts ex ammonium tetrathiotungstate*. *Journal of Catalysis*, 1997. **171**(1): p. 325-328.
23. Gunturu, A.K., et al., *A kinetic model for the synthesis of high-molecular weight alcohols over a sulfided Co-K-Mo/C catalyst*. *Industrial & Engineering Chemistry Research*, 1998. **37**(6): p. 2107-2115.

### 3 SYNTHESIS, CHARACTERIZATION AND EVALUATION OF $\text{MoS}_2$ BASED CATALYSTS

#### 3.1 INTRODUCTION

Oxygenates and alcohols from CO hydrogenation were first reported amongst the hydrocarbon products by Fischer & Tropsch <sup>[1-2]</sup> and Frolich & Cyder <sup>[3-4]</sup>. Further experimentation in catalyst synthesis lead to increased productivity (both activity and selectivity) of alcohols. The effect of alkali as a promoter in alcohol synthesis catalysts for F-T type reactions became evident in the mid century with further research in the subject by Anderson <sup>[5]</sup> and Wender <sup>[6-7]</sup>. In the 70s, ethanol and  $\text{C}_{2+}$  oxygenates could be selectively produced over Rh based catalysts <sup>[8-9]</sup>. Development of low-temperature methanol catalysts by ICI provided yet another catalyst variation for producing higher alcohols when these copper based catalysts were altered with alkali promoters <sup>[10-12]</sup>. Another discovery was  $\text{MoS}_2$  based catalysts, which when doped with an alkali, produces alcohols with significantly improved selectivity. These were patented by Dow <sup>[13]</sup> and Union Carbide <sup>[14]</sup>. A review of literature on this subject is presented in Chapter 1.

$\text{MoS}_2$  based catalysts are good for methanation and hydrodesulfurization (HDS) processes. Extensive work has been done in improving the activity, selectivity and reaction mechanisms of these HDS catalysts <sup>[15-24]</sup>. In one of the early attempts to develop catalysts for syngas to alcohols, these conventional HDS catalysts were examined and it was observed that  $\text{MoS}_2$  based catalysts show significant improvements in the catalytic activity and selectivity towards alcohols. However, considering the increasing importance of syngas to alcohols synthesis, the current level of activity/selectivity is not adequate for economic viability. It is with this objective the present work was undertaken to develop improved catalysts for syngas conversion to HAS. The purpose of this research was to develop active catalysts for higher

alcohols and investigate the parameters which might possibly lead to breakthroughs in the performance of the catalysts. This work was focused on investigations of the following parameters in the synthesis and evaluation of MoS<sub>2</sub> based catalysts:

- Effect of metal loading
- Effect of support characteristic
- Effect of co-promoters
- Effect of alkali promoter
- Effect of synthesis conditions
- Effect of operating conditions

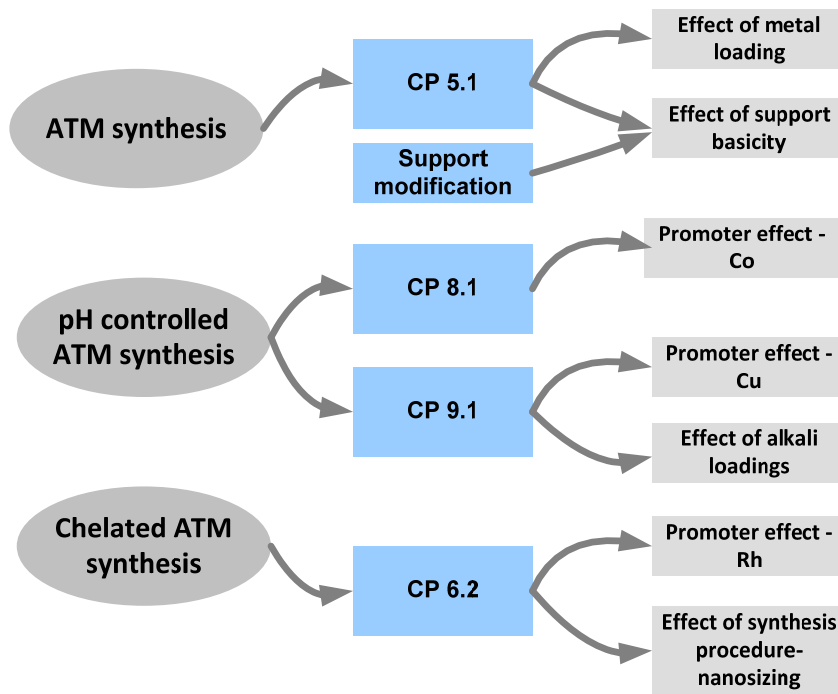


*Figure 3-1 General scheme of catalysts prepared and tested according to project goals*

The surest test for such an intuitive sampling approach is the catalytic performance test itself. The experimental results are presented in subsequent sections. Firstly, the various catalysts synthesized and prepared are described. Subsequently, the results of their catalytic performance

evaluations are categorized according to the project goals. Important observations, discussions and characterization results are presented accordingly. Later sections provided conclusions and future recommendations outlining which parameters affected HAS performance the most and which should be further explored and researched. Figure 3-1 describes the general scheme of catalyst preparation and testing according to the goals outlined above.

### 3.2 CATALYST PREPARATION

All catalysts were synthesized according to the three synthesis procedures described in section 2.4.1. Four main formulations of the catalysts were prepared to evaluate their performance in syngas conversion. Table 3-1 summarizes the preparation of these catalysts based on synthesis technique employed.

Name	Synthesis procedure	Description
CP.5	Normal ATM synthesis, section 3.4.1.1	Calcined in inert (N <sub>2</sub> ) atmosphere
CP.5.1		CP.5 + K <sub>2</sub> CO <sub>3</sub> @ K:Mo=0.6:1
CP.6.2	chelated ATM synthesis, section 3.4.1.3	Nanosized Rh-MoS <sub>2</sub> catalyst
CP.6.2.1		CP.6.2 + K <sub>2</sub> CO <sub>3</sub> @ K:Mo=0.5:1
CP.8.1.1	pH controlled ATM synthesis, section 3.4.1.2	CoMoS type with 2-step alkali promotion
CP.9.1	pH controlled ATM synthesis, section 3.4.1.2	CuCoMoS based catalyst

*Table 3-1 Catalysts prepared with reference to synthesis technique*

However, the final composition of the catalysts tested were significantly varied based on further alterations affected through physical mixing and/or alkali impregnation. These are described in Table 3-2 accordingly. The classification/nomenclature described in Table 3-2 is henceforth used throughout the remaining text

<b>Test run</b>	<b>Base Catalyst</b>	<b>Final modification</b>
<b>CT.15</b>	CP.5.1	CP.5.1- 15 wt%, Bentonite clay-85 wt%
<b>CT.16</b>	CP.5.1	CP.5.1- 40 wt%, Bentonite clay-60 wt%
<b>CT.17</b>	CP.5.1	CP.5.1- 60 wt%, Bentonite clay-40 wt%
<b>CT.21</b>	CP.5.1	CP.5.1- 78 wt%, Bentonite clay-22 wt%
<b>CT.18</b>	CP.5.1	CP.5.1- 40 wt% + Cs-Bentonite-60 wt%
<b>CT.20</b>	CP.5.1	CP.5.1- 40 wt% + K-Bentonite-60 wt%
<b>CT.22</b>	CP.5.1	CP.5.1- 40 wt% + K-Y zeolite-60 wt%
<b>CT.23</b>	CP.6.2	CP.6.2.1- 60 wt%, K-Y zeolite-40 wt%.
<b>CT.29A</b>	CP.8.1	
<b>CT.29B</b>	CP.8.1	CP.8.1 -90 wt% + K <sub>2</sub> CO <sub>3</sub> 10 wt.%
<b>CT.39</b>	CP.8.1	(CP.8.1-72wt%+ K <sub>2</sub> CO <sub>3</sub> 8 wt.%) + Bentonite-20wt%
<b>CT.32</b>	CP.9.1	CP.9.1 - 95 wt% + K <sub>2</sub> CO <sub>3</sub> - 5 wt%
<b>CT.33</b>	CP.9.1	CP.9.1 - 97 wt% + K <sub>2</sub> CO <sub>3</sub> - 3 wt%
<b>CT.34</b>	CP.9.1	CP.9.1 - 92 wt% + K <sub>2</sub> CO <sub>3</sub> - 8 wt%

*Table 3-2 Nomenclature for catalyst tested- includes final composition of catalyst before loading*

BET surface areas were low for all the catalysts tested (Table 3-3). This is not surprising as all the catalysts were prepared through a common synthesis technique. When supported on zeolite, some surface area increase did take place, but this was still not an intrinsic property of the metal catalyst component.

Sample ID	Surface area, m <sup>2</sup> /g
CP.5.1	13.3
Y-zeolite	497.6
22 <sup>nd</sup> (CP.5.1 40 wt% on K-Y zeolite)	257.7
CP.6.2	2.3
CP.8.1.	8.5
29 <sup>th</sup> used (CP.8.1 + 10 wt.% K <sub>2</sub> CO <sub>3</sub> )	4.6
CP.9.1	19.9
32 <sup>nd</sup> Used (CP.9.1+ 5wt.% K <sub>2</sub> CO <sub>3</sub> )	17.2

Table 3-3 BET surface areas of catalyst samples tested

Pore size analysis was performed for the catalysts and it also revealed a similarity in composition of the pore structure due to similar synthesis methods. Figure 3-2 represents the typical adsorption isotherm obtained over these unsupported catalysts.

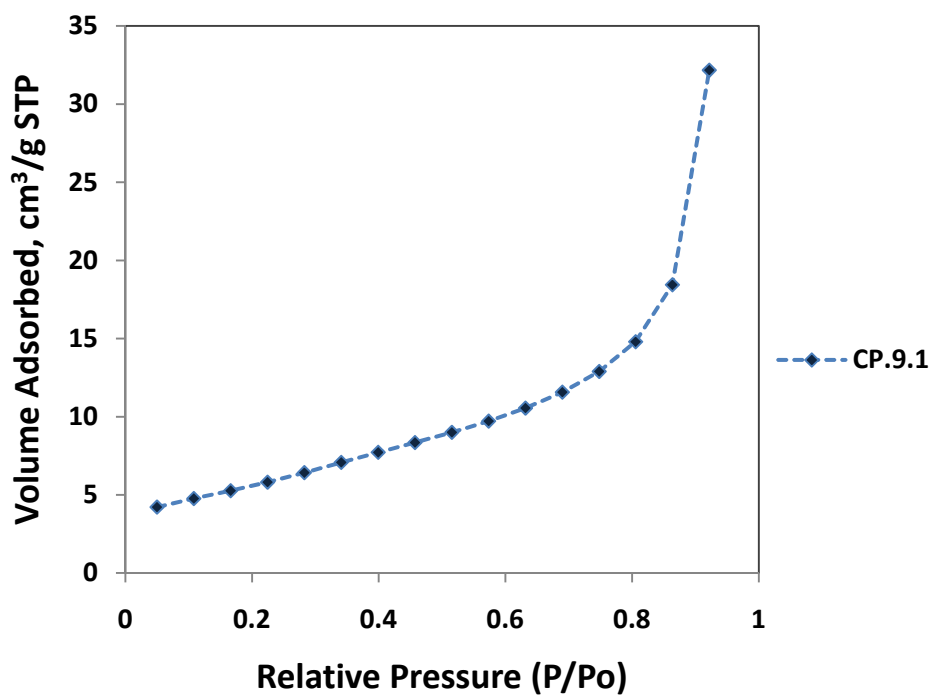


Figure 3-2 Type-I isotherm for CP.9.1, indicating pore size distribution



The plot indicates a TYPE-I isotherm, indicating normal pore size distribution. Desorption curve could not be obtained due to equipment limitations. About 60% of the pore surface area lies within pore range of 171-400 Å (17-40 nm), whereas the rest lies within smaller pores, down to 19 Å (1.9 nm). This indicates a meso-porous substance (Wikipedia-IUPAC)

Packed densities of the catalyst material depended upon the diluent used. Packed densities tested were in the ranges below. These three values are characteristic of all the catalysts tested as they are represented by one of these values depending upon their type:

$$22^{\text{nd}}\_U \text{ (zeolite supported)} = (2.022\text{g}/4.1\text{cc}) = 0.493 \text{ g/cc}$$

$$39^{\text{th}}\_U \text{ (clay supported)} = (1.72\text{g}/2.6\text{cc}) = 0.662 \text{ g/cc}$$

$$34^{\text{th}}\_U \text{ (unsupported)} = (2.938\text{g}/2.9\text{cc}) = 1.013 \text{ g/cc}$$

The catalyst density can play an important as most comparisons of catalyst performance are based on 'per mass' basis. The above values indicate that for a similar weight loading, catalysts supported on zeolite would occupy twice the volume than if the active catalyst material was loaded as an un-supported material.

The catalyst fraction sieved was between 120 and 200 mesh. Thus the particle range is 0.075-0.125 mm (75-125 micron).

### 3.3 RESULTS, CHARACTERIZATION AND DISCUSSION

For evaluation of catalyst performance in a continuous reactor system, only steady state data provides meaningful results. The initial experiments indicated that for alcohol synthesis catalysts, a set-in period (induction period) is required to achieve a steady state activity. A typical time-on-stream performance for catalyst CT.22 is shown in Figure 3-3. During this initial period, a steady increase in the alcohol selectivity was observed with a decrease in alkane selectivity, whereas the conversion does not vary that much. This consistent observation indicates

transformation of the catalyst precursors to active species responsible for promoting alcohol formation.

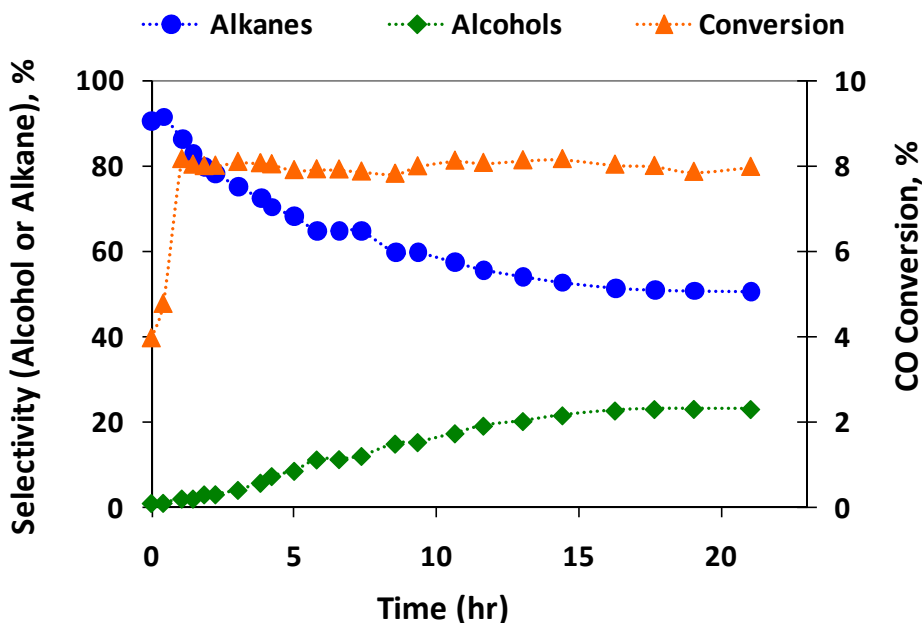


Figure 3-3 Onstream time required at reaction startup to achieve steady state performance.  $MoS_2-K_2CO_3$  catalyst, 40 wt% loading on clay. 330°C, 68 bar,  $CO:H_2=2.0$ , 6000L/kg.cat/hr

The reasons for this variation in product selectivity of alcohols and alkanes are not clear. Possible explanations are:

**Alkali redistribution:** It is believed that re-distribution of alkali promoter takes place on the surface of the catalyst. This seems probable, as SEM/EDS analysis performed on fresh and used catalyst indicated surface enrichment of potassium (CT.16 discussed later). Similar effect was noted by Woo<sup>[25]</sup> and Iranmahboob<sup>[26]</sup> for  $K_2CO_3$  doped  $MoS_2$  catalysts. However, it is necessary to note, that this alkali distribution or thermal migration happens under a syngas environment. In some cases, alkali addition is usually before calcination<sup>[27]</sup>. Thus, these catalysts that have the alkali premixed before calcination should have enough opportunity to distribute and properly disperse during calcination conditions, i.e. 400-500°C for 2 hours. Even for these catalysts, the induction period that is a prequel to the steady state is still needed<sup>[27]</sup>.

**Sulfide stabilization:** Another explanation for the development of steady state is the stabilization of the sulfide species. Christensen reported that the induction period is shortened by inclusion of H<sub>2</sub>S in the feed<sup>[28]</sup>. Again it seems necessary that the H<sub>2</sub>S needs to be pre-fed with CO and H<sub>2</sub>, i.e. the stabilization occurs in the presence of syngas. Catalysts that are calcined in a H<sub>2</sub>S/H<sub>2</sub> stream, before catalytic testing, also needed this induction period<sup>[28-29]</sup>.

Other than the induction time required to achieve a steady state performance, an important observation was made for some of the catalysts (CT.21, CT.23, CT.29, Ct.32). This was the oscillatory behavior of the exit concentration profile and hence the reactor performance, as shown in Figure 3-4 for Rh-MoS<sub>2</sub> catalyst.

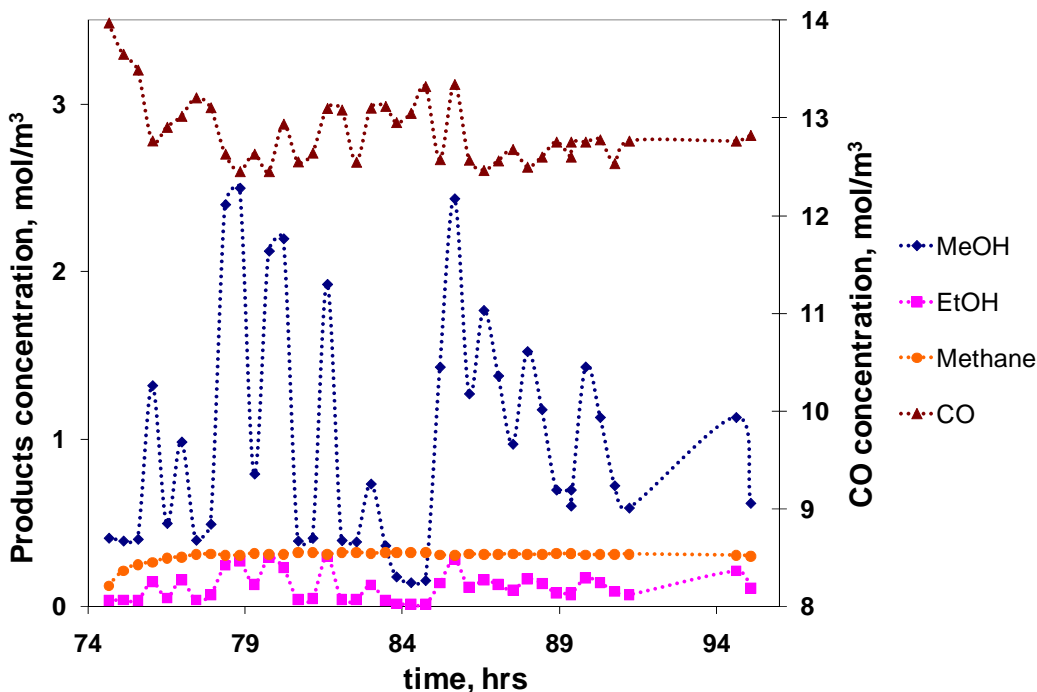


Figure 3-4 Transient state with varying concentrations as measured by GC. Run 23<sup>rd</sup>\_I, Rh-MoS<sub>2</sub> catalyst, 335°C, 90 bar, CO:H<sub>2</sub>=0.5 and 6,000 L/kg.cat/hr

For assessment of catalyst performance in such cases of transients in catalyst activity, an average performance was calculated. This is based on quantification of the amount of liquid products collected, as shown in Table 3-4.

Activity	Methanol concentration, mol/m <sup>3</sup>	Alcohol yield, g/kg.cat/hr	CO Conversion, %
High	2.3	720	29.0
Intermediate + liquid collected	1.1	408	19.4
Low	0.4	158	12.8

*Table 3-4 Alcohol yield selection based on averaged values, that match the liquid product collected.*

Such transient behavior has not been reported for alcohol synthesis catalysts from this family, though it has been reported for F-T synthesis [30-31]. Schuth [30] described oscillatory behavior to occur on transition metals like Fe,Co,Ni and zeolites. Others researched reaction rate oscillations, specifically for FT synthesis, over Fe [32] and Fe-zeolite catalyst [31]. Considering the complex reaction scheme, there can be multiple reasons that can cause this oscillatory phenomenon. Based on the literature for oscillatory behavior in F-T systems, transient behavior in our system could be due to:

- Complex kinetics associated with changes in the active species
- Non-Isothermal behavior
- Phase separation or onset of supercritical fluid phase
- WGS reaction, producing water
- Adsorption on active sites

The actual cause for such an oscillatory behavior cannot be elucidated without further research on the subject.

An important criterion for evaluation of catalysts in a fixed bed catalytic reactor is to ensure that heat and mass transfer limitations within the catalyst particle and from bulk gas

phase to the catalyst surface are not significant. Intraparticle mass transfer resistance was evaluated according to the Weisz and Prater criteria [33-34].

$$\Phi = \frac{R.r^2\rho}{C_s D_e} \ll 1 \quad \text{for non - zero order} \quad \text{Eq. 3-1}$$

$R$ , observed reaction rate, mol/g.cat/s

$r$ , catalyst particle radius, cm

$\rho$ , catalyst density, g/cm<sup>3</sup>

$C_s$ , CO concentration at surface, mol/cm<sup>3</sup>

$D_e$ , CO diffusivity, cm<sup>2</sup>/s

For one of the most active catalysts (CT.23), the  $\Phi$  factor was evaluated as  $\sim 0.01$ , indicating that the catalytic system is free from intraparticle mass transfer limitations. The activation energy (84 kJ/kmol) was evaluated for one of the catalysts discussed in section 3.3.7.2, which also indicates that the reaction is in the regime of kinetic control.

### **3.3.1 EFFECT OF METAL LOADING**

Several catalysts consisting of K<sub>2</sub>CO<sub>3</sub> doped MoS<sub>2</sub> on bentonite support were prepared according to the procedure described for CP. 5.1, to study the effect of active metal (Mo) loading. The active metal was thoroughly ad-mixed with the support until the metal ‘disappeared’ into the support and the final catalyst developed a consistent color. Thus, the final catalyst was considered a diluted catalyst, **with K<sub>2</sub>CO<sub>3</sub>/MoS<sub>2</sub> as the active metal component of this material**. Other researchers have also used similar ‘diluted’ catalysts and achieved significant alcohol yields [35-36]. Elsewhere it was reported that physical mixing is known to impart improvement in F-T activity [37-38]. Xu et. al. [37] noticed a drastic increase in the CO hydrogenation activity of Fe-Cu catalyst when physically mixed with zeolites. Increased quantities of branched and heavier hydrocarbons

were obtained. Kang et. al. [38] evaluated impregnated and physically mixed FeCuK/ZSM-5 catalysts. The later was more active but had lower olefin selectivity.

The catalysts with varying metal content (15, 40, 60 and 78%, w/w) were prepared and evaluated under uniform conditions. The results are presented in Table 3-5

<b>Metal Loading, %</b>	<b>15</b>	<b>40</b>	<b>60</b>	<b>78</b>
Temp, °C	302	304	302	302
Pressure, atm	90	88	88	87
CO/H <sub>2</sub>	2	2	2	2
GHSV, L/kg.cat/hr	6000	6000	6000	6000
Space time Yield (STY), g/kg.cat/hr				
Methanol	3.0	18.0	42.3	43.1
Ethanol	3.2	14.5	19.7	25.3
Propanol	1.5	0.0	4.6	8.1
DiMethyl Ether	36.9	5.9	4.9	5.2
Methane	1.8	12.3	20.1	22.0
Ethane	3.3	15.2	8.3	11.1
<b>Total Alcohols</b>	<b>7.7</b>	<b>32.5</b>	<b>66.6</b>	<b>76.5</b>
Molar yields, mol/kg.cat/hr				
Total Alkanes	0.6	3.1	1.9	2.4
Total Alcohols	0.2	0.9	1.4	2.0
Other Oxygenates	0.8	0.2	0.2	0.2
<b>Conversion, %</b>	<b>1.4</b>	<b>4.2</b>	<b>4.8</b>	<b>4.9</b>
Selectivity, CO <sub>2</sub> free basis				
Methanol	13.8	22.7	32.2	38.7
Ethanol	5.2	6.3	6.6	7.9
Propanol	1.2	0.0	1.7	1.3
Methane	7.3	24.7	26.8	29.8
Ethane	7.7	13.2	10.7	8.6
Propane	6.3	12.3	8.7	7.0
Total Alcohols	20.2	39.1	47.6	49.9
Total Alkanes	40.0	58.0	50.1	48.5
Other oxygenates	39.8	2.9	2.3	1.6

*Table 3-5 Effect of metal loading on performance of K<sub>2</sub>CO<sub>3</sub>-MoS<sub>2</sub> catalyst (K:Mo = 0.6:1)*

One of the prominent results is that a minimum amount of metal loading is needed to promote alcohol yields. By increasing the metal loading, acidic sites on the clay material are suppressed and secondary reactions of alcohols are minimized. The source of surface acidity over

bentonite is believed to arise from its ability to donate protons (Bronsted acidity) and the polarizing ability of the network cation (Lewis acidity)<sup>[39]</sup>. Thus, acidity results from the clays ability to form OH<sup>-</sup> groups from hydrated water and the subsequent availability of H<sup>+</sup> to reacting species<sup>[40]</sup>.

For CT.15, catalyst with 15% metal loading, it is seen that a significant amount of DiMethyl Ether is formed (represented as other oxygenates in Table 3-5). Methanol is known to easily condense to DME over acidic sites<sup>[41-42]</sup>. Therefore, at 15% loading not enough surface coverage is achieved to suppress the acidic sites.

For loadings higher than 15%, formation of DME and other oxygenates was significantly lower. At higher Mo loadings, the byproduct DME formation was suppressed and alcohol yields improved. Further increase in metal content improved alcohol selectivity further, with a decline in total alkane formation. Again, this can be attributed to suppression of acidic sites which are known to dehydrogenate alcohols to alkanes. E.g. Murchison et. al.<sup>[43]</sup> compared the effect of activated carbon and alumina as supports for CoMoS catalysts. Alumina having more surface acidity than Act. C., produced more alkanes than alcohols. Alcohol selectivity was **75%** over the Act. C supported catalyst vs. **12%** with alumina supported catalyst. Bian<sup>[44]</sup> suppressed acidity on Al<sub>2</sub>O<sub>3</sub> by increasing the K-MoS<sub>2</sub>/ Al<sub>2</sub>O<sub>3</sub> catalyst calcination temperature from 500°C to 800°C. This resulted in an increase in alcohol yields/selectivity with a concomitant decrease in alkane selectivity. For unsupported K-MoS<sub>2</sub> increase in calcination temperature did not yield any improvement in alcohol selectivity.

Thus, increased quantities of active metal (**K<sub>2</sub>CO<sub>3</sub>/MoS<sub>2</sub>**) in the clay not only provided greater surface coverage required to suppress the surface acidity but also provided increased alkali which neutralized the acidic sites<sup>[45-46]</sup>.

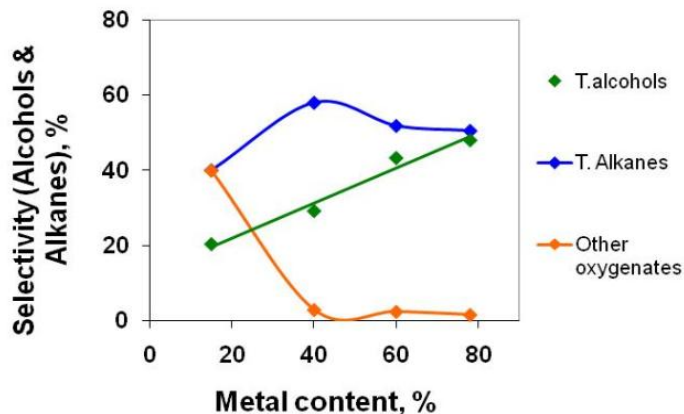


Figure 3-5 Variation in selectivity of total alcohols, alkanes and other oxygenates at different metal loadings at similar operating conditions: 300°C, 1300 psi, CO:H<sub>2</sub> = 2, GHSV = 6000 ml/g.cat/hr.

Increasing Mo loading from 60% to 78% did not show significant variation in the yield and selectivity pattern. The conversion remained the same with only higher alcohols showing an improvement (Table 3-5). However, for the catalyst with 78% Mo loading, temperature had little effect on alcohol selectivity, whilst the yields increased with increasing temperature as shown in Figure 3-6. In Figure 3-6, the effect of temperature on alcohol selectivity and alcohol yield is plotted for different metal loadings. There is only one data point for the catalyst with 15% metal loading, because the catalyst appeared inactive for alcohol synthesis at conditions that many report as optimum. Unknowingly, further testing was abandoned as it was considered that the catalyst was not properly synthesized.

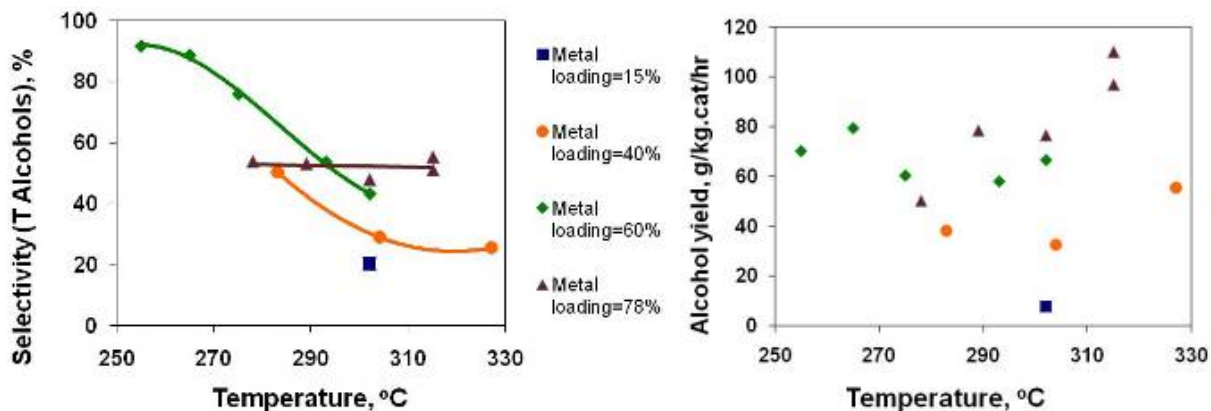


Figure 3-6 Effect of temperature on total alcohol selectivity (left) and yields (right) at varying metal loadings



The active metal component,  $K_2CO_3$  doped  $MoS_2$ , is the same for all the four catalysts tested in this case. The material was characterized using TEM, SEM / EDS, FTIR and XRD.

SEM images for **CP.5.1** revealed a very homogeneous size distribution of spherical  $MoS_2$  particles. For catalyst CP5.1, size distribution was limited to 200-300nm after calcination and  $K_2CO_3$  doping. Generally,  $MoS_2$  has a tendency to form arbitrary stacked layers during calcination [47-48]. Producing sulfides in narrow size distribution was noted as a significant improvement by Haruta [49], who produced molybdenum and cobalt sulfides with distribution between 100nm-600nm by controlling the pH of the liquor. Inamura [15] advocated a homogenous distribution of CoMoS to be better for HDS. Perhaps, the greatest advantage of such homogenous size distribution is realized in application areas other than HDS and HAS. As a semiconductor material, a well controlled size distribution is of utmost importance for reliable performance in photocatalytic materials [50]. A narrow size distribution is also extremely important in tribology, where  $MoS_2$  materials are used as lubricating agents [51].

Spot analysis (EDS) revealed that the clusters that appeared to be more bright/white, had more  $K_2CO_3$  loading. Potassium varied from 6% to 9%, between points A and B (see Figure 3-7). The non-uniform  $K_2CO_3$  doping was also studied in a similar manner by Iranmahboob [26]. The atomic ratios of Mo:S are 1:2, indicating that the calcined material consists of stoichiometric  $MoS_2$ .

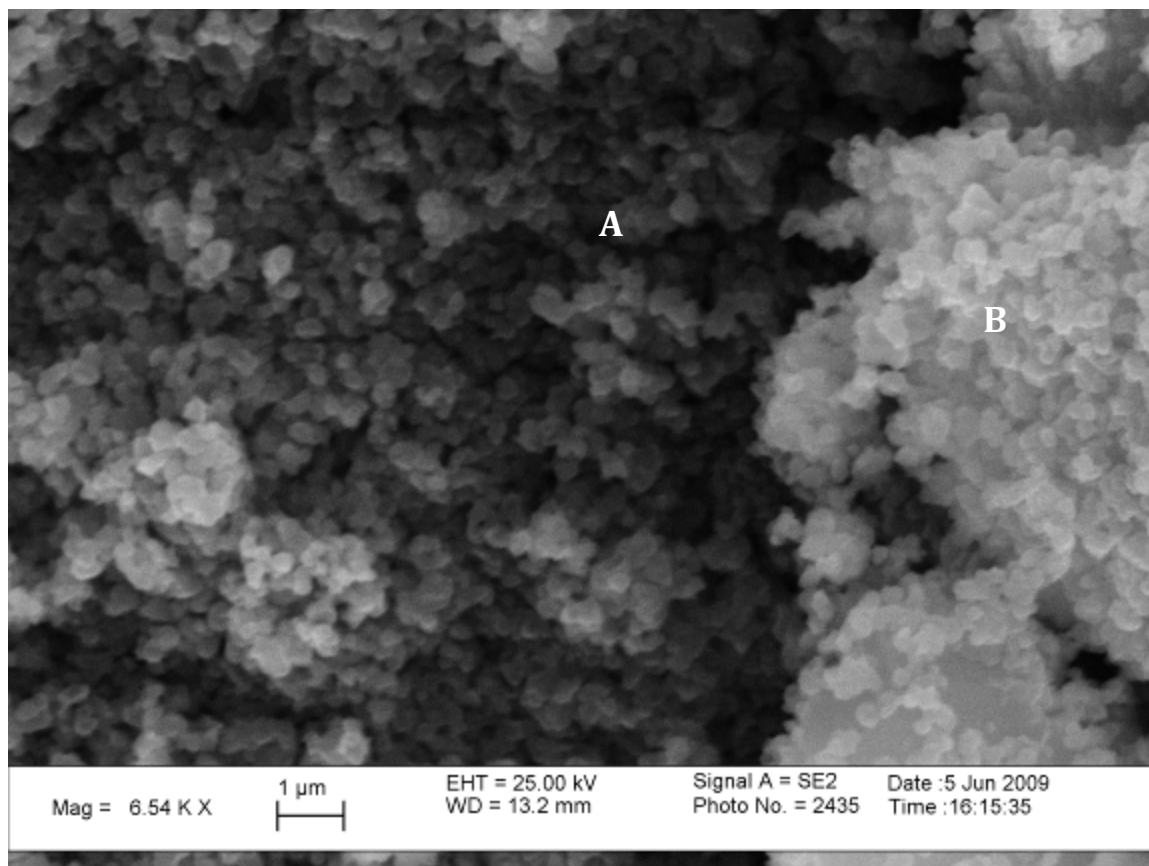


*Figure 3-7 SEM of CP5.1, showing homogeneous size distribution. A and B represent locations for EDAX analysis*

TEM analysis shows how nearly spherical molecules of  $\text{MoS}_2$  agglomerate together to form arbitrary shapes. From SEM and TEM images it appears that for CP5.1 catalyst, the synthesized  $\text{MoS}_2$  is not necessarily stacked together into layers, as is the usual case for  $\text{MoS}_2$ . Commercial  $\text{MoS}_2$  was used to calibrate EDS machines of SEM and TEM equipment. Peaks for molybdenum and sulfur co-evolve in the spectra, but are adequately resolved.

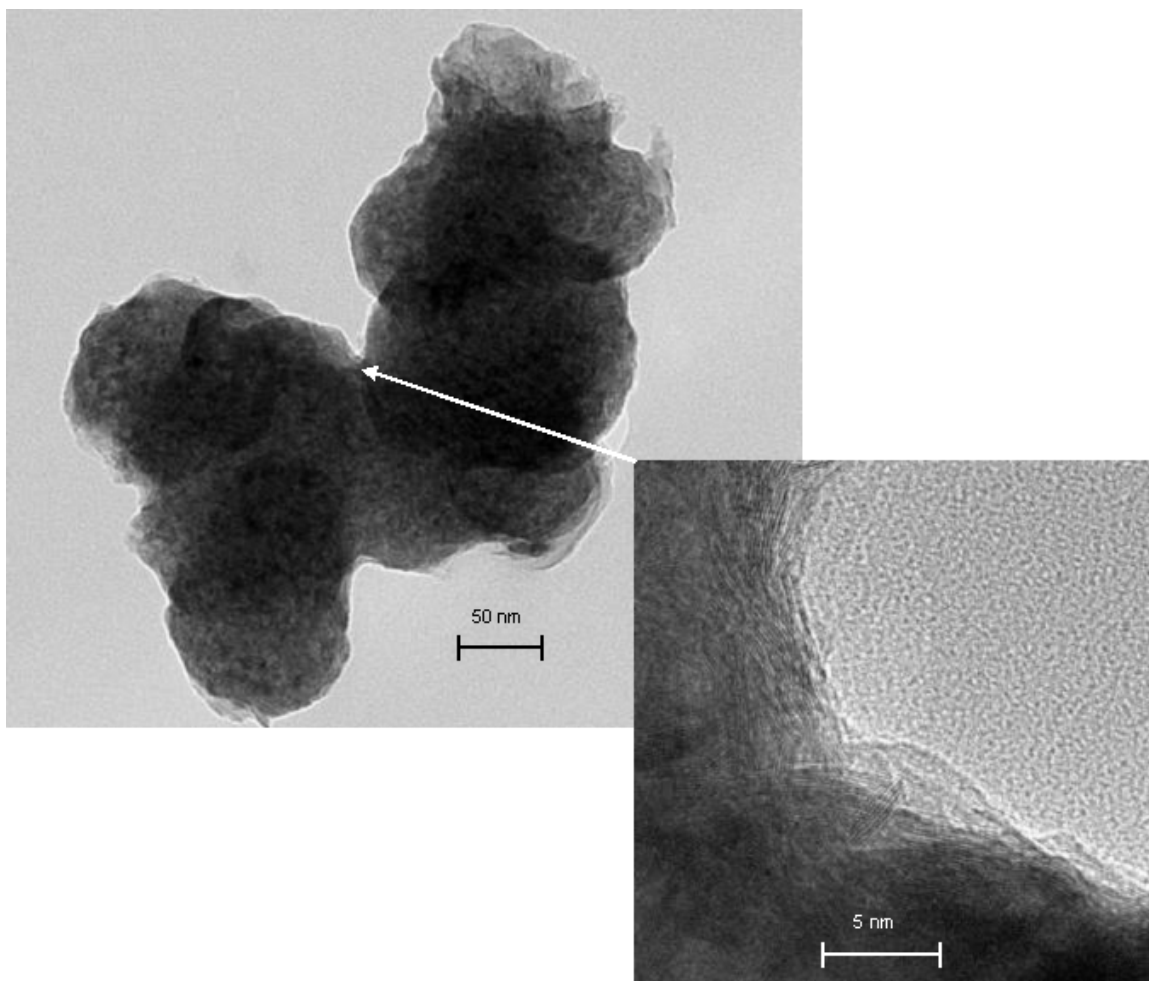


*Figure 3-8 TEM of CP5.1, showing how semi-spherical MoS<sub>2</sub> are bundled together.  
Insert: Zoom indicating fringe patterns and crystallinity of MoS<sub>2</sub>*

SEM of CT.16 (40% metal loading) is shown in Figure 3-9. The pillared structure of the clay is somewhat visible. EDS spectra revealed the following interesting features:

1. Presence of Fe and Mg
2. K distribution limited, even in Figure 3-9, which is a zoom in on a pile of metal catalyst

3. Spectra doesn't show carbon

The SEM/EDS data for the same catalyst after testing, CT.16U, are shown in Figure 3-11 and Figure 3-12. They show a uniform distribution of MoS<sub>2</sub> catalyst. Some thermal migration and surface reconfiguration takes places, as chunks of MoS<sub>2</sub> evident in SEMs before reactions are not visible after reaction. EDS reveals the following:

1. K is much more uniform over the surface. Moreover, an increase in K concentrations is noticed, which reflects on the fact that significant alkali redistribution does take place. K concentrations increase from an average of 1.0% to 8.0%.
2. Mo:S ratio is maintained at 1:2, indicating stability of the catalyst. Moreover, surface enrichment of MoS<sub>2</sub> also takes place, i.e. concentrations of MoS<sub>2</sub> also increase on the surface.

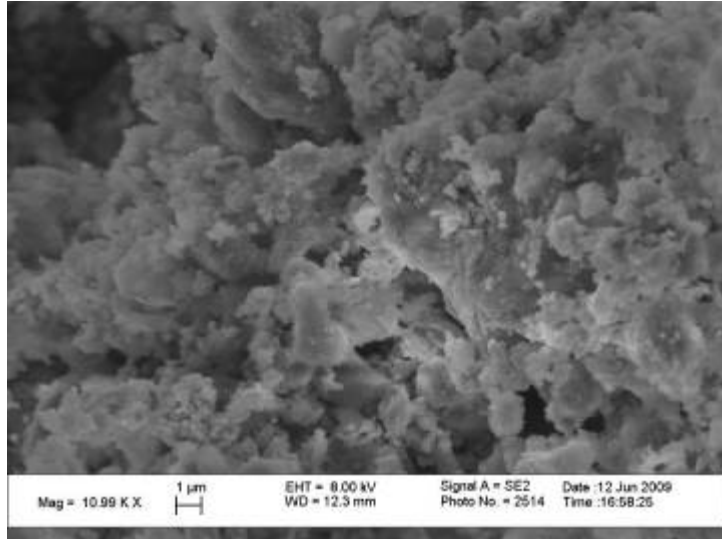


Figure 3-9 SEM of CT.16 (CP5.1+ Bentonite)

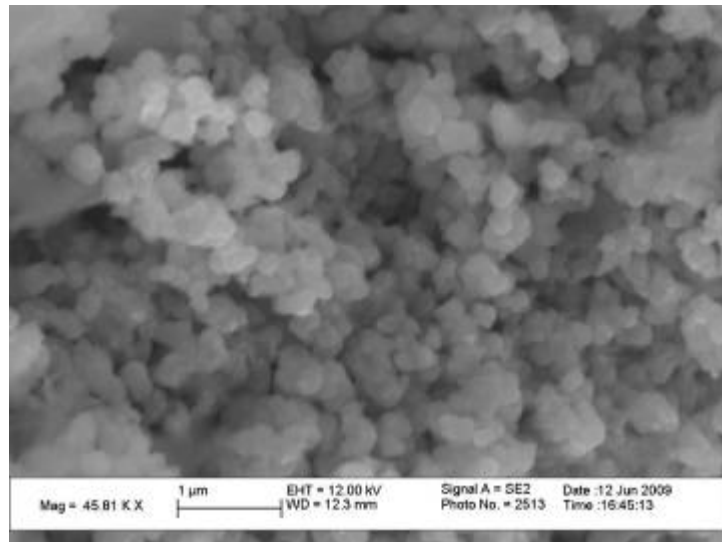


Figure 3-10 CT.16 SEM-zoom in on a chunk of K-MoS<sub>2</sub> precursor in bentonite

3. For Figure 3-12, two spot analysis reveal almost exact concentrations, the difference being in surface concentration of K; this is the surface enrichment with K

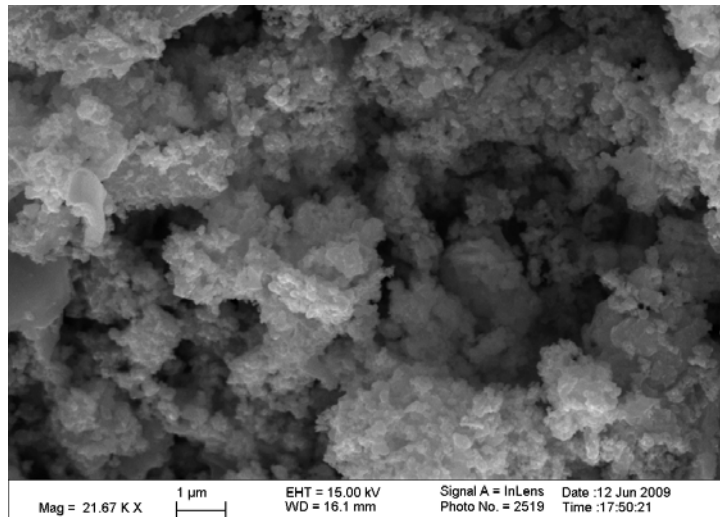
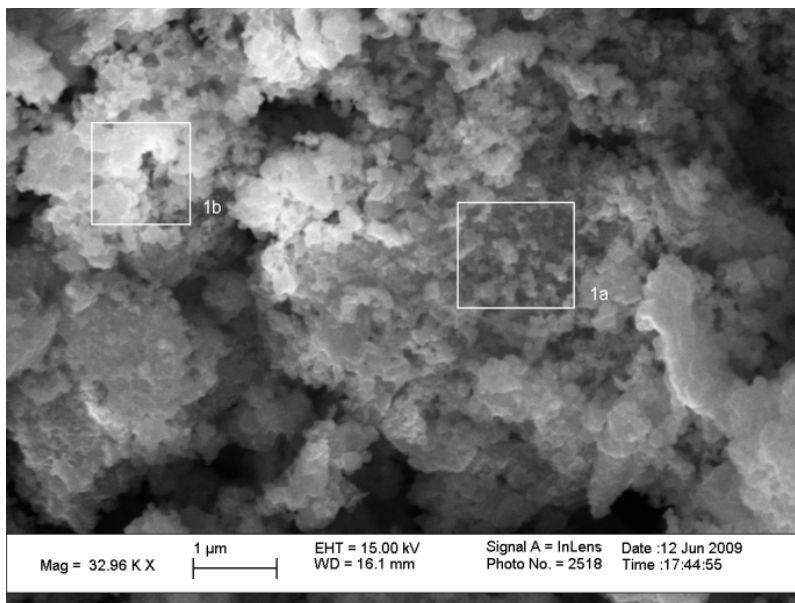


Figure 3-11 SEM of used catalyst CT.16U



	O	Fe	Na	Mg	Al	Si	Mo	S	K
<b>1A</b>	33.80	9.55	1.22	0.22	0.45	0.62	14.75	31.62	7.77
<b>1B</b>	32.79	7.60	0.00	0.00	0.86	0.54	14.72	33.87	9.62

Figure 3-12 SEM+EDs of CT.16U, homogeneity in chemical composition

### 3.3.2 ALTERING SUPPORT BASICITY

As discussed before, support acidity can have a negative effect on alcohol selectivity and yield. It was therefore anticipated that varying the support acidity, or conversely its basicity, would have a beneficial effect on alcohol selectivity..

For aluminosilicate materials, it is known that support acidity (or basicity) can be altered by interchanging the framework cations. Barthomeuf <sup>[52]</sup> has researched and postulated the reasons what affects the basicity in zeolites. Some important findings are summarized below:

1. **Framework Oxygen atoms:** As the negative charge is borne by the oxygen atoms, base strength can be expressed by the negative charge on the O<sup>-2</sup>. Moreover, as the oxygen is not mobile (as opposed to the mobile H<sup>+</sup> in acidic zeolites), the framework orientation also dictates on how many basic sites are accessible by the reactants.
2. **Si/Al :** Basic strength decreases with increase in framework Si/Al ratio. E.g. Dealumination is used to increase the zeolite acidity. Basicity in descending order in different zeolites is:

<b>Zeolite</b>	<b>Si/Al</b>
FAU-X (Faujasite)	1.2
FAU-Y (Faujasite)	2.4
MOR (Mordenite)	5
MFI (ZSM-5)	10

3. **Framework cation :** Basicity increases with increase in electropositivity of the counter cation, Cs > K > Na

Thus, a way of inducing basicity in aluminosilicates is by the addition of a stronger cation into the zeolite/clay structure, referred to as addition of ‘nonframework basicity’. Procedure for modifying supports in this way has been discussed in section 2.4.1.4.

Results of changing the basicity of supports are presented in Table 3-6. At similar operating conditions and constant metal loading, it is clearly seen that framework cation has a significant impact on the alcohol selectivity and yield, in the following order:

**Cs-Bentonite > K-Bentonite > Na-Bentonite**

Support	Na-Bentonite	K-Bentonite	Cs-Bentonite	K-Y zeolite
Temp, °C	304	305	304	305
Pressure, atm	88	85	85	89
CO/H <sub>2</sub>	2	2	2	2
GHSV, L/kg.cat/hr	6,000	6,000	6,000	6,000
Space time Yield (STY), g/kg.cat/hr				
Methanol	18.0	27.2	42.6	29.7
Ethanol	14.5	16.9	36.2	39.0
Propanol	0.0	6.1	17.2	18.5
DME	5.9	29.1	37.6	6.5
Methane	16.2	13.7	11.9	7.2
Ethane	15.2	9.8	6.9	7.6
Total Alcohols	32.5	50.2	96.0	87.2
C <sub>2+</sub> /C <sub>1</sub>	0.8	0.8	1.3	2.1
Molar yield, mol/kg.cat/hr				
Total Alcohols	0.9	1.3	2.4	2.2
Total Alkanes	3.1	2.2	1.4	1.6
Other Oxygenates	0.1	0.6	0.9	0.2
Conversion, %				
	4.7	4.0	4.3	3.5
Selectivity, CO <sub>2</sub> free basis				
Methanol	22.7	33.0	42.0	39.6
Ethanol	6.3	7.1	12.4	18.1
Propanol	0.0	1.3	3.0	4.4
Methane	24.7	20.4	14.9	19.2
Ethane	13.2	8.3	4.9	5.8
Propane	12.3	7.4	3.8	3.8
Total Alcohols	29.1	41.4	57.4	62.8
Total Alkanes	68.0	50.2	33.6	34.8
Other oxygenates	2.9	8.4	9.0	2.4

Table 3-6 Effect of support basicity on performance of K<sub>2</sub>CO<sub>3</sub>-MoS<sub>2</sub> catalyst(K:Mo = 0.6:1)

Both alcohol selectivity and activity increased with support basicity. However, CO conversion is similar for all these base modified clay supported catalysts. The total molar activity (mol/kg.cat/hr) of all products over individual catalysts is similar too. This gives an indication that altering the basicity of the support does not impact the inherent activity of the active metal loaded, rather it alters the product distribution. A look at the reaction scheme over MoS<sub>2</sub> catalysts (Figure 1-5) can further elucidate this: Note that all products are formed through common intermediates. Thus, the increased basicity provided by the support merely provides an environment that is more conducive for conversion of the intermediate to alcohols.

It could also be that the increased basic environment of the support stabilizes the acyl intermediate ( $C_xH_{(2x-1)}O^*$ ), which is responsible for alcohol formation. The transformation of the acyl ( $C_xH_{(2x-1)}$ ) species to the alkyl species by dehydration and subsequent H<sup>\*</sup> insertion leads to alkanes. Stabilization of the acyl/alkyl specie, might also explain a higher alcohol fraction in the product crude, as there would be more chances for CO insertion to produce higher alcohols.

Note that clay or bentonite has been used as a support /diluent. In a US patent<sup>[13]</sup> by Dow, bentonite clay was used as the preferred diluent/support for a number of MoS<sub>2</sub> based catalysts. Iranmahboob<sup>[35]</sup> also used bentonite as a support and quantified the benefit of using bentonite clay as a support. At 310°C, clay supported Co-MoS<sub>2</sub> catalysts showed higher oxygenate activity **320 g/kg.cat/hr** vs. **120 g/kg.cat/hr** for unsupported catalysts. The alcohol selectivity was 70% and ~85% respectively.



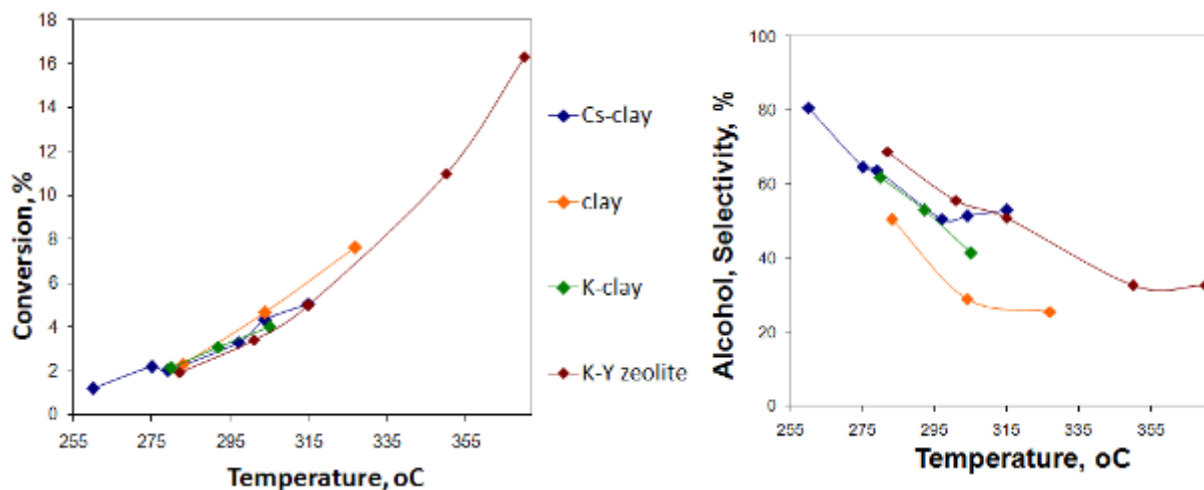


Figure 3-13 Effect of temperature on conversion and alcohol selectivity for catalysts + support with varying basicity

The beneficial effect of altering the support basicity is evident at higher temperatures where higher alcohol selectivity is observed (Figure 3-13). Higher temperatures are known to promote alcohol formation, but at the same time increase the alkane productivity to a much larger extent. Altering support basicity is an effective way to reduce alkane selectivity at higher temperatures and promote alcohol formation. Figure 3-14 examines the alcohol productivity of these catalysts at two different temperatures, and also provides a breakup of products in terms of  $C_1$  and  $C_{2+}$  components. Along with an increase in alcohol productivity, temperature also alters the product profile by increasing the  $C_{2+}$  content relative to  $C_1$  homologue. Note the shootup of alkane productivity for the Na-bentonite supported catalyst with an increase in temperature of only 10 °C. Bentonite supported catalysts have a strong tendency to drastically increase alkane productivity, sometimes at the expense of alcohol productivity <sup>[35]</sup>. This tendency has been effectively curtailed by increasing the basicity of the bentonite clay. Data for the K-bentonite supported catalyst was not recorded at 315 °C and is not presented in Figure 3-14. The trend is nonetheless, as described in general.

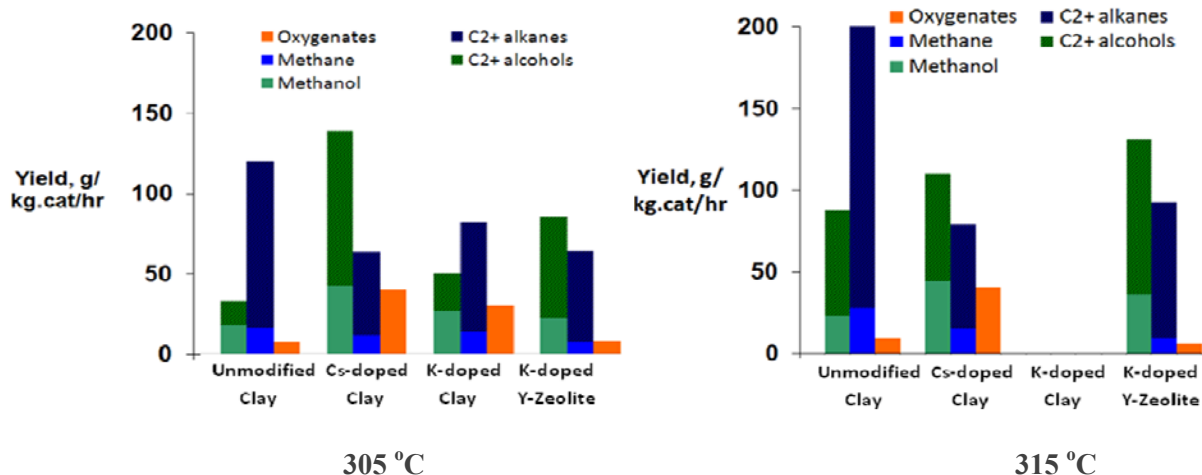
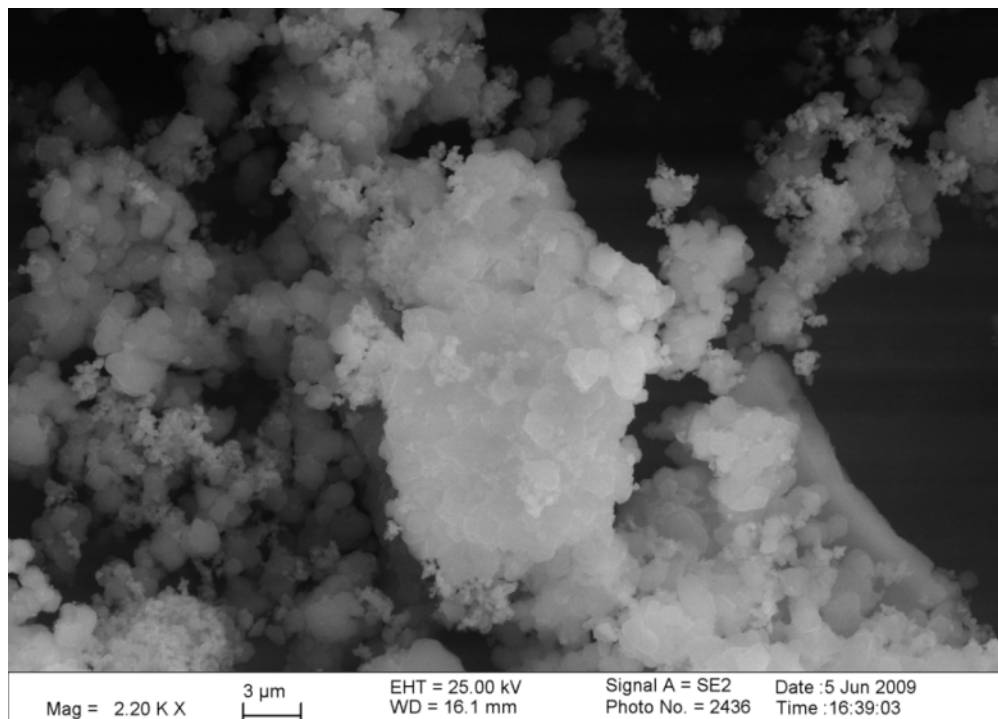


Figure 3-14 Effect of temperature on product yields on catalysts + support with varying basicity

An interesting aspect of K-Y zeolite as a support is the promotion of higher alcohols over methanol. KY zeolite supported catalyst produced  $C_{2+}/C_1$  ratios as high as 4.9 at 350°C, 87 atm and a space velocity of 4,000 ml/g.cat/hr. This is significant, as generally  $MoS_2$  catalyst, without additional co-promoter like Co or Ni, does not give a high  $C_{2+}/C_1$  alcohol ratio.

Figure 3-15 represents a SEM micrograph of catalyst CT.22, in which  $MoS_2$  catalyst can be seen randomly distributed. SEM also shows that the zeolite structure remains intact after affecting the solid state interaction between the active metal and the zeolite. Joshi<sup>[53]</sup> noticed a reduction in the particle size for a similar zeolite material after 30 minutes of ball milling. This resulted in some destruction of the zeolite network and loss in catalytic activity. EDS revealed the following:

1. Mo:S = 1:2.2
2. A significant amount of carbon (33.8%), which could have resulted from the organic template used in the synthesis of the commercial zeolite<sup>[54]</sup>



*Figure 3-15 SEM of CT.22(CP.5.1+KY zeolite)*

SEM/EDS of this used catalyst, CT.22U, indicated that the original MoS<sub>2</sub> structure and size are preserved (Figure 3-16). EDS showed:

1. A consistent Al/Si ratio.
2. Mo:S = 1:1.5; indicating probably loss of sulfur from the catalyst as it was operated at 350 °C for extended period.
3. Again, enrichment of surface concentrations of Mo, although K remained the same

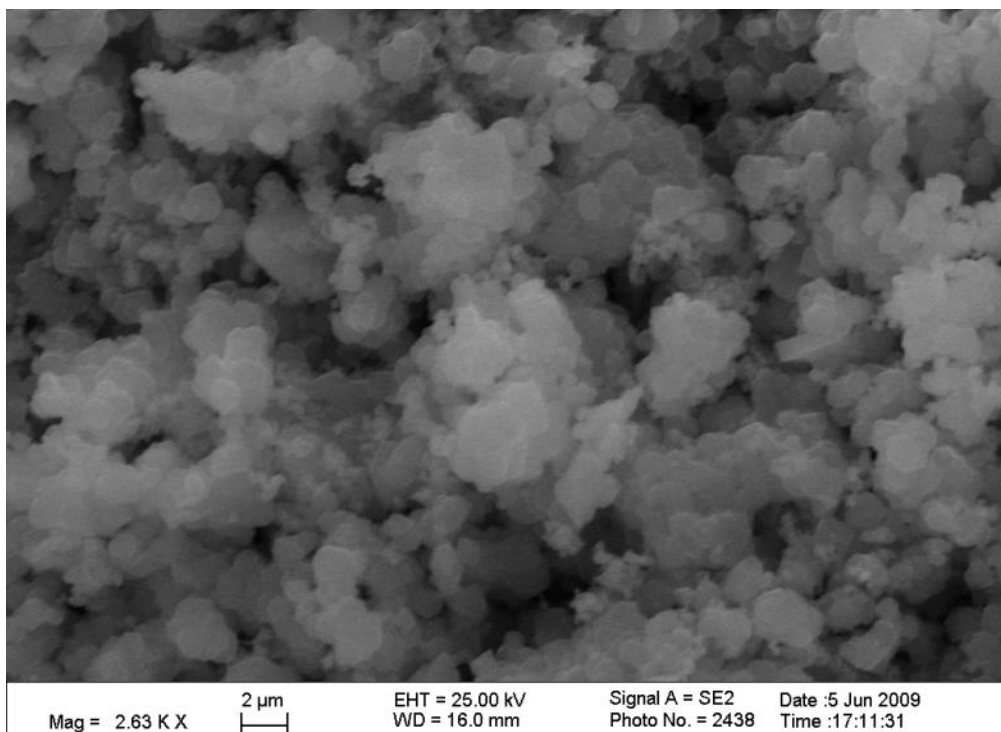


*Figure 3-16 SEM of used catalyst, CT.22U*

XRD pattern comparison for CP5.1 (K doped MoS<sub>2</sub> precursor), CT.22 (MoS<sub>2</sub>+KY zeolite) and CT.22U (used CT.22) is shown in Figure 3-17. On supporting CP5.1 in the zeolite, the characteristic peaks of MoS<sub>2</sub> somewhat disappear. After 140 hours of operation, the peaks for zeolite are still strong, indicating stability of the zeolite (and catalyst). This also indicates that the zeolite catalyst works well under HAS conditions, in which water is generated due to the various reactions involved.

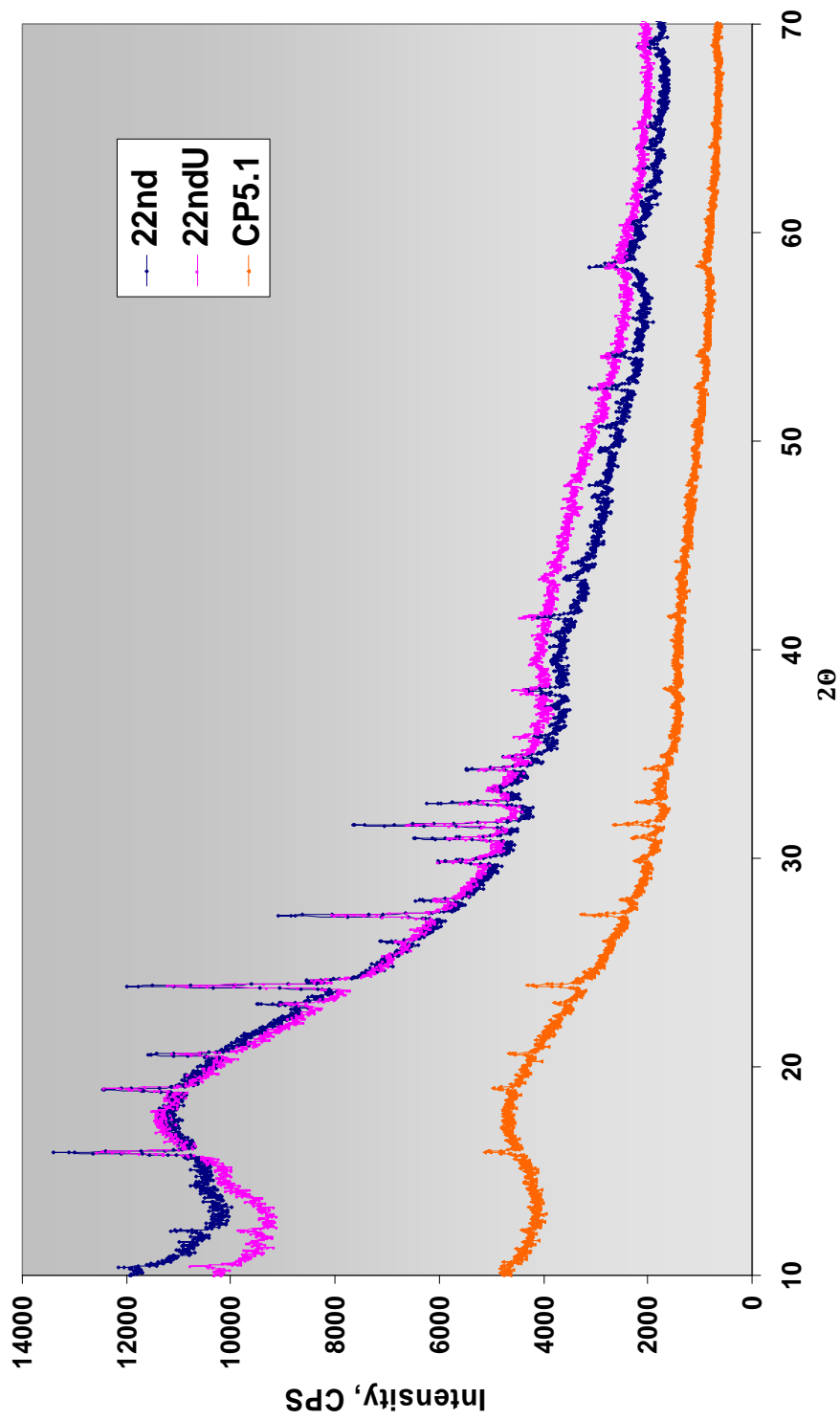


Figure 3-17 XRD comparison of CP.5.1, CT.22 and CT.22U. Patterns indicate that zeolite structure remains intact after the reaction

### 3.3.3 EFFECT OF COBALT AS CO-PROMOTER

Cobalt catalysts are known to promote a wide variety of reactions including the homologation of alcohols. Extensive work has been done previously on Co catalyzed homologation of methanol to ethanol<sup>[55-56]</sup>. On the other hand, Co is also known to be an effective Fischer-Tropsch catalyst, used for alkane production. In fact cobalt is the catalyst of choice for many F-T commercial processes<sup>[57-58]</sup>.

Co inclusion in MoS<sub>2</sub> catalysts increases selectivity of higher alcohols and improves overall alcohol yields. This has been confirmed by many researchers<sup>[13, 27, 59]</sup> and interpreted as result of strong C<sub>1</sub>-C<sub>2</sub> homologation chemistry. Particularly cobalt promotes formation of ethanol amongst higher alcohols. This also skews the Anderson Schulz Flory (ASF)<sup>‡</sup> distribution in favor of ethanol. Due to its dual mode of action, an increase in methane is also seen over these catalysts.

It has been argued that Co is the most effective when present in the **CoMoS** phase instead of **Co<sub>x</sub>S<sub>y</sub>**. In the field of Hydrodesulfurization (HDS), it is reported that active sites on CoMoS/Al<sub>2</sub>O<sub>3</sub> catalysts, are the edge planes<sup>[60]</sup>. For Co to be a part of the Co-Mo-S matrix, it is required to be present below a specific Co/Mo ratio, whereby it is preferentially occupies the end locations. At higher Co/Mo loading cobalt will segregate out and form a Co<sub>9</sub>S<sub>8</sub> bulk phases. Li<sup>[59]</sup> has shown that Co<sub>9</sub>S<sub>8</sub> phase is inactive for alcohol synthesis. The optimum loading is widely accepted to be Co/Mo=0.5 for the sulfided catalyst<sup>[59] [61]</sup>. Cobalt helps in shrinking the size of MoS<sub>2</sub> particles on a carbon support, while it also dampens the effect of operating conditions. Co-MoS<sub>2</sub> seems to work well without the inclusion of H<sub>2</sub>S, which has been reported to enhance C<sub>2+</sub> alcohol selectivity over K-MoS<sub>2</sub> catalysts. Elsewhere, Iranmahboob et. al<sup>[62]</sup> have correlated the loss of activity of their CoMoS type catalyst with the growth/agglomeration of Co<sub>9</sub>S<sub>8</sub> phase and also found a decrease in the surface area of the catalyst after reaction. They attribute this to the

loss of sulfur from the catalyst, which under the syngas environment, gets converted into H<sub>2</sub>S. Christensen <sup>[28]</sup> also speculated that some sulfur is lost from the catalyst. They analyzed the liquid products obtained over their K<sub>2</sub>CO<sub>3</sub>/Co-MoS<sub>2</sub>/Act. C catalyst and found contamination with sulfur derivatives. However, they used a feed containing H<sub>2</sub>S as a reactant and hence, it is not surprising that some 'sulfur slip' occurs. What is interesting is that as the feed is shifted to H<sub>2</sub>S-free stream, there is a linear decreasing trend of sulfur contamination in the liquid products.

As described before, clay supported Co-MoS<sub>2</sub> catalysts have been known to perform better. A comparison is presented in Table 3-7 between a K<sub>2</sub>CO<sub>3</sub> doped CoMoS catalyst and the same catalyst diluted/supported with clay at a catalyst:clay = 80:20 ratio on weight basis.

For the clay diluted catalyst, surprisingly, the catalyst performance is virtually the same when compared with the undiluted catalyst at similar operating conditions. Note that the catalyst performance is compared based on total weight of catalyst and is **not normalized** to 'active metal content'. This is possibly due to the reason described above in section 3.3.1, where by increase in metal content after the optimum loading on the clay diluent does not significantly increase the alcohol yields and selectivity.

Catalyst	CoMoS+K <sub>2</sub> CO <sub>3</sub>			CoMoS+K <sub>2</sub> CO <sub>3</sub> /clay
	310	315	330	330
Temp, °C	310	315	330	330
Pressure, atm	91	89	90	89
CO/H <sub>2</sub>	1	1	1	1
GHSV, L/kg.cat/hr	3000	3000	3000	3000
<b>Space time Yield (STY), g/kg.cat/hr</b>				
Methanol	130.2	118.6	107.6	115.7
Ethanol	116.6	123.3	128.2	130.0
Propanol	28.9	43.4	71.9	71.4
DME	0.0	0.0	2.7	4.4
Methane	16.5	22.0	31.2	34.4
Ethane	1.5	1.9	2.7	9.1
Total Alcohol	275.8	285.3	325.8	327.3
C <sub>2+</sub> /C <sub>1</sub>	1.1	1.4	2.0	1.8
<b>Molar yield, mol/kg.cat/hr</b>				
Total Alcohols	7.1	7.1	7.6	7.8
Total Alkanes	1.1	1.5	2.2	2.7
Othe oxygenates	0.1	0.1	0.2	0.2
<b>Conversion, %</b>				
	15.4	17.5	22.6	24.6
<b>Selectivity, CO<sub>2</sub> free basis</b>				
Methanol	48.9	42.6	33.8	33.9
Ethanol	30.5	30.8	28.0	26.5
Propanol	5.8	8.3	12.0	11.1
Methane	12.4	15.8	19.6	20.2
Ethane	0.6	0.8	1.0	3.1
Propane	0.0	0.0	0.0	1.9
Total Alcohols	85.2	81.7	76.2	73.1
Total Alkanes	13.7	17.3	22.0	25.4
Other oxygenates	1.1	1.0	1.8	1.5

Table 3-7 Performance evaluation of CoMoS type catalysts. K<sub>2</sub>CO<sub>3</sub> loading at 10 wt%.



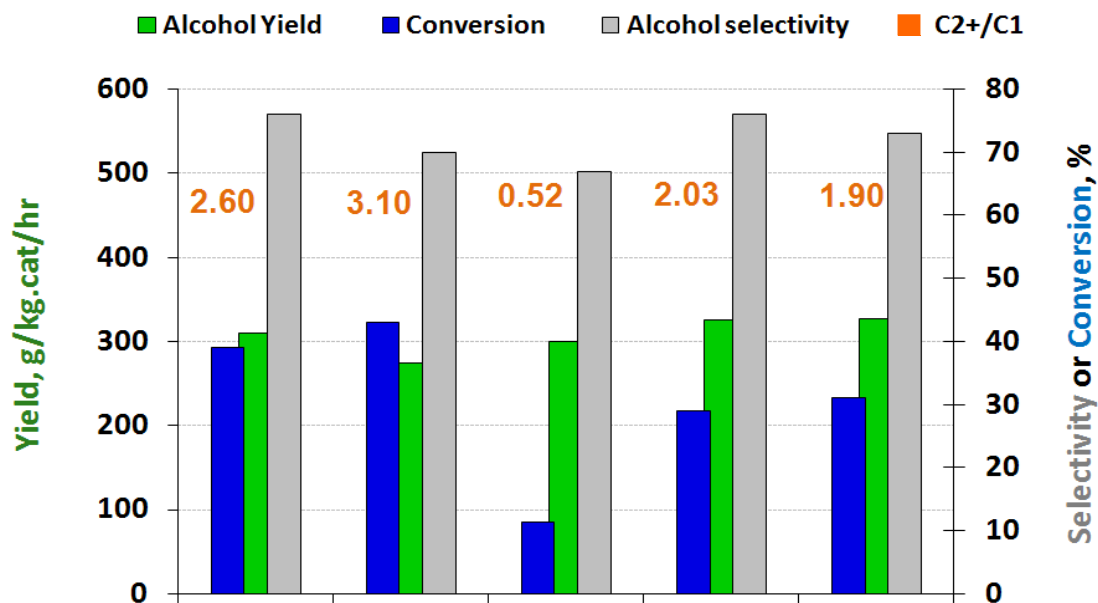
For CP.8.1, note that alkali was introduced twice: first before calcination and second after calcination. Why that was done should be obvious from Table 3-8; Catalysts prepared with  $K_2CO_3$  addition before calcination, gave no significant alcohol activity. But the same catalyst, when physically mixed with an additional amount of  $K_2CO_3$  gave much greater alcohol selectivity.

Alcohol selectivity increases from **14% to 91%**, while the alkane selectivity reduces correspondingly. This is also exhibited in the overall decrease in CO conversion. The K:Mo and Co:Mo ratios for CP.8.1 were also confirmed via SEM/EDS and TEM/EDS characterization studies. EDS results show that despite starting the catalyst synthesis with a Co/Mo ratio of 0.5 (of precursor salts) the eventual Co/Mo in the final catalyst is 0.2. A similar problem was also observed by Iranmahboob<sup>[61]</sup>: to obtain a Co/Mo=0.5 ratio, the precursor materials should have a starting ratio Co/Mo=1. Despite the fact that the Co/Mo is not at the optimum, CT.29B compared well with reported catalysts; even better at higher GHSVs.

Before doping with additional amount of  $K_2CO_3$ , the K:Mo ratio was at **0.42**, which is not far from the intended **0.5**. This catalyst is referred to as 29thA. After doping an additional 10wt% of  $K_2CO_3$  (relative to the catalyst weight), the K:Mo increased to an average of **0.90**. Alkali amounting to 10 wt% on a CoMoS catalyst would give a K:Mo of 0.35; thus the total enrichment, theoretically, should be **0.77** (0.42+0.35), instead of **0.90**. However, the catalyst was characterized after its use and catalyst surface enrichment with K does take place. What is important is that a K:Mo ratio of ~0.5 is considered to be an optimum for alcohol synthesis. However, as revealed in this experiment, the optimum ratio depends upon the mode and sequence of alkali addition. The optimum ratio for this catalyst appears to be around K:Mo = 1.

<b>Catalyst</b>	<b>29<sup>th</sup>-A</b>	<b>29<sup>th</sup>-B</b> K <sub>2</sub> CO <sub>3</sub> added again
Temp, °C	295	300
Pressure, atm	68	68
CO/H <sub>2</sub>	1	0.5
GHSV, L/kg.cat/hr	6000	6000
<b>Space time Yield (STY), g/kg.cat/hr</b>		
Methanol	2.2	72.2
Ethanol	18.7	26.0
Propanol	0.0	0.0
Methane	12.1	4.7
Ethane	13.8	0.2
Propane	32.2	0.0
Butane	23.7	0.0
Total Alcohols	20.9	98.2
Total Alkanes	133.6	4.7
<b>Conversion, %</b>		
	<b>4.6</b>	<b>4.6</b>
<b>Selectivity, CO<sub>2</sub> free basis</b>		
MeOH	2.1	71.2
EtOH	12.2	17.8
PrOH	0.0	0.0
Total Alcohols	14.3	89.1
Total Alkanes	85.5	9.9
Other oxygenates	0.2	1.0

*Table 3-8 Effect of additional alkali salt doping post-calcination: product selectivity shifts from alkanes to alcohols*



	CoMoS+ K <sub>2</sub> CO <sub>3</sub> /clay <sup>[1]</sup> <sub>31</sub>	CoMoS+ K <sub>2</sub> CO <sub>3</sub> /clay <sup>[6]</sup> <sub>11</sub>	Cs- MoS <sub>2</sub> <sup>[45]</sup>	CoMoKS + K <sub>2</sub> CO <sub>3</sub>	CoMoKS+ K <sub>2</sub> CO <sub>3</sub> /clay
Temp, °C	305	300	295	330	330
Pressure, atm	105	136	85	89	90
CO/H <sub>2</sub>	1.0	0.9	1	1	1
GHSVs, L/kg.cat/hr	2000 <sup>†</sup>	3000 <sup>†</sup>	7760	3000	3000

Figure 3-18 Comparison between reported alcohol synthesis catalysts of CoMoS type

<sup>†</sup> GHSV converted from hr<sup>-1</sup> basis by using a catalyst density of ~0.66 g/cc

SEM and TEM image reveal a very non-homogeneous size and shape distribution of Co-MoS<sub>2</sub> particles. From the SEM in Figure 3-19, it can be seen that there are smaller spherical particles distributed on top of big slab like particles/layers. These are the CoMoS and the MoS<sub>2</sub> phase, respectively. It is believed that the Co is incorporated as a CoMoS mixed phase, which itself is supported on the MoS<sub>2</sub> phase<sup>[59, 63]</sup>. For the CoMoS phase, there is a consistency in size and shape, 200-300nm.

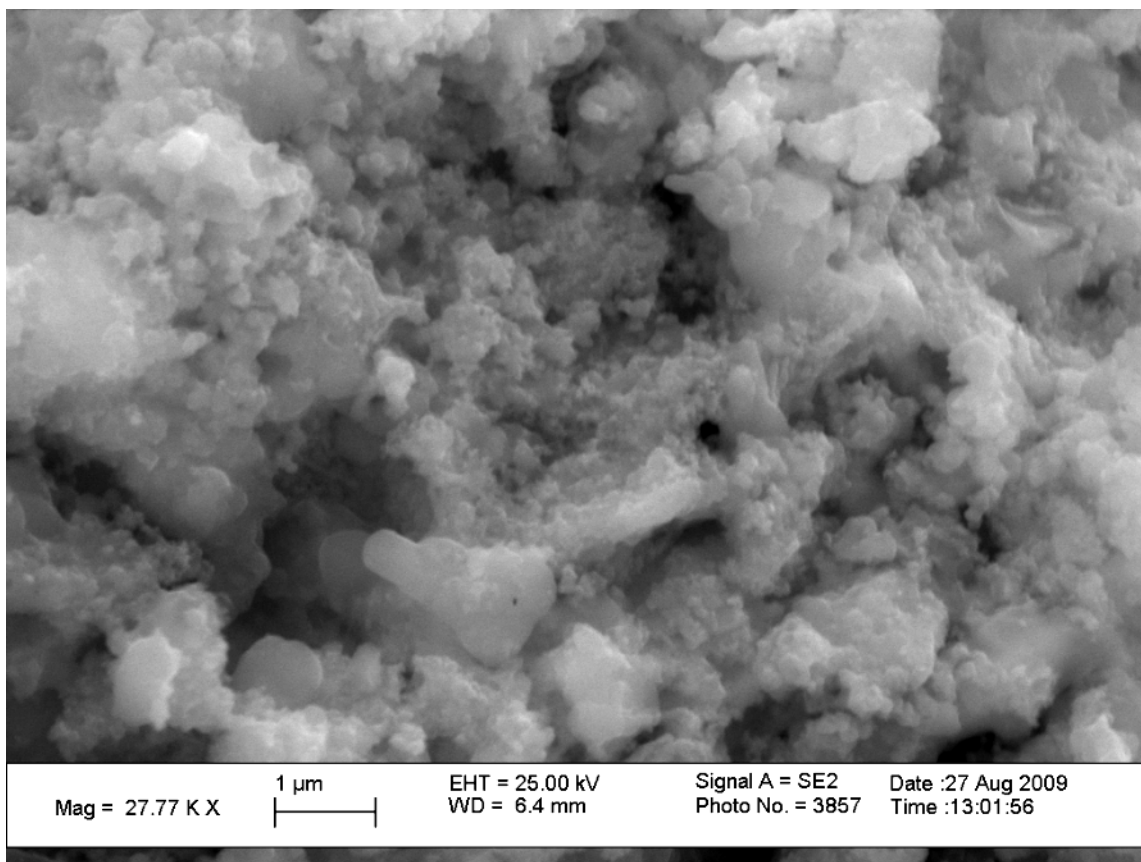


*Figure 3-19 SEM image of used catalyst CT.29U. The smaller particles are believed to be CoMoS mixed phase supported on MoS<sub>2</sub> layers*

TEM (Figure 3-20) micrograph also supports the above discussion: smaller particles are supported on larger slab like particles. EDS spectra reveal that the concentration of Co in these smaller particles is greater than in the bigger, slab like particles. Moreover it is seen that the smaller CoMoS phase, supported above the MoS<sub>2</sub> phase, exhibits strong fringe patterns at the edges/corners, showing its crystalline form. Earlier studies have revealed, that below a Co:Mo = 0.5 ratio, inclusion of Co in the MoS<sub>2</sub> material does not destroy the characteristic peaks of MoS<sub>2</sub> observed in XRD spectra<sup>[63]</sup>. The peak intensity is reduced, which points towards smaller crystal sizes. Indeed, it has been pointed out in numerous studies that Co can alter the physical structure of the MoS<sub>2</sub> slabs by inducing defects, which result in smaller crystallites and greater edges<sup>[64-65]</sup>.

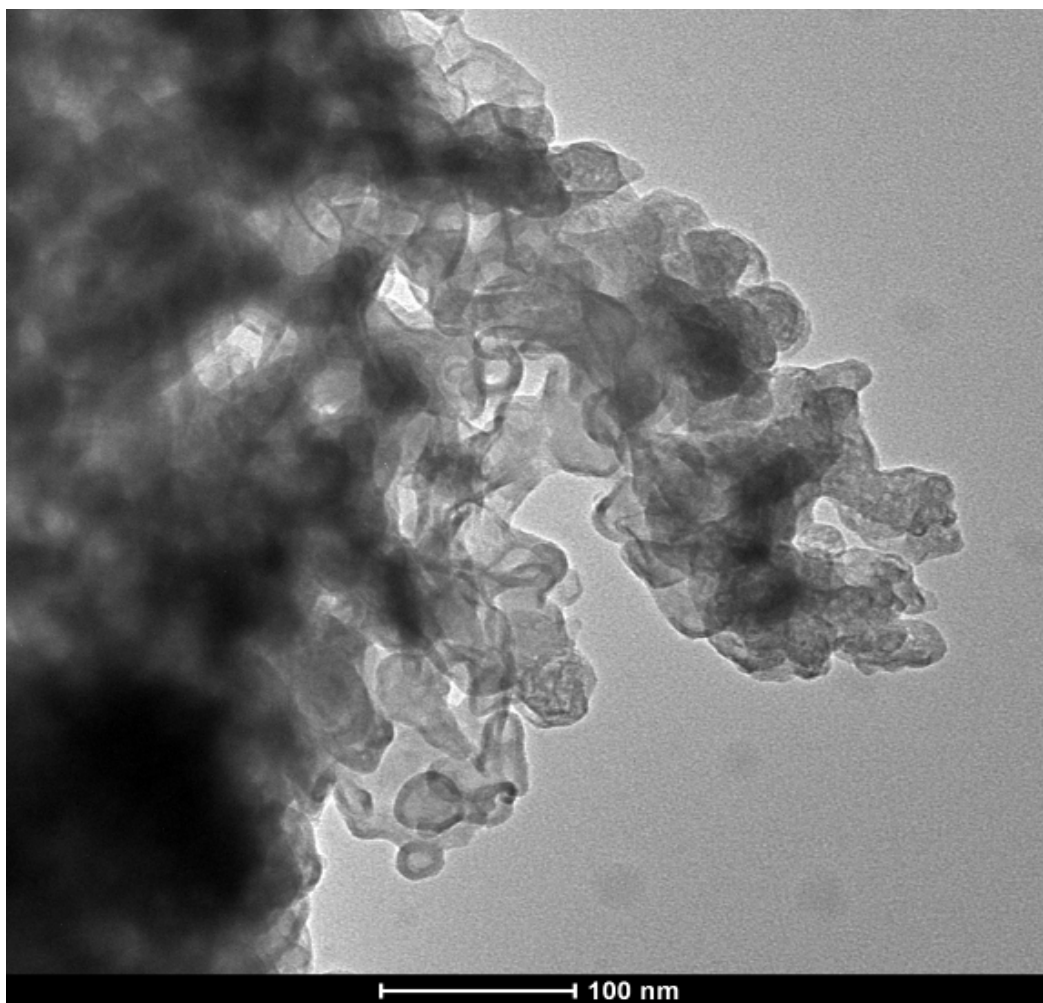


*Figure 3-20 TEM of CP.8.1. Smaller CoMoS particles display strong diffraction patterns at edges, characteristic of crystalline material*

FTIR spectra were also obtained for this catalyst (Figure 3-21), before and after the reaction. Peaks at  $620\text{ cm}^{-1}$  are associated with terminal Mo-S bonds or C-S bonds. Interestingly, this peak was stronger for used catalysts, indicating some transformation of the sulfur bonds

Infrared spectroscopy has been used previously to evaluate the effect of the alkali doping on MoS<sub>2</sub> catalyst.. Strong stretching occurs at the  $1300\text{-}1100\text{ cm}^{-1}$  for 'C-O' and around  $1700$

( $\pm 100$ )  $\text{cm}^{-1}$  for 'C=O' bond, depending upon the type of compound. These bonds are present in the carbonate salt, K-O-CO-O-K.

Peaks at **1130  $\text{cm}^{-1}$**  are strong which result from C-O stretching. Increased intensity of this peak can be associated to the surface enrichment with alkali, which occurs during the reaction.

Peaks at **1400  $\text{cm}^{-1}$**  and **1650  $\text{cm}^{-1}$**  are not prominent for CP.8.1. After additional alkali doping, these peaks become detectable. Over  $\text{MoS}_2$  catalysts, Woo<sup>[25]</sup> and Klier<sup>[45]</sup> identified these characteristic peaks as being responsible for enhancing the alcohol selectivity. Alkali salts that did not exhibit these peaks, 1650  $\text{cm}^{-1}$  (C-O-H) and 1400  $\text{cm}^{-1}$  (C-O-K), were not found to be active for alcohol formation, e.g. KCl and  $\text{K}_2\text{SO}_4$ . A similar behavior is noticed for this catalyst. What is probable is that the  $\text{K}_2\text{CO}_3$  introduced before catalyst calcination was subsequently decomposed. Although potassium was retained (as detected in SEM/EDS spectra), the conjugate salt was lost.

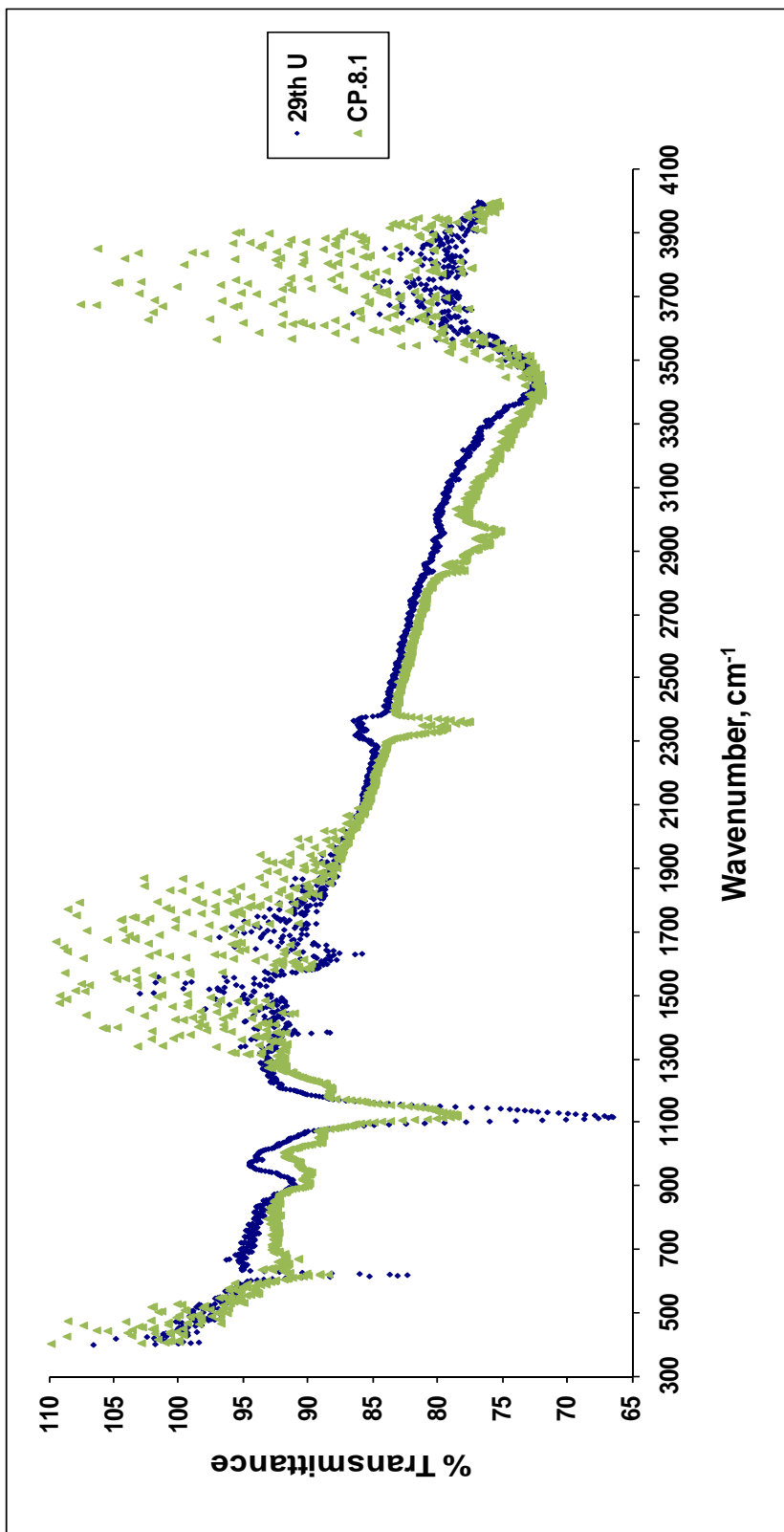


Figure 3-21 FTIR spectra of CP.8.1 (without alkali) and 29<sup>th</sup>\_U (CP.8.1. with alkali and post reaction)

### 3.3.4 EFFECT OF RHODIUM AS CO-PROMOTER

Although rhodium is an active catalyst for direct synthesis of C<sub>2</sub> oxygenate from syngas, it is also an effective promoter in Mo or MoS<sub>2</sub> based catalysts for CO hydrogenation. Synthesis of oxygenates from syngas was first reported by Foley<sup>[42]</sup> and Sudahakar<sup>[66]</sup> on a Rh-Mo/Al<sub>2</sub>O<sub>3</sub> catalyst. The incorporation of Mo in the Rh/Al<sub>2</sub>O<sub>3</sub> catalyst led to increase in the CO hydrogenation activity by **ten times**<sup>[66]</sup>. For Rh-Mo type catalyst, the bi-metallic interaction exhibits features different from either metal alone<sup>[67]</sup>.

Koizumi<sup>[68]</sup> developed sulfur tolerant catalyst for syngas conversion and found that Rh and Pd sulfide catalysts were active for methanol synthesis. They had appreciable activity and selectivity, which still did not compare well to the industrial Cu/ZnO types. But under a feed with a few ppm of H<sub>2</sub>S, the activity of the Cu catalyst reduced significantly, whereas that of Rh and Pd sulfides did not.

In CO hydrogenation, Rh can perform multiple functions and the extent of each function depends upon the support. Rh can adsorb CO associatively (forming methanol/alcohol) or dissociatively (forming hydrocarbons). Other functions are discussed earlier in section 1.4.2.1.

The Rh-MoS<sub>2</sub> catalyst tested was prepared from chelated precursors, which successfully limited the size of the MoS<sub>2</sub> slabs to less than 20 nm and provided a homogeneous size distribution. The nanosized catalyst gave a significant improvement in the selectivity and yield of alcohols (Table 3-9). The rhodium loading is based on a 1 wt% of MoS<sub>2</sub> or Rh:Mo=0.015:1. CP.6.2.1. was made by impregnating the catalyst with K<sub>2</sub>CO<sub>3</sub> solution, which corresponds to 18 wt.% loading of K<sub>2</sub>CO<sub>3</sub> on the Rh-MoS<sub>2</sub> or a K:Mo=0.5:1.

Some peculiar observations arising from the results are:

1. Ethanol selectivity is not high, but overall the C<sub>2+</sub> alcohol selectivity is good. At 350°C, CO<sub>2</sub> free C<sub>2+</sub> alcohol selectivity is **40% vs. 36%** for methanol. Over Rh promoted catalysts, this is considered a significant improvement.



2. Catalyst produced more alcohols when the CO:H<sub>2</sub> ratio was changed from 1.0 to 0.5. Production of higher alcohols also increased, which actually means that the catalyst was not limiting in C<sub>1</sub> to C<sub>2</sub> chain propagation as much as it was in production of the C<sub>1</sub> alcohol (i.e. methanol synthesis)

Catalyst	RhMoS+K <sub>2</sub> CO <sub>3</sub> /K-Y zeolite			
Temp, °C	335		350	
Pressure, atm	90		90	
CO/H <sub>2</sub>	<b>1.0</b>	<b>0.5</b>	<b>1.0</b>	<b>0.5</b>
GHSV, L/kg.cat/hr	6000		6000	
<b>Space time Yield (STY), g/kg.cat/hr</b>				
Methanol	63.3	191.6	102.5	182.8
Ethanol	31.6	103.9	63.7	127.2
Propanol	24.7	100.8	58.4	174.1
DME	4.4	6.4	4.0	5.8
Methane	23.8	26.0	35.8	39.2
Ethane	10.0	11.2	17.3	18.0
Total Alcohol	119.7	407.5	236.2	538.2
C <sub>2+</sub> /C <sub>1</sub>	0.9	1.1	1.3	1.9
<b>Molar yield, mol/kg.cat/hr</b>				
Total Alcohols	3.1	10.1	5.7	12.1
Total Alkanes	2.3	2.5	3.6	3.8
Other oxygenates	0.2	0.2	0.1	0.2
<b>Conversion, %</b>				
	7.4	19.4	11.7	23.7
<b>Selectivity, CO<sub>2</sub> free basis</b>				
Methanol	35.6	47.1	33.8	35.5
Ethanol	12.4	17.8	14.6	17.2
Propanol	7.4	13.2	10.3	18.0
Butanol	0.0	1.2	1.6	4.5
Methane	26.7	12.8	23.6	15.3
Ethane	6.41	3.1	6.5	4.0
Propane	4.5	2.2	4.4	2.4
Total Alcohols	55.3	79.4	60.5	75.6
Total Alkanes	41.9	19.3	38.1	23.4
Other oxygenates	2.8	1.3	1.3	1.0

Table 3-9 Performance of Rh-MoS<sub>2</sub> catalyst. Rh:Mo=0.015:1; K:Mo=0.5:1; 60%loading on KYzeolite

3. Alkane activity remained the same on change of CO:H<sub>2</sub> ratio, although total alkane selectivity went down (which is a relative property).
4. Rhodium enhances the alcohol activity of the MoS<sub>2</sub> based system. It's inclusion does not alter the product profile of the MoS<sub>2</sub> catalyst. Typical Rh/SiO<sub>2</sub> products (C<sub>2+</sub> oxygenates) are not observed in significant quantities over the Rh-MoS<sub>2</sub> catalyst.

Potassium amounts have not been optimized and it is probable that lower amounts would be the optimum. From the above, it is difficult to conclude whether H<sub>2</sub> adsorption was the rate limiting step because alkane activity remained the same. Generally, alkanes and methanol benefit the most when CO:H<sub>2</sub> = 0.5.

An alternative explanation can be provided in terms of CO adsorption: CO\* or C\*O\*. Rhodium can promote associative adsorption of CO depending upon the support. With SiO<sub>2</sub> it can be associative, whereas with Al<sub>2</sub>O<sub>3</sub> it is dissociative<sup>[69]</sup>. Ichikawa also commented that for rhodium based catalysts, the product spectrum varies with support. More basic supports favored alcohols, acidic favored alkanes<sup>[8]</sup>. This is inline with our earlier results (section 3.3.2), that by increasing the framework basicity, higher alcohol selectivities are achievable.

Thus, if CO dissociative adsorption is limiting, alkane synthesis from the classical FT mechanism of 'C\* + H\*' would be limiting. Alcohol formation, on the other hand, is according to CO\* insertion mechanism; thus the higher availability of CO\* (instead of C\*O\*) would also correspond to the increased amounts of C<sub>2+</sub> alcohols. It could simply be that alcohol synthesis was limited by the availability of the C<sub>1</sub> formyl intermediate specie, which is derived from methanol. If the catalyst is active enough, then methanol activity would obviously be better at the stoichiometric ratio of CO:H<sub>2</sub> = 0.5.

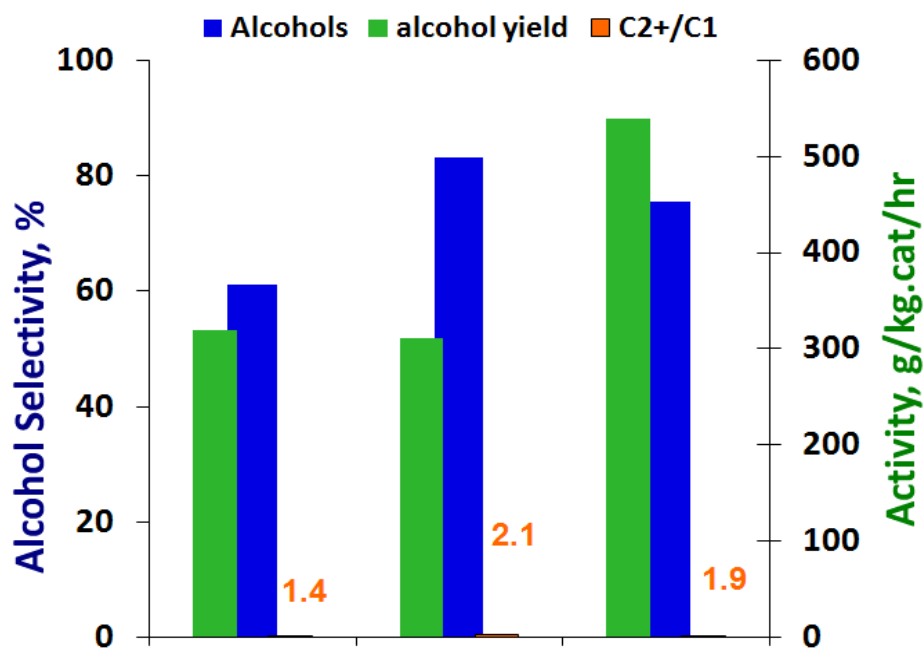
This explanation is rife with speculation though. Amongst other things, it also assumes that the acyl intermediate is more stable than the alkyl intermediate; acyls form alcohols and alkyls form alkanes

(see Figure 1-5) OR that H• addition to alkyl specie is still limiting. This would be despite the fact that an increased amount of adsorbed hydrogen is now available as the CO:H<sub>2</sub> ratio decreases from 1.0 to 0.5. However, this could be due to the basic environment provided by the support. Additional in-depth research would be needed to probe and confirm the beneficial effect of increased support basicity on stabilization of the intermediates.

For higher alcohol synthesis Storm<sup>[70]</sup> and Li<sup>[67]</sup> have studied catalysts containing Rh as a co-promoter. Storm et. al. compared a K/Co/Mo/Al<sub>2</sub>O<sub>3</sub> with a K/Rh/Co/Mo/Al<sub>2</sub>O<sub>3</sub> catalyst and tested out supports like SiO<sub>2</sub>, MgO and alumina. The Rh doped catalyst performed better, not necessarily for higher alcohols though. At lower K loadings, alcohol yields of 1,100 g/kg.cat/h with a 80% selectivity could be obtained, but methanol was dominant in the products. Attempts to increase higher alcohol selectivity reduced total alcohol yields to almost the same as that without Rh. Amongst the supports tested, Al<sub>2</sub>O<sub>3</sub> was found to be the better support as it gave a higher total alcohol yields and higher alcohol selectivity. Fig 4.2.6 compares performance of this catalyst with others reported in literature.

Li et. al. used sulfided Rh/Mo/Al<sub>2</sub>O<sub>3</sub> catalysts, with an optimized loading of 0.5 wt%. Rh incorporation alters the properties of Mo metal by:

- Altering the electronic distribution of the Mo species
- Enhancing interaction between metal and support, stronger Mo-O bonds
- Changing orientation of MoS<sub>2</sub> slabs relative to the support and enhancing dispersion. Instead of interacting with the support through its basal planes, a perpendicular orientation of the MoS<sub>2</sub> is achieved, which exposes greater edge sites to the reacting species.



	RhCoMoK / Al <sub>2</sub> O <sub>3</sub> <sup>[70]</sup>	RhMoK-S / Al <sub>2</sub> O <sub>3</sub> <sup>[67]</sup>	RhMoK-S / K-Y zeolite
Temp, °C	350	350	350
CO/H <sub>2</sub>	0.5	0.5	0.5
GHSV, hr <sup>-1</sup>	<b>14,400</b>	<b>28,000</b>	<b>4,000</b>

Figure 3-22 Performance comparison of between different Rh-Mo based systems

TEM image (Figure 3-23) shows that the synthesis procedure was successful in limiting the size of the MoS<sub>2</sub> particles. These are essentially agglomerates of nano-sized particles with the agglomerate size being restricted to < 20 nm. Moreover, there is a narrow size distribution, which as discussed in section Effect of Metal Loading, is particularly valuable. Elsewhere<sup>[71-72]</sup>, sonochemical synthesis methods resulted in average sizes of 15-20 nm. These are considered significant improvements over conventional techniques where the agglomerates increase to 100-200 nm<sup>[73-74]</sup>. These agglomerates usually bundle together into larger irregular shapes.

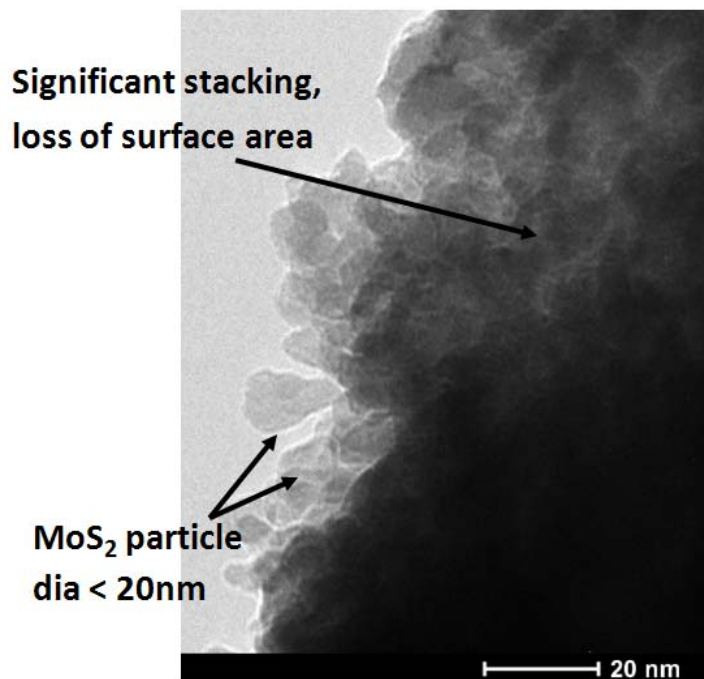


*Figure 3-23 TEM of CP.6.2, indicating nanosized MoS<sub>2</sub> particles. Darker areas show MoS<sub>2</sub> layers stacked on top of one another*

SEM micrograph (Figure 3-24) indicates severe stacking of the MoS<sub>2</sub> layers for CP.6.2 . BET analysis of this catalyst showed a very low surface area of 2 m<sup>2</sup>/g. However, the performance of this catalyst with respect to HAS is extraordinary. Due to the nanosize of the catalyst particles and severe stacking, this catalyst has a high ratio of edge area/basal area. In HDS, it is now well recognized that a higher ratio of edge area/basal area results in greater edge sites. The edge sites, according to the Topsoe CoMoS model, are responsible for breaking the C-S and S-S bonds of the sulfur compounds, and thus imparting desulfurization capacity to these HDS catalysts <sup>[48, 64, 75]</sup>. Chianelli <sup>[47]</sup> reported that due to the anisotropic layered structure of MoS<sub>2</sub>, HDS activity does not correlate well with BET surface area. Better agreement was seen between HDS activity and O<sub>2</sub> chemisorption of the HDS catalyst. Such explanations can also be extended to the Rh-MoS<sub>2</sub> catalyst, as despite having a low surface area, the HAS activity is very high.

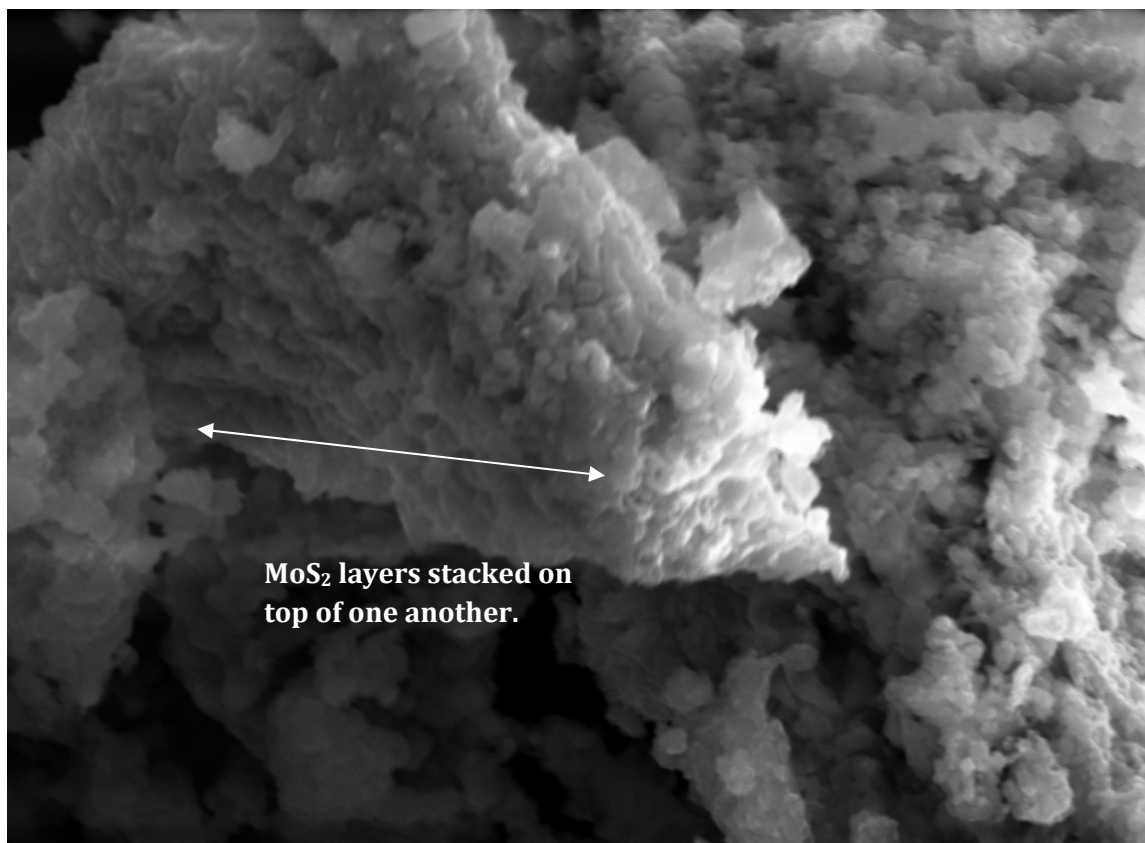


*Figure 3-24 SEM of CP.6.2 (Rh- MoS<sub>2</sub> particles). A MoS<sub>2</sub> high rise is visible*

Average compositions revealed by SEM/EDS suggest that a perfect stoichiometry of 1:2 between Mo:S is not achieved:

$$\text{K:Mo} = 0.45:1$$

$$\text{Mo:S} = 1:1.6$$

Rh – below detection limit of EDS

This could be effect of the chelating agent as it provides a slow release of Mo ions and discourages fast sulfidation. It could also be that rhodium modifies the MoS<sub>2</sub> structure. Li<sup>[67]</sup> reported that Rh modified the MoS<sub>2</sub> crystal orientation and Mo-support interaction.

### 3.3.5 EFFECT OF COPPER AS CO-PROMOTER

Copper is an industrial catalyst for methanol synthesis and is also an extremely good higher alcohol synthesis catalyst as discussed in section 1.4.2.2. It has been used as the co-promoter in modified FT catalyst, discussed in section 1.4.2.3. However, in conjunction with MoS<sub>2</sub>, there have been no reports of use of copper as a promoter. CuS is not known to be of catalytic importance, in fact Cu catalysts are the most sensitive to sulfur poisoning and usually do not regain their activity after poisoning.

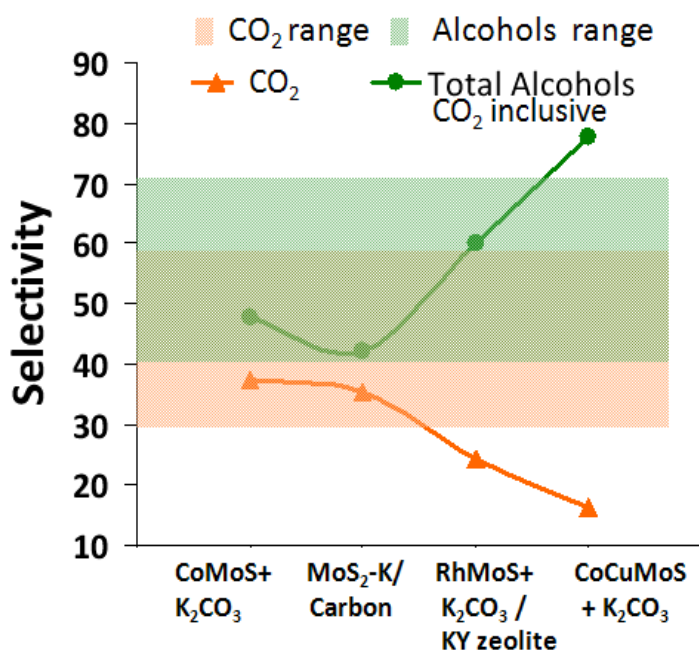


Figure 3-25 CO<sub>2</sub> inclusive selectivities of different catalysts tested. Shaded regions depict normal ranges reported in literature. Similar operating conditions of 330°C, 90 bar, 3000 h<sup>-1</sup>, CO/H<sub>2</sub>=1

Our experimentation with a CuCoMoS catalyst showed that Cu did not necessarily enhance the activity of the catalyst nor altered the product portfolio, but significantly decreased CO<sub>2</sub> generation. Figure 3-25 compares this catalyst to other catalysts tested in-house with comparable performances. Use of CO<sub>2</sub> inclusive alcohol selectivities, instead of CO<sub>2</sub> exclusive selectivities, presents a much broader picture in terms of the whole syngas conversion process. It accounts for net carbon utilization and overall

GHG emissions associated with the process. It is seen that addition of Cu to the CoMoS catalyst significantly improves the total alcohol selectivity.

<b>Catalyst</b>	<b>CuCoMoS+8wt% K<sub>2</sub>CO<sub>3</sub></b>		
Temp, °C	330	330	350
Pressure, atm	90	90	90
CO/H <sub>2</sub>	1	1	1
GHSV, L/kg.cat/hr	1500	3000	3000
<b>Space time Yield (STY), g/kg.cat/hr</b>			
Methanol	28.2	118.8	104.6
Ethanol	68.9	150.1	137.0
Propanol	40.2	29.5	34.3
DME	0.0	0.0	0.0
Methane	9.6	8.3	17.2
Ethane	1.0	0.7	1.6
Total Alcohol	141.7	298.4	275.9
C <sub>2+</sub> /C <sub>1</sub>	4.0	1.5	1.6
<b>Molar yield, mol/kg.cat/hr</b>			
Total Alcohols	3.1	7.5	6.8
Total Alkanes	0.6	0.6	1.2
Other oxygenates	0.0	0.0	0.1
<b>Conversion, %</b>			
	16.4	13.6	15.7
<b>Selectivity, CO<sub>2</sub> free basis</b>			
Methanol	23.3	45.9	40.6
Ethanol	39.5	40.4	37.0
Propanol	17.6	6.1	7.1
Methane	15.8	6.4	13.4
Ethane	0.9	0.3	0.7
Total Alcohols	82.4	92.6	85.0
Total Alkanes	17.0	6.8	14.3
Other oxygenates	0.7	0.6	0.7

*Table 3-10 Performance of CuCoMoS catalyst. Cu:Mo=0.2:1; Co:Mo=0.4:1; 8wt% K<sub>2</sub>CO<sub>3</sub>*

Table 3-10 details the performance of this catalyst. Even at high temperatures CO<sub>2</sub> yields were not significant. Over MoS<sub>2</sub> based catalysts this represents a significant improvement in carbon utilization. If the results are compared to CoMoS catalyst (Table 3-7), it is clear that along with an improvement in



overall alcohol selectivity and carbon utilization, there is decline in catalyst activity (or CO conversion). This decline in activity is due to a decline in alkane formation and corresponding decline in CO<sub>2</sub> production. The alcohol activity is also affected but not significantly. This can be due to the lower starting ratio of Co:Mo=0.4 vs. 0.5 for the CoMoS catalyst. Nonetheless, it is evident that the addition of copper significantly improved the alcohol selectivity. Another significant effect was the reduced quantity of alkali dopant necessary for selective alcohol production. Alkali doping reduces surface area of the final catalyst.

However, it is interesting to discuss the production of CO<sub>2</sub> associated with HAS and the reason for reporting selectivity on a CO<sub>2</sub> free basis. Under steady state conditions, CO<sub>2</sub> is only produced as a result of WGS (from H<sub>2</sub>O & CO) or if the oxygen rejection associated with product formation is directly as CO<sub>2</sub>, instead of H<sub>2</sub>O (Eq.1-13 to Eq.1-17). Because the WGS is at equilibrium over MoS<sub>2</sub> catalysts and in the forward direction at our operating temperatures <sup>[76-77]</sup>, most of the water produced as a side product is converted to CO<sub>2</sub>. Oxygen rejection (or CO<sub>2</sub> production) is a direct measure of the productivity of a catalyst. If the alcohol productivity over this CuCoMoS catalyst is similar to CoMoS catalyst and if the water content in the liquid products from both catalysts is similar too, then what would the reason be for the low CO<sub>2</sub> production observed over this CuCoMoS catalyst? A closer look at the products formed in Table 3-10 vs. Table 3-7 furnishes these answers:

1. **Lower alkane formation:** The reaction stoichiometry reveals (Eq.1-13 to Eq.1-17) that any alkane produced will reject one more mole of oxygen than a corresponding alcohol. Lower alkane formation over Cu promoted catalyst translates to lower CO<sub>2</sub> production.
2. **Decreased Higher alcohols/alkanes:** Higher carbon products reject even more oxygen. Actually, from C<sub>2</sub> onwards, every carbon added into the chain is accompanied by an oxygen rejection. Thus lower the amount of higher carbon products, lower would be the carbon dioxide produced

One of the reasons for increased activity in Cu catalysts used for higher alcohol synthesis could be its **inherent ability for associative adsorption of CO** <sup>[78]</sup>. FT catalysts and MoS<sub>2</sub> will activate both H<sub>2</sub> and CO dissociatively, whereas in the linear chain growth scenario where higher alcohols are produced via CO insertion, associatively adsorbed CO is required. This also coincides with one of the prime functions of alkali addition: suppression of the dissociative adsorption of CO in favor of associative adsorption. Thus, the higher availability of associatively adsorbed surface CO species, due to Cu addition, provides for better alcohol selectivity and reduced amounts of alkali.

An ethanol yield of **150 g/kg.cat/hr** and ethanol selectivity of **40%** (34% CO<sub>2</sub> inclusive) are one of the highest reported values in previous literature. Due to the extremely narrow product distribution, methanol recycle would have significant effects as it would promote ethanol formation dominantly.

### **3.3.6 EFFECT OF ALKALI PROMOTER**

Sometimes a promoter can function as a poison by blocking the active sites responsible for by-product formation. Alkali metals have long been known as useful ingredients in heterogeneous catalysis for improving catalyst performance <sup>[79]</sup>. As early as 1924, alkali metals or salts were reported to be effective promoters for oxygenate synthesis by Fischer and Tropsch. Through numerous studies, it is now well understood that oxygenate/alcohol selectivity cannot be developed without alkali doping over catalysts active in CO hydrogenation. Thus, all families, other than noble metals, require some alkali doping for increased production of alcohols. It is not exactly clear how the alkali affects the alcohol selectivity; its multi-functional role is indeed plausible<sup>[45, 79]</sup>:

1. Suppression of surface acidity
2. Promotion of CO associative adsorption and insertion
3. Decrease in H<sub>2</sub> adsorption and insertion

#### 4. Altering surface characteristics, imparting stability to active species

Variation of alkali loading was limited in our experiments. Potassium carbonate,  $K_2CO_3$  was the alkali of choice. In one series of experiments, for the CuCoMo type catalysts (CT.32, CT.33, CT.34),  $K_2CO_3$  loading was varied. There was no suggestion available for optimum alkali loading as this is the first time such a catalyst was prepared.

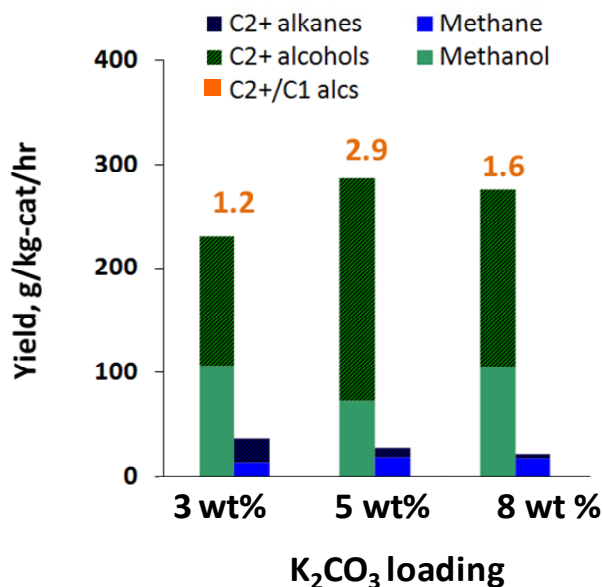


Figure 3-26 Effect of potassium loading on product yields over CuCoMoS catalyst. Similar operating conditions @  $350^\circ C$ , 88 atm,  $CO:H_2 = 1$  and  $GHSV=3,000 L/kg.cat/hr$

It can be seen in Figure 3-26 that the optimum  $K_2CO_3$  loading is 5 wt%. This is different from the 17 wt% reported for  $MoS_2$  catalyst<sup>[25, 77]</sup> and 12.5 wt% for Co- $MoS_2$  catalyst<sup>[61]</sup>. The different optimums vary because of the role the alkali performs. Better said, the optimum varies with the balance of various functions performed by the alkali dopant. In this case, as the ‘**CO associative adsorption**’ function is also performed by the copper, a lower amount of alkali is needed for the same. Any additional amount would lead to excessive surface coverage by CO and the reaction could become limiting in  $H_2$  adsorption.

Also note that the relative amounts of higher alcohols to methanol, reflected by the  $C_{2+}/C_1$  ratio (fig 4.2.8), also changes with the alkali loading. Again, this might represent an additional function which the alkali is performing. Klier<sup>[45]</sup> also claimed that the alkali functioned in carbon chain growth.

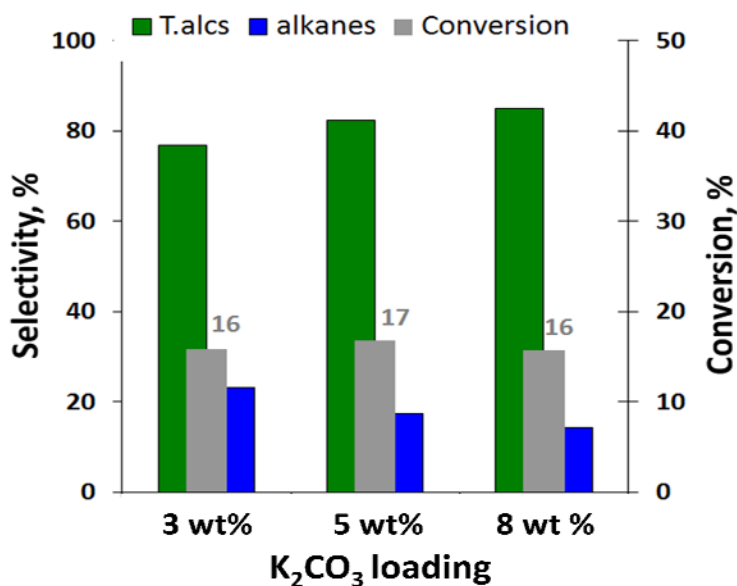
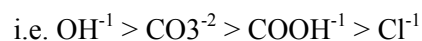


Figure 3-27 Effect of potassium loading on catalytic performance of CuCoMoS. Similar operating conditions @ 350°C, 88 atm,  $CO:H_2 = 1$  and  $GHSV=3,000 L/kg.cat/hr$

Figure 3-27 shows the variation in product selectivity with alkali loading. Whereas the conversion remains the same, overall alcohol selectivity increases.

Woo and Klier<sup>[45]</sup> correlated the effect of pKa of alkali with the doped salt and alcohol activity. It was noticed that alcohol yield increased as the basicity of the conjugate ion increased,



On the other hand basicity of the alkali ion itself is also a contributor. Subramani<sup>[80]</sup> in their review have pointed out the following order:



However, no matter what the alkali metal, a maxima will be observed in the alcohol yield; additional alkali doping will negatively affect the alcohol yields<sup>[27]</sup>. It would appear that the only benefit

of using a more basic ion is to reduce the amount of dopant for achieving the ‘optimum performance’, which a less basic alkali would eventually achieve with increased doping (Cs vs. K). Thus, one can find different researchers having different alkalis as the best promoter for alcohol synthesis.

Woo et. al. <sup>[25]</sup> commented on alkali post-addition techniques, specifically physical mixing and impregnation of  $K_2CO_3$  solutions. They found no difference in activity or selectivity for both techniques. Tatsumi <sup>[81]</sup> reported that co-impregnation of  $K_2CO_3$  and Mo on  $SiO_2$  favored hydrocarbon formation and was not as effective for alcohol production as post impregnation. A similar effect was observed in our catalyst synthesis and discussed in section 3.3.3. Catalysts that had  $K_2CO_3$  added to them before calcination, by either physical mixing or impregnation, did not provide much activity for alcohols. The same catalyst when removed and physically mixed with  $K_2CO_3$  became selective to alcohol formation.

Optimum alkali/metal ratio also varies with type of catalyst and interestingly with researching group. Ranges of 0.4-1.2 (K/Mo) are seen. For Dadyburjor’s group, who develop their sulfided catalysts by an in-situ sulfidation procedure involving exposure to  $H_2S$  gas at high temperatures, alkali doping is before the calcination/sulfidation step. Optimum K/Mo for their catalysts is on the higher side; K/Mo = 1-1.3 <sup>[27, 29]</sup>. For researchers preferring the simple physical mixing of  $MoS_2$  (already sulfided) and  $K_2CO_3$ , the K/Mo ratios were optimal at 0.5 (also often referred to as 17 wt% loading of  $K_2CO_3$ ) <sup>[25, 77]</sup>. Li reported optimum K/Mo as 0.8, where they first impregnated with  $K_2CO_3$  first and calcined it at 300 °C <sup>[59]</sup>.

Here it is important to realize that the optimum K/Mo ratio would actually depend upon the catalyst. It is already different for the different families of catalysts.

Concerning the mechanism of alkali promotion, it is proposed that the alkali stabilizes the surface adsorbed CO, by increasing the interaction between the alkali metal (electron deficient) and electron rich oxygen of adsorbed CO. This results in weaker M-CO bonds, the stabilization of which requires electrons from the catalytic species, which results in weaker M-H bonds and therefore decreased  $H_2$  adsorption <sup>[25]</sup>.

Woo<sup>[82]</sup> also found that oxidized  $K_2CO_3/MoS_2$  samples (left in an open atmosphere for an extended period of time) lose their alcohol selectivity to alkanes. With transformation of potassium's conjugate by oxidation, potassium ions diffuse through the semi-crystalline  $MoS_2$  material. This enriches the metal species with electrons and increases the F-T activity. Papageorgopoulos<sup>[83]</sup> and Karolewski<sup>[84]</sup> also confirm the increased oxygen uptake by alkali doped  $MoS_2$ . The former also describes the alkali penetration into the subsurface and the later found increased dissociative adsorption of certain molecules.

From the above: metal electron enrichment leads to hydrocarbons

### ***3.3.7 EFFECT OF OPERATING CONDITIONS***

Operating conditions play an important part in this catalytic system. Not only do they affect the conversions and yields, they can also alter the product distribution. Depending upon their types, a catalyst can show a significant sensitivity to a particular operating variable. Results from operating condition analysis for **CT.22** are primarily presented and discussed.

#### **3.3.7.1 Pressure**

It would appear that pressure is one condition that least affects the catalyst performance. Its effect is to increase the conversion and activity. This is in accordance with the law of mass action: as there is a decrease in volume with progression of reaction, the reaction will move forward with increase in pressure. The sensitivity to pressure is the highest at low pressures, and as the system pressure increases, its effect becomes less and less

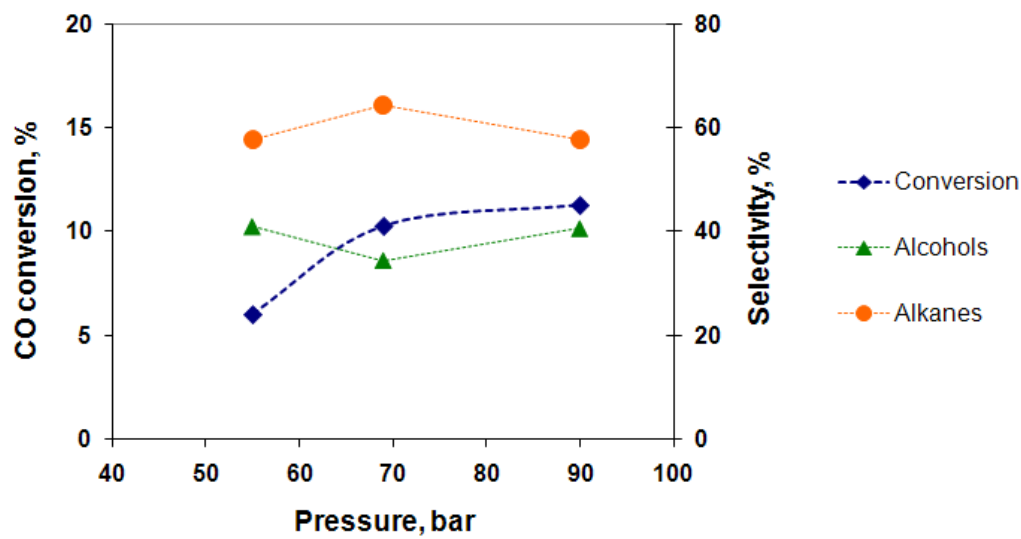


Figure 3-28 Effect of temperature on product yields,  $MoS_2+K_2CO_3/K-Y$  zeolite;  $\sim 90$ bar,  $CO:H_2=2$ , 6000 L/kg.cat/hr

Different catalysts might show increased dependence to pressure. The Rh- $MoS_2$  catalyst showed the least dependence on pressure. If some of the activity is imparted by Rh, then this is expectable, as rhodium is active even at lower pressures.

### 3.3.7.2 Temperature

Temperature plays a significant role in HAS. Increase in temperature upto an optimum leads to an increase in alcohol activity and selectivity. Further increase encourages alkane formation dramatically, methane being the most problematic. Significant increase in temperature can also decrease total alcohol yield due to greater activity of side reactions which consume alcohols depending upon the type of catalyst.

From Figure 3-29, increase in temperature drives alcohol productivity other than methanol and also alkane productivity. Figure 3-30 describes the effect of temperature on product selectivities. At temperatures higher than 315oC, alkane selectivity supersedes that of alcohol.

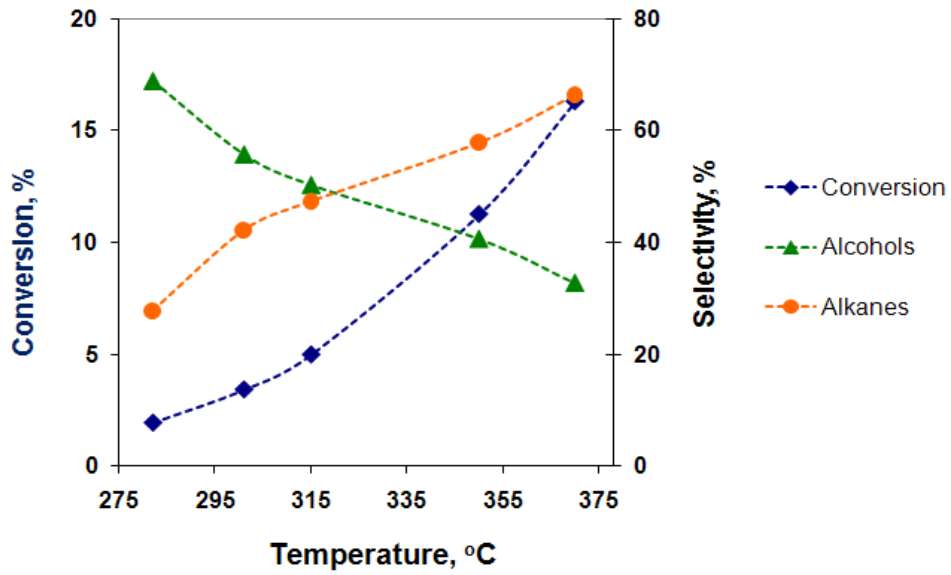


Figure 3-29 Effect of temperature on catalyst performance,  $\text{MoS}_2+\text{K}_2\text{CO}_3/\text{K-Y}$  zeolite; ~ 90bar,  $\text{CO}:\text{H}_2=2$ , 6000 L/kg.cat/hr

At higher temperatures, methanol production becomes constant Figure 3-30, as higher alcohols are preferred at higher temperatures. It is also interesting to note that majority of alkanes over this catalyst are alkanes other than methane. In other cases, methane is the dominant alkane.

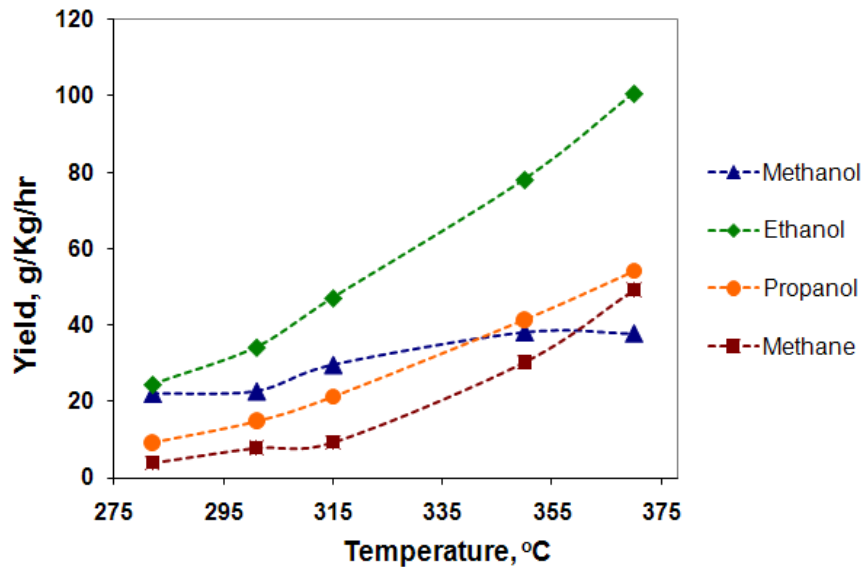
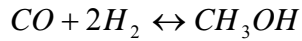


Figure 3-30 Effect of temperature on product yields,  $\text{MoS}_2+\text{K}_2\text{CO}_3/\text{K-Y}$  zeolite; ~ 90bar,  $\text{CO}:\text{H}_2=2$ , 6000 L/kg.cat/hr

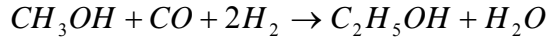


A look at the thermodynamics of the prominent reactions involved reveals the problem:

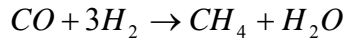
methanation



$$\Delta H_{298}^{\circ} = -90.5 \text{ kJ/mol} \quad \Delta G_{298}^{\circ} = -25.1 \text{ kJ/mol}$$



$$\Delta H_{298}^{\circ} = -165.1 \text{ kJ/mol} \quad \Delta G_{298}^{\circ} = -97.0 \text{ kJ/mol}$$



$$\Delta H_{298}^{\circ} = -205.9 \text{ kJ/mol} \quad \Delta G_{298}^{\circ} = -141.9 \text{ kJ/mol}$$

Methanation is highly favored at all temperatures and is also exothermic. Thermodynamic equilibrium sets in for methanol synthesis at 150°C and for ethanol at 280°C. Higher alcohols follow a similar trend, their equilibrium restrictions occur at increasing temperatures. Higher temperatures needed for greater C<sub>3+</sub> production can also produce significant methane (and higher alkanes)

The actual problem is kinetics, as the tendency of the catalyst to form alkanes is countered by alkali doping. Despite the fact that higher alcohols (C<sub>3+</sub>) are not limited by equilibrium at 300°C, the dominant alcohol is still methanol. The system is kinetically controlled and many have suggested the C<sub>1</sub>→C<sub>2</sub> alcohol formation the limiting step [29, 85].

Temperature dependence of the reaction rate is also plotted as an Arrhenius plot in . A straight line is obtained indicating a strong dependence on temperature. The activation energy, extracted from the plot, is 84 kJ/kmol. This value also indicates that the reaction is under ‘kinetic control’ and as a rule of thumb, is devoid of mass and heat transfer limitations. The activation energy is calculated from the slope of the straight line, according to the equation [34].

$$\ln k = -\frac{E}{R} \frac{1}{T} + \ln A_o \quad \text{Eq. 3-2}$$

$T$  = temperature, °K

$R$  = gas constant, kJ/kmol.°K

$E$  = activation energy, kJ/kmol

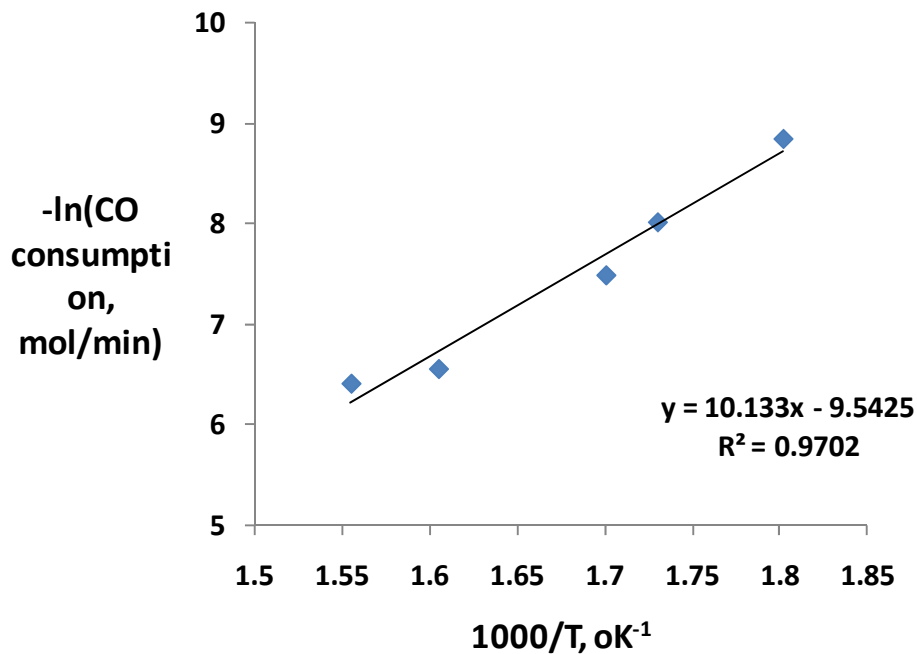


Figure 3-31 Arrhenius plot of reaction rate dependence on temperature.

### 3.3.7.3 Syngas ratio

Higher alcohols are favored at higher CO:H<sub>2</sub> ratios. As the CO partial pressure increases, more opportunities for ‘CO insertion’ into the acyl species (C<sub>x</sub>H<sub>(2x-1)</sub>O\*) become available. Another effect is the decrease in alkane and CO<sub>2</sub> formation and an overall decrease in CO conversion. However, very high CO:H<sub>2</sub> ratios are not effective in enhancing the alcohol selectivity nor are the feasible from the technical standpoint of syngas generation. Results are tabulated in Table 3-11.

Catalyst	MoS <sub>2</sub> +K <sub>2</sub> CO <sub>3</sub> /K-Y zeolite			
Temp, °C	350			
Pressure, bar	87	87	90	69
CO/H <sub>2</sub>	0.5	1	2	3
GHSV, L/kg.cat/hr	6000			
Space time Yield (STY), g/kh/hr				
Methanol	39.0	45.0	38.2	23.0
Ethanol	41.2	63.7	78.0	52.8
Propanol	16.0	31.3	41.5	26.2
DME	21.2	18.3	12.0	5.3
Methane	57.2	47.4	30.3	18.5
Ethane	45.0	44.4	34.6	23.5
Propane	57.2	67.9	55.3	39.7
Butane	39.2	62.5	59.3	43.9
Total Alcohol	102.9	160.1	197.8	141.3
C <sub>2+</sub> /C <sub>1</sub>	1.6	2.6	4.2	5.2
<b>Conversion</b>	21.3	16.6	11.3	6.9
<b>Selectivity, CO<sub>2</sub> free basis</b>				
Total Alcohols	25.5	32.7	40.6	40.4
Total Alkanes	72.2	65.3	57.8	58.5
Other oxygenates	2.2	1.9	1.6	1.1

Table 3-11 Effects of syngas ratio on catalyst performance

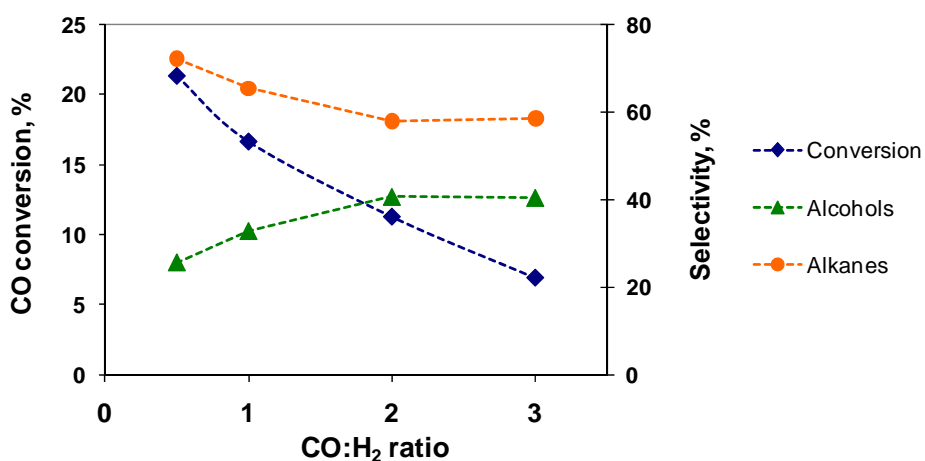


Figure 3-32 Effect of CO:H<sub>2</sub> ratio on catalyst performance, MoS<sub>2</sub>+K<sub>2</sub>CO<sub>3</sub>/K-Y zeolite; 350°C, ~ 90bar, 6000 L/kg.cat/hr

As seen in fig. 4.2.14, different catalysts respond differently to change in CO:H<sub>2</sub> ratio. It seems that, other than increasing the higher alcohol content in the liquid product, predicting catalyst performance with increase in CO:H<sub>2</sub> ratios strongly depends upon the catalyst characteristics.

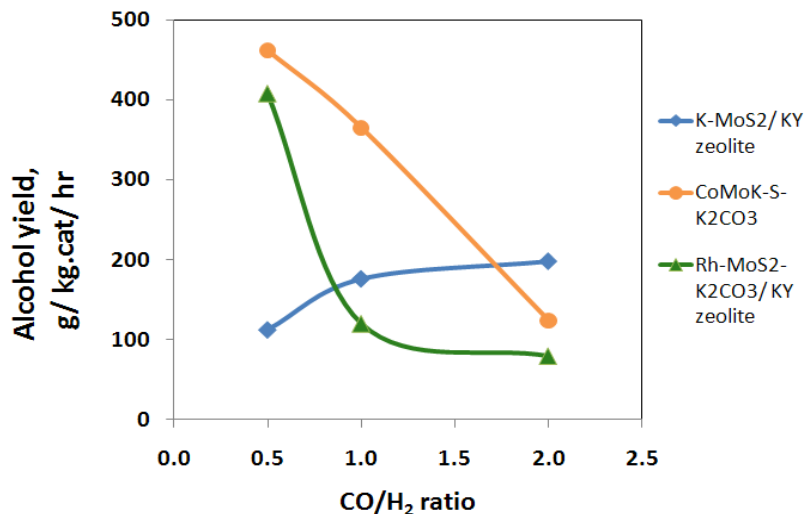


Figure 3-33 Comparison of alcohol yield over different catalyst as a function of CO:H<sub>2</sub>. Conditions: 330-350°C, ~ 90bar, 6000 L/kg.cat/hr

### 3.3.7.4 Gas Hourly Space velocity (GHSV)

Increase in feed flowrates decrease the CO conversion. Other than that it

- alters the product selectivity, promoting alcohols instead of alkanes
- decreases C<sub>2+</sub>/C<sub>1</sub> ratios for both alcohols and alkanes

The effect is the same for other catalysts as well: product selectivities do not vary much, whereas the conversion goes down. Within the alcohols, higher GHSV would favor more methanol as the residence time directly affects the successive homologies for higher alcohols. Methane activity does not vary much.

It is important to note that an optimum GHSV for a particular catalyst would depend upon the temperature. At higher temperatures, a higher GHSV might be required to lower the alkane selectivity/activity.

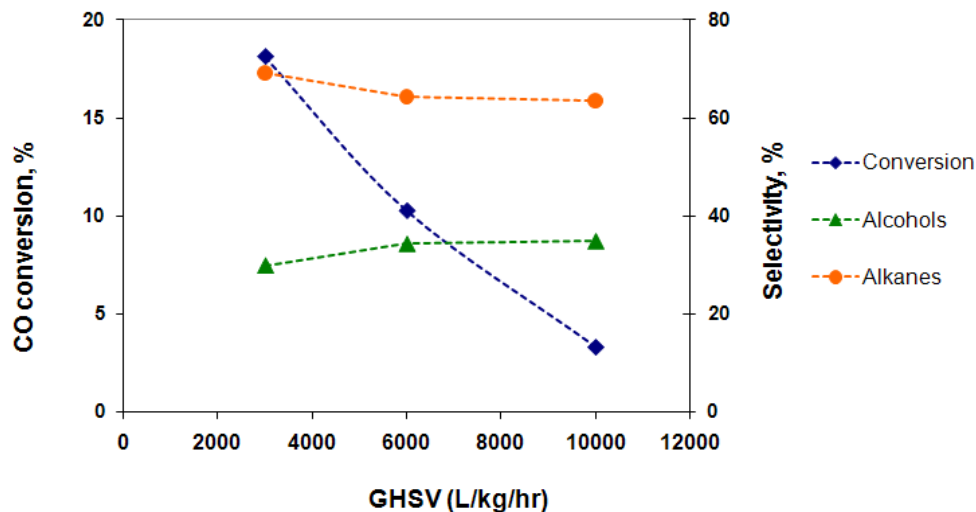


Figure 3-34 Effect of GHSV on catalyst performance,  $\text{MoS}_2 + \text{K}_2\text{CO}_3 / \text{K-Y zeolite}$ ;  $350^\circ\text{C}$ ,  $\sim 90\text{bar}$ ,  $\text{CO}:\text{H}_2=2$

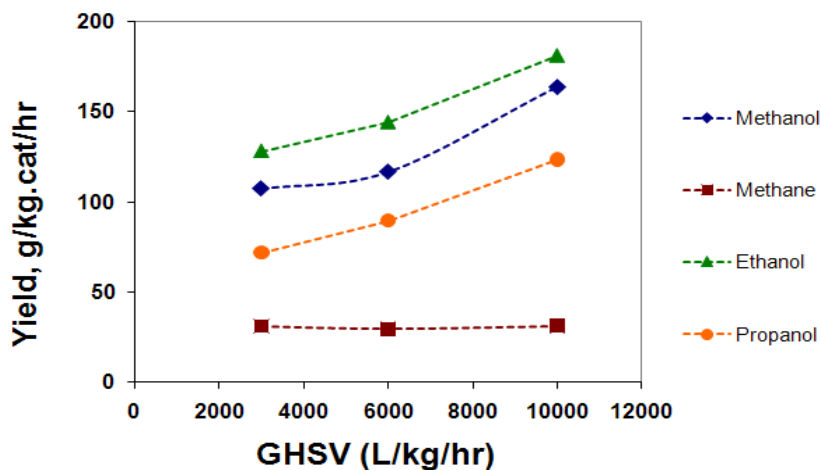


Figure 3-35 Effect of GHSV on product yields,  $\text{CoMoS} + \text{K}_2\text{CO}_3$ ;  $330^\circ\text{C}$ ,  $\sim 90\text{bar}$ ,  $\text{CO}:\text{H}_2=1$

### 3.3.7.5 Methanol recycle

In syngas based systems, the unconverted feed is recycled back to the reactor. One of the advantages in using  $\text{MoS}_2$  based catalysts is that methanol can be recycled as a feed along with syngas.

Over MoS<sub>2</sub> catalysts, C-O bond of methanol breaks down to give a methyl group. With ‘CO’ insertion this transforms into an acyl group, which upon subsequent hydrogenation gives ethanol. This scheme is represented in the mechanism described earlier (section 1.5). Santiestesban <sup>[86]</sup> used labeled methanol to study the mechanism of alcohol formation over alkali/Co-MoS<sub>2</sub> catalyst. An increase in both alcohols and hydrocarbons was observed. Gunturu <sup>[29]</sup> reached a similar conclusion upon injecting methanol into the feed stream over a K-Co/MoS<sub>2</sub>/Act.C catalyst.

Catalyst	CT.22 : CP.5.1+KY zeolite	
Temp, °C	350	350
Pressure, atm	1300	1300
CO/H <sub>2</sub>	2.0	2.0
GHSV, L/kg.cat/hr	6,000	6,000
% Methanol in feed	0	3
Space time Yield (STY), g/kg.cat/hr		
Methanol	38.2	76.7
Ethanol	78.0	106.7
Propanol	41.5	47.6
Butanol	40.0	54.1
DME	12.1	43.5
Methane	30.3	47.9
Ethane	34.6	37.9
CO <sub>2</sub>	443.5	598.8
C <sub>2+</sub> alcohols	159.0	208.6
C <sub>2+</sub> /C <sub>1</sub>	4.2	
Conversion, %	11.3	16.4

*Table 3-12 Increase in C<sub>2+</sub> alcohols over Ct.22 catalyst upon cofeeding methanol with syngas*

In one run with CT.22, methanol was injected into the feed stream at the tune of 3 volume % of the feed syngas. Besides an increase in both alkanes and higher alcohols, an increase in DME was observed. This is reasonable as dehydration of methanol to DME is a practiced art over zeolite materials (CT.22 consists of 60 wt% zeolite)

**Conversion increased from 11 to 16%, whereas a 33% increase in C<sub>2+</sub> productivity was witnessed.**

This shows that recycle of methanol can be an effective means of increasing higher alcohol yields. An MoS<sub>2</sub> based catalyst that offers good selectivity to alcohols should provide a good starting point for optimizing catalyst performance with methanol enriched syngas.

### 3.4 GLOSSARY

DME – DiMethyl Ether

ASF – Anderson-Schulz-Flory

EDS - [Energy-dispersive X-ray Spectroscopy](#)

EDAX – Company providing EDS instrument

FTIR – Fourier Transform InfraRed

HDS – HydroDeSulfurization

WGS-Water Gas Shift

HAS – Higher Alcohol Synthesis

SEM - [Scanning Electron Microscope](#),

TEM - [Transmission Electron Microscopy](#)

XRD – X-Ray Diffraction

XPS - [X-ray Photoelectron Spectroscopy](#), also known as ESCA



### 3.5 REFERENCES

1. Tropsch, H., *Problems in the chemistry of coal*. Chemical Reviews, 1929. **6**(1): p. 63-90.
2. Fischer, F., *The Conversion of Coal into Oils*. 1925: Ernst Benn Limited.
3. Frolich, P.K. and D.S. Cryder, *Catalysts for the formation of alcohols from carbon monoxide and hydrogen VI Investigation of the mechanism of formation of alcohols higher than methanol*. Industrial and Engineering Chemistry, 1930. **22**: p. 1051-1057.
4. Frolich, P.K. and W.K. Lewis, *Synthesis of alcohols higher than methanol from carbon monoxide and hydrogen*. Industrial and Engineering Chemistry, 1928. **20**(1): p. 354-359.
5. Anderson, R.B., J. Feldman, and H.H. Storch, *Synthesis of alcohols by hydrogenation of carbon monoxide*. Industrial and Engineering Chemistry, 1952. **44**(10): p. 2418-2424.
6. Wender, I., R. Levine, and M. Orchin, *Homologation of alcohols*. Journal of the American Chemical Society, 1949. **71**(12): p. 4160-4161.
7. Wang, J., et al., *Alcohol synthesis from CO/H<sub>2</sub> over Co/Cu/Zn/Al<sub>2</sub>O<sub>3</sub> - in-situ addition of CH<sub>3</sub>NO<sub>2</sub>*. Journal of Catalysis, 1995. **153**(1): p. 100-107.
8. Ichikawa, M., *Catalysis by supported metal crystallites from carbonyl clusters .2. Catalytic ethanol synthesis from CO and H<sub>2</sub> under atmospheric-pressure over supported rhodium crystallites prepared from Rh carbonyl clusters deposited on TiO<sub>2</sub>, ZrO<sub>2</sub>, and La<sub>2</sub>O<sub>3</sub>*. Bulletin of the Chemical Society of Japan, 1978. **51**(8): p. 2273-2277.
9. Ichikawa, M., *Catalytic synthesis of ethanol from CO and H<sub>2</sub> under atmospheric-pressure over pyrolyzed rhodium carbonyl clusters on TiO<sub>2</sub>, ZrO<sub>2</sub>, and La<sub>2</sub>O<sub>3</sub>*. Journal of the Chemical Society-Chemical Communications, 1978(13): p. 566-567.
10. Calverley, E.M. and R.B. Anderson, *Synthesis of higher alcohols over promoted copper-catalysts*. Journal of Catalysis, 1987. **104**(2): p. 434-440.
11. Smith, K.J. and R.B. Anderson, *The synthesis of higher alcohols on Cu/ZnO catalysts promoted with K<sub>2</sub>CO<sub>3</sub>*. Abstracts of Papers of the American Chemical Society, 1984. **188**(AUG): p. 68-FUEL.
12. Smith, K.J. and R.B. Anderson, *A chain growth scheme for the higher alcohols synthesis*. Journal of Catalysis, 1984. **85**(2): p. 428-436.
13. Stevens, R.R., *Alcohols from synthesis gas*. 1986, (Dow Chemical Co., USA). US 4,752,622. p. 31 pp.
14. Kinkade, N., *Tantalum containing catalyst useful for producing alcohols from synthesis gas*. Union Carbide: US patent 4994498, 1991.
15. Inamura, K., et al., *Preparation of active HDS catalysts by controlling the dispersion of active species*. Applied Surface Science, 1997. **121**: p. 468-475.
16. Alonso, G., et al., *Preparation of WS<sub>2</sub> catalysts by in situ decomposition of tetraalkylammonium thiotungstates*. Applied Catalysis a-General, 2000. **197**(1): p. 87-97.
17. Okamoto, Y. and H. Katsuyama, *Intrazeolite nanocomposite catalysts: Co-Mo Sulfides for Hydrodesulfurization*. AIChE Journal, 1997. **43**(S11): p. 2809-2819.
18. Vissers, J.P.R., et al., *Effect of the support on the structure of mo-based hydrodesulfurization catalysts - activated carbon versus alumina*. Journal of Catalysis, 1987. **105**(2): p. 277-284.
19. Okamoto, Y., et al., *Effects of support on the activity of Co-Mo sulfide model catalysts*. Applied Catalysis A: General, 2002. **226**(1-2): p. 115-127.
20. Coulier, L., et al., *Correlation between hydrodesulfurization activity and order of Ni and Mo sulfidation in planar silica-supported NiMo catalysts: The influence of chelating agents*. Journal of Catalysis, 2001. **197**(1): p. 26-33.
21. Medici, L. and R. Prins, *The influence of chelating ligands on the sulfidation of Ni and Mo in NiMo/SiO<sub>2</sub> hydrotreating catalysts*. Journal of Catalysis, 1996. **163**(1): p. 38-49.

22. Nicosia, D. and R. Prins, *The effect of glycol on phosphate-doped CoMo/Al<sub>2</sub>O<sub>3</sub> hydrotreating catalysts*. Journal of Catalysis, 2005. **229**(2): p. 424-438.
23. Mahajan, D., et al., *Sono synthesis and characterization of nano-phase molybdenum-based materials for catalytic hydrodesulfurization*. Applied Catalysis a-General, 2004. **258**(1): p. 83-91.
24. Yoneyama, Y. and C.S. Song, *A new method for preparing highly active unsupported Mo sulfide. Catalytic activity for hydrogenolysis of 4-(1-naphthylmethyl)bibenzyl*. Catalysis Today, 1999. **50**(1): p. 19-27.
25. Woo, H.C., et al., *Structure and distribution of alkali promoter in K/MoS<sub>2</sub> catalysts and their effects on alcohol synthesis from syngas*. Journal of Catalysis, 1993. **142**(2): p. 672-690.
26. Iranmahboob, J., H. Toghiani, and D.O. Hill, *Dispersion of alkali on the surface of CO-MoS<sub>2</sub>/clay catalyst: a comparison of K and Cs as a promoter for synthesis of alcohol*. Applied Catalysis a-General, 2003. **247**(2): p. 207-218.
27. Li, X.G., et al., *Higher alcohols from synthesis gas using carbon-supported doped molybdenum-based catalysts*. Industrial & Engineering Chemistry Research, 1998. **37**(10): p. 3853-3863.
28. Christensen, J.M., et al., *Effects of H<sub>2</sub>S and process conditions in the synthesis of mixed alcohols from syngas over alkali promoted cobalt-molybdenum sulfide*. Applied Catalysis A: General, 2009. **366**(1): p. 29-43.
29. Gunturu, A.K., et al., *A kinetic model for the synthesis of high-molecular weight alcohols over a sulfided Co-K-Mo/C catalyst*. Industrial & Engineering Chemistry Research, 1998. **37**(6): p. 2107-2115.
30. Schuth, F., B.E. Henry, and L.D. Schmidt, *Oscillatory reactions in heterogeneous catalysis*. Advances in Catalysis, Vol 39, 1993. **39**: p. 51-127.
31. Tsotsis, T.T., V.U.S. Rao, and L.M. Polinski, *Reaction-rate oscillations during fischer-tropsch synthesis on fe-precipitated Nu-1 zeolite-type catalysts*. Aiche Journal, 1982. **28**(5): p. 847-851.
32. Snel, R., *Supported iron catalysts in Fischer-Tropsch synthesis: influence of the preparation method*. Industrial & Engineering Chemistry Research, 1989. **28**(6): p. 654-659.
33. Madon, R.J. and M. Boudart, *Experimental criterion for the absence of artifacts in the measurement of rates of heterogeneous catalytic reactions*. Industrial & Engineering Chemistry Fundamentals, 1982. **21**(4): p. 438-447.
34. G.F.Froment and K.B.Bischoff, *Chemical Reactor Analysis and Design* 2nd ed. 1990: Wiley.
35. Iranmahboob, J., et al., *The influence of clay on K<sub>2</sub>CO<sub>3</sub>/Co-MoS<sub>2</sub> catalyst in the production of higher alcohol fuel*. Fuel Processing Technology, 2002. **79**(1): p. 71-75.
36. Liu, Z.Y., et al., *Screening of alkali-promoted vapor-phase-synthesized molybdenum sulfide catalysts for the production of alcohols from synthesis gas*. Industrial & Engineering Chemistry Research, 1997. **36**(8): p. 3085-3093.
37. Xu, Q.A., et al., *Improved activity of Fe-Cu catalysts by physical mixing with zeolites for the hydrogenation of carbon dioxide*. Journal of Molecular Catalysis A-Chemical, 1997. **120**(1-3): p. L23-L26.
38. Kang, S.-H., et al., *Fischer-Tropsch Synthesis Using Zeolite-supported Iron Catalysts for the Production of Light Hydrocarbons*. Catalysis Letters, 2008. **125**(3): p. 264-270.
39. Mokaya, R. and W. Jones, *Pillared clays and pillared acid-activated clays - a comparative-study of physical, acidic, and catalytic properties*. Journal of Catalysis, 1995. **153**(1): p. 76-85.
40. Frenkel, M., *Surface acidity of Montmorillonites*. Clays and Clay Minerals, 1974. **22**(5-6): p. 435-441.
41. Spivey, J.J. and A. Egbebi, *Heterogeneous catalytic synthesis of ethanol from biomass-derived syngas*. Chemical Society Reviews, 2007. **36**(9): p. 1514-1528.
42. Foley, H.C., E.E. Lowenthal, and S. Schwarz, *Surface-chemistry of Rh-Mo/gamma-Al<sub>2</sub>O<sub>3</sub> - An analysis of surface-acidity*. Journal of Catalysis, 1995. **156**(1): p. 96-105.
43. Murchison, C.B., et al., *Mixed Alcohols from syngas over moly catalysts*. Proceedings of the 9th International Congress of Catalysis, 1988. **2**: p. 626-633.

44. Bian, G.Z., et al., *Mixed alcohol synthesis from syngas on sulfided K-Mo-based catalysts: Influence of support acidity*. Industrial & Engineering Chemistry Research, 1998. **37**(5): p. 1736-1743.
45. Klier, K., R.G. Herman, and M. Deemer, *Ethanol synthesis and water gas shift over bifunctional sulfide catalysts. Technical progress report*, OSTI ID: 10133374 1992.
46. Forzatti, P., E. Tronconi, and I. Pasquon, *Higher alcohol synthesis*. Catalysis Reviews-Science and Engineering, 1991. **33**(1-2): p. 109-168.
47. Chianelli, R.R., *Fundamental-studies of transition-metal sulfide hydrodesulfurization catalysts*. Catalysis Reviews-Science and Engineering, 1984. **26**(3-4): p. 361-393.
48. Furimsky, E., *Role of MoS<sub>2</sub> and WS<sub>2</sub> in hydrodesulfurization*. Catalysis Reviews-Science and Engineering, 1980. **22**(3): p. 371-400.
49. Haruta, M., et al., *preparation and properties of colloidal spherical-particles of molybdenum and cobalt sulfides*. Journal of Colloid and Interface Science, 1984. **101**(1): p. 59-71.
50. Pourabbas, B. and B. Jamshidi, *Preparation of MoS<sub>2</sub> nanoparticles by a modified hydrothermal method and the photo-catalytic activity of MoS<sub>2</sub>/TiO<sub>2</sub> hybrids in photo-oxidation of phenol*. Chemical Engineering Journal, 2008. **138**(1-3): p. 55-62.
51. Parenago, O.P., et al., *Molybdenum sulfide nanoparticles as new-type additives to hydrocarbon lubricants*. Doklady Chemistry, 2002. **383**(1-3): p. 86-88.
52. Barthomeuf, D., G. Coudurier, and J.C. Vedrine, *Basicity and basic catalytic properties of zeolites*. Materials Chemistry and Physics, 1988. **18**(5-6): p. 553-575.
53. Joshi, U.D., et al., *Effect of nonframework cations and crystallinity on the basicity of NaX zeolites*. Applied Catalysis a-General, 2003. **239**(1-2): p. 209-220.
54. Robson, H., *Verified Synthesis of Zeolitic Materials*. 2nd ed. 2001: Elsevier Science.
55. Sugi, Y., K.I. Bando, and Y. Takami, *The homologation of methanol - the modification of cobalt catalyst by diphosphines*. Chemistry Letters, 1981(1): p. 63-64.
56. Walker, W.E., *Process for the selective homologation of methanol to ethanol*, Union Carbide ,US patent 4277634, 1981.
57. Dry, M.E., *The Fischer-Tropsch process: 1950-2000*. Catalysis Today, 2002. **71**(3-4): p. 227-241.
58. Dalai, A.K. and B.H. Davis, *Fischer-Tropsch synthesis: A review of water effects on the performances of unsupported and supported Co catalysts*. Applied Catalysis A: General, 2008. **348**(1): p. 1-15.
59. Li, Z.R., et al., *Effect of cobalt promoter on Co-Mo-K/C catalysts used for mixed alcohol synthesis*. Applied Catalysis a-General, 2001. **220**(1-2): p. 21-30.
60. Topsoe, H., et al., *Recent basic research in hydrodesulfurization catalysis*. Industrial & Engineering Chemistry Fundamentals, 2002. **25**(1): p. 25-36.
61. Iranmahboob, J., D.O. Hill, and H. Toghiani, *K<sub>2</sub>CO<sub>3</sub>/Co-MoS<sub>2</sub>/clay catalyst for synthesis of alcohol: influence of potassium and cobalt*. Applied Catalysis a-General, 2002. **231**(1-2): p. 99-108.
62. Iranmahboob, J. and D.O. Hill, *Alcohol synthesis from syngas over K<sub>2</sub>CO<sub>3</sub>/CoS/MoS<sub>2</sub> on activated carbon*. Catalysis Letters, 2002. **78**(1-4): p. 49-55.
63. Inamura, K. and R. Prins, *The role of Co in unsupported Co-Mo sulfides in the hydrodesulfurization of thiophene*. Journal of Catalysis, 1994. **147**(2): p. 515-524.
64. Prins, R., V.H.J. Debeer, and G.A. Somorjai, *Structure and function of the catalyst and the promoter in co-mo hydrodesulfurization catalysts*. Catalysis Reviews-Science and Engineering, 1989. **31**(1-2): p. 1-41.
65. Candia, R., B.S. Clausen, and H. Topsoe, *On the role of promoter atoms in unsupported hydrodesulfurization catalysts - influence of preparation methods*. Bulletin Des Societes Chimiques Belges, 1981. **90**(12): p. 1225-1232.

66. Sudhakar, C., et al., *Chemically modified rhodium-alumina catalysts for CO hydrogenation*. Abstracts of Papers of the American Chemical Society, 1986. **191**: p. 16-PETR.
67. Li, Z.R., Y.L. Fu, and M. Jiang, *Structures and performance of Rh-Mo-K/Al<sub>2</sub>O<sub>3</sub> catalysts used for mixed alcohol synthesis from synthesis gas*. Applied Catalysis a-General, 1999. **187**(2): p. 187-198.
68. Koizumi, N., et al., *Development of sulfur tolerant catalysts for the synthesis of high quality transportation fuels*. Catalysis Today, 2004. **89**(4): p. 465-478.
69. Trautmann, S. and M. Baerns, *Infrared spectroscopic studies of CO adsorption on rhodium supported by SiO<sub>2</sub>, Al<sub>2</sub>O<sub>3</sub>, and TiO<sub>2</sub>*. Journal of Catalysis, 1994. **150**(2): p. 335-344.
70. Storm, D.A., *The production of higher alcohols from syngas using potassium-promoted Co/Mo/Al<sub>2</sub>O<sub>3</sub> and Rh/Co/Mo/Al<sub>2</sub>O<sub>3</sub>*. Topics in Catalysis, 1995. **2**(1-4): p. 91-101.
71. Dhas, N.A., A. Ekhtiarzadeh, and K.S. Suslick, *Sonochemical preparation of supported hydrodesulfurization catalysts*. Journal of the American Chemical Society, 2001. **123**(34): p. 8310-8316.
72. Mdleleni, M.M., T. Hyeon, and K.S. Suslick, *Sonochemical synthesis of nanostructured molybdenum sulfide*. Journal of the American Chemical Society, 1998. **120**(24): p. 6189-6190.
73. Verma, A., et al., *Tribological behavior of deagglomerated active inorganic nanoparticles for advanced lubrication*. Tribology Transactions, 2008. **51**(5): p. 673-678.
74. Moreno, B., et al., *Synthesis and characterization of molybdenum based colloidal particles*. Journal of Colloid and Interface Science, 1998. **207**(2): p. 251-257.
75. Chianelli, R.R., et al., *The single-layered morphology of supported MoS<sub>2</sub>-based catalysts - The role of the cobalt promoter and its effects in the hydrodesulfurization of dibenzothiophene*. Applied Catalysis A-General, 2008. **345**(1): p. 80-88.
76. Lund, C.R.F., *Effect of adding Co to MoS<sub>2</sub>/Al<sub>2</sub>O<sub>3</sub> upon the kinetics of the water-gas shift*. Industrial & Engineering Chemistry Research, 1996. **35**(9): p. 3067-3073.
77. Park, T.Y., I.S. Nam, and Y.G. Kim, *Kinetic analysis of mixed alcohol synthesis from syngas over K/MoS<sub>2</sub> catalyst*. Industrial & Engineering Chemistry Research, 1997. **36**(12): p. 5246-5257.
78. Sun, Y.H., et al., *A short review of heterogeneous catalytic process for mixed alcohols synthesis via syngas*. Catalysis Today, 2009. **147**(2): p. 133-138.
79. Mross, W.D., *Alkali doping in heterogeneous catalysis*. Catalysis Reviews-Science and Engineering, 1983. **25**(4): p. 591-637.
80. Subramani, V. and S.K. Gangwal, *A review of recent literature to search for an efficient catalytic process for the conversion of syngas to ethanol*. Energy & Fuels, 2008. **22**(2): p. 814-839.
81. Tatsumi, T., A. Muramatsu, and H.O. Tominaga, *Effects of alkali-metal halides in the formation of alcohols from CO and H<sub>2</sub> over silica-supported molybdenum catalysts*. Chemistry Letters, 1984(5): p. 685-688.
82. Woo, H.C., et al., *Room-temperature oxidation of K<sub>2</sub>CO<sub>3</sub>/MoS<sub>2</sub> catalysts and its effects on alcohol synthesis from CO and H<sub>2</sub>*. Journal of Catalysis, 1992. **138**(2): p. 525-535.
83. Papageorgopoulos, C.A., *Adsorption of Cs and O<sub>2</sub> on MoS<sub>2</sub>*. Surface Science, 1978. **75**(1): p. 17-28.
84. Karolewski, M.A. and R.G. Cavell, *Sims study of Cs/MoS<sub>2</sub>(0001) .2. Chemisorption of O<sub>2</sub>, H<sub>2</sub>O, HCOOH, CO<sub>2</sub> and CS<sub>2</sub>*. Surface Science, 1989. **219**(1-2): p. 261-276.
85. Klier, K., J.G. Santiesteban, and J.G. Nunan, *Molybdenum-disulfide as catalyst for alcohols*. Abstracts of Papers of the American Chemical Society, 1987. **193**: p. 64-PETR.
86. Santiesteban, J.G., et al., *Mechanism of C<sub>1</sub>-C<sub>4</sub> alcohol synthesis over alkali/MoS<sub>2</sub> and alkali/Co/MoS<sub>2</sub> catalysts*. Proc. 9th Int. Congress on Catalysis, 1988. **2**: p. 561-568.

## 4 CONCLUSIONS AND RECOMMENDATIONS

### 4.1 CONCLUSIONS

This research has provided significant insight into the parameters that dramatically improve the performance of MoS<sub>2</sub> based catalysts for aliphatic alcohol synthesis. By extensive catalytic testing at scales > 1g of catalyst and on-stream hours >200, it is shown that MoS<sub>2</sub> based catalysts are suitable and stable catalysts for larger scale commercial operation. Some of the prominent results are summarized below:

1. The analytical setup can perform online analysis of alcohols and other oxygenate products whilst volatile, with a 30 minute interval; whereas other researchers generally analyzed their alcohol products after collecting them as liquids. This capability revealed that transient states can develop within the reactor, which strangely only affect the oxygenate products. Further research work is needed to elucidate the cause of such oscillations and optimize reactor operation where conversion is higher.
2. With supported MoS<sub>2</sub> catalysts, surface acidity of the support negatively affects alcohol yields and selectivity. A minimum amount of active metal component is necessary to achieve greater alcohol selectivity amongst the products, by suppressing the acidic sites on the support.
3. Beyond the minimum metal loading, significant increase in metal loading does not necessarily provides significant increase in alcohol selectivity or CO conversion.
4. Increasing support basicity improves alcohol selectivity and yields. By varying between aluminosilicate types and their framework cation, selectivity for alcohols as well as overall alcohol yields were improved by 3 times at temperatures > 300°C;

5. By incorporating a modified zeolite as support, significant improvement in higher alcohol yields was achieved.  $C_{2+}/C_1$  alcohol ratios were increased from 2 to 4-5. Generally, large  $C_{2+}/C_1$  alcohol ratios are not observed over the  $K_2CO_3$ - $MoS_2$  catalyst without a co-promoter like Co, Ni or Fe.
6. Co- $MoS_2$  catalyst can achieve greater alcohol yields than those without co-promoters. However, methanation becomes particularly strong over this catalyst.
7. Over unsupported CoMoS type catalysts, the sequence of alkali introduction is critical. Addition of  $K_2CO_3$  after calcination of the catalyst material achieves greater alcohol selectivity and activity.
8. Unsupported CoMoS catalysts remain stable and active even at higher temperatures. This can be due to the fact that  $MoS_2$  is structured and stable material. Catalyst performance between unsupported and supported CoMoS (80 wt% on bentonite) was virtually the same. Conversely, this also supports point 3 above, whence further metal loading does not improve HAS.
9. Novel synthesis techniques, which can restrict the size of  $MoS_2$  particles in the unsupported mode, can be a significant impact in improving HAS catalyst.
10. Co-promoters other than Co and Ni can be effective in HAS composite catalysts also. Rh as co-promoter, at 1 wt% of the  $MoS_2$  material, provided significant improvements in alcohol yields **under optimized operating conditions**. Higher alcohol yields were better than similar catalysts reported in literature.
11. Cu as a co-promoter in a CoMoS catalyst improved alcohol selectivity. Under similar operating conditions, alcohol selectivity improved from 76% to 93% ( $CO_2$  free basis),  $CO_2$  production decreased from 261 to 70 g/kg.cat/hr, alcohol yields decreased slightly from 325 to 298 g/kg.cat/hr.
12. Optimum alkali loading depends upon the catalyst OR the co-promoters used in the  $MoS_2$  material. Moreover, by varying the  $K_2CO_3$  loading and operating conditions, it is possible to

narrow down the product distribution. On the CuCoMoS catalyst with 8% wt/wt loading of  $K_2CO_3$ , alcohol distribution was concentrated between methanol and ethanol.

13. From a process engineering perspective, methanol (or lower alcohols) can be recycled back with unconverted syngas to increase higher alcohol production. However this method also increases productivity of alkanes and other oxygenates. Over a very selective alcohol catalyst however, methanol recycle would provide significant results.
14. Operating conditions have a significant impact on performance of HAS catalyst. Other than the obvious effects on conversion and yields, the operating parameters can significantly vary the products formed. This is in part due to the complex reaction scheme of HAS. Although each individual catalyst exhibits a different sensitivity to a particular operating parameter, the impact of these variables can be summarized as follows:

**Temperature > Space velocity > CO/H<sub>2</sub> ratio > Pressure**

## 4.2 FUTURE PATH

Based on the research performed and existing literature, following avenues are proposed for further research:

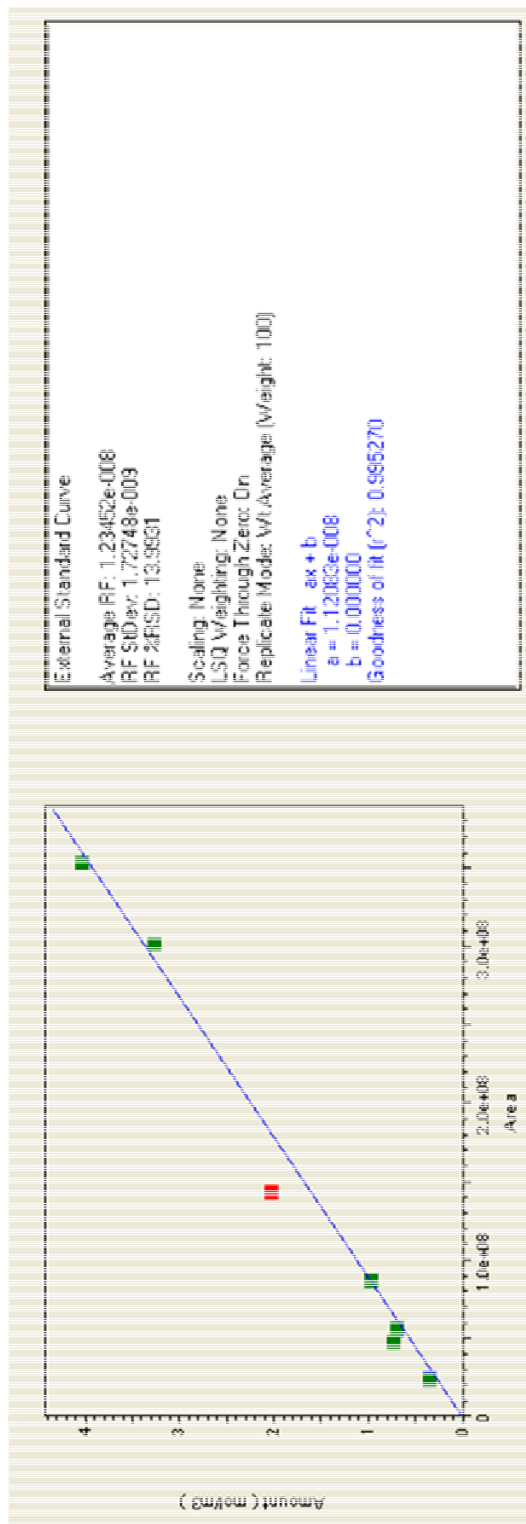
1. The ability to analyze oxygenates online in the gas phase has disclosed that transients can develop within the reactor. The cause of this behavior must be researched and ascertained. It is possible, that if the limitations are removed, the reactor can be operated in a state where the alcohol productivity is maximized.
2. Increased basicity of the support improves alcohol selectivity and productivity. Other reports indicate that the increased basicity of an alkali also has a similar effect. It is worthwhile to explore the effect of adding a base stable at high temperatures.

3. Dual alkali promotion method, i.e. once before calcination and once after it, seems to be an interesting technique in stabilizing and increasing HAS performance. Obviously, the optimum alkali amount would change in this dual promotion technique and needs evaluation.
4. Use of supports like clays and zeolites and their basic variants, provided an interesting route to enhanced alcohol performance. Novel synthesis techniques, which encapsulate active metals in the zeolite pores, can be employed to significantly improve active metal dispersion and decrease the required amounts of metal.
5. Experimenting and perfecting synthesis techniques, which produce homogeneous and nanosized sulfide particles, appears to offer the greatest incentive in enhancing alcohol productivity.
6. Inclusion of copper as a co-promoter, to an improved catalyst composition active for alcohols, should help in improving total alcohol selectivity. If ethanol is the desired product, addition of copper and optimization of operating conditions can narrow the alcohol products to methanol and ethanol.
7. By recycling methanol over a Cu-promoted MoS<sub>2</sub> catalyst, one can significantly improve the overall syngas conversion to ethanol. Ethanol productivity at 150 g/kg.cat/hr over the CuCoMoS is already one of the highest reported in literature for the MoS<sub>2</sub> catalyst family.
8. Cu-promoted catalyst should be particularly tested with a syngas containing CO<sub>2</sub>. Biomass gasified syngas would contain CO<sub>2</sub> and it is reported that C<sub>2+</sub> alcohol activity suffers under CO<sub>2</sub> containing syngas. Cu catalysts are known to be stable under such conditions and can even activate CO<sub>2</sub> to CO.
9. Improvement in higher alcohol selectivity of a catalyst has been attributed to its ability to adsorb 'CO' associatively and insert it into acyl intermediates. However, this has not been proved conclusively for MoS<sub>2</sub> based catalysts. In situ spectroscopic studies are proposed to evaluate a catalyst's relative ability to adsorb CO associatively and dissociatively.



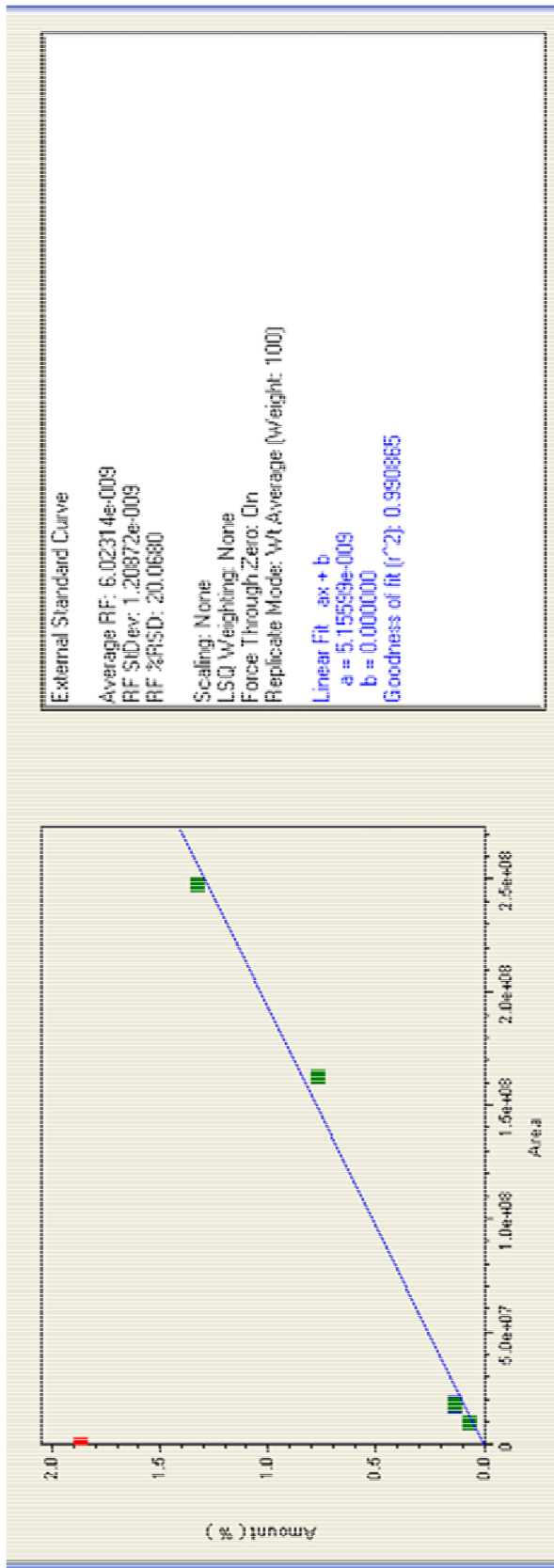
10. As HAS is an extremely exothermic process, reactor engineering concepts improving heat transfer can improve alcohol selectivity, e.g. slurry reactor. Slurry reactors can offer other advantages as well. As opposed to plug flow in a fixed bed reactor, a slurry reactor offers a homogenous exposure between the catalyst, reactants and intermediate species. This inherently makes a slurry reactor more favorable to oxygenates synthesis than alcohols. An interesting modification could be inclusion of a CO homologation catalyst along with the HAS catalyst in the slurry. Use of two catalysts in a single reactor can also be evaluated for fixed bed reactors. First bed can provide increased amounts of lower alcohols, whereas the following CO homologation catalyst can tune the oxygenate carbon chain growth to the desired alcohol range.
11. Tools such as XRD and chemisorption should be used extensively to characterize the catalyst surface, structure and active metal dispersion.
12. In light of possible release of sulfur from the catalyst and downstream contamination, unsulfided CoMo type catalyst should also be researched. It was previously discussed that sulfided catalysts perform better than unsulfided catalysts due to increased selectivity to alcohols. However, the catalysts compared were prepared via conventional techniques. It has been suggested, but not confirmed, that through novel synthesis techniques, better homogeneity, dispersion and alcohol activity can be achieved for the unsulfided CoMo catalysts.

## 5 APPENDIX

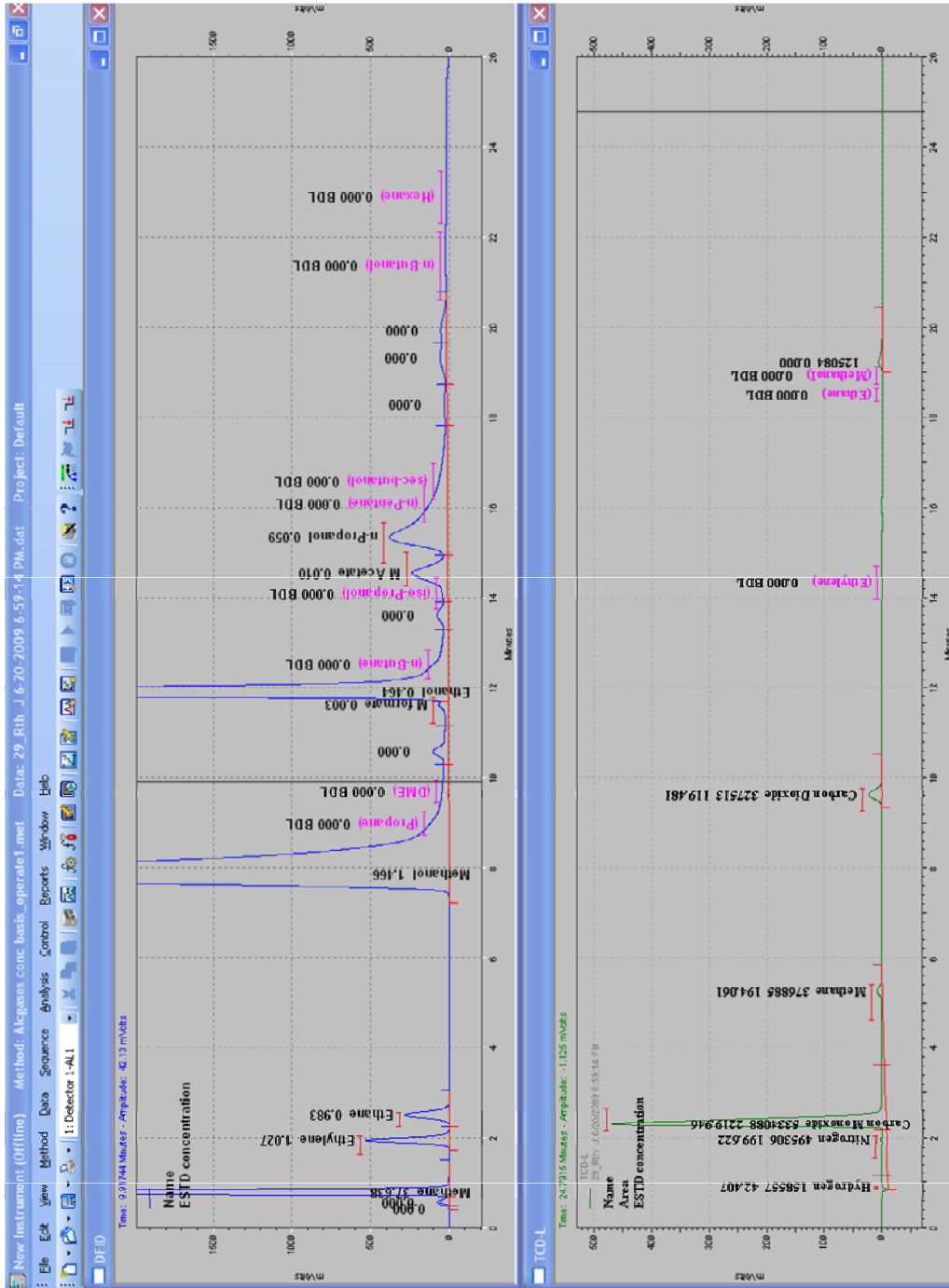


Appendix 1- Calibration curve for methanol – Shimadzu GC software EZStart

Note that an erroneous calibration point is turned off (marked red) and not included in the response factor (RF) calculation. The software automatically calculates the average RF factor and also the error in curve fitting



Appendix 2 - Calibration curve for ethanol – Shimadzu GC software EZStart



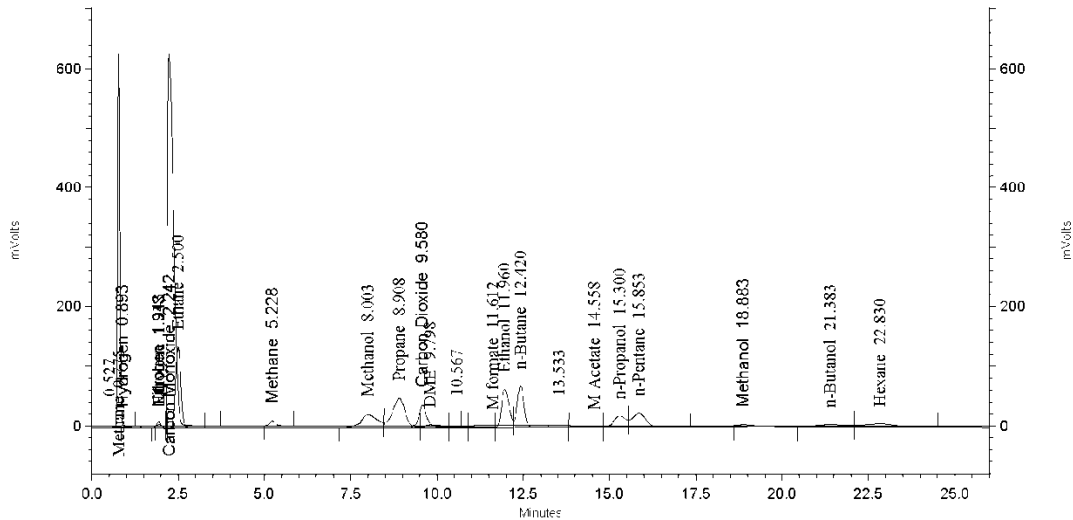
Appendix 3 – Sample chromatogram from online gas sampling GC. The software is adjusted such that it automatically picks up the peaks (already calibrated) and displays the calculated concentration

Calibration sample ID	3.1	Date	2/2/2008				
For preparation of gas phase calibration sample, a metered dose of a liquid mixture is injected into a heated stream of nitrogen gas. The calibration units are mol/m <sup>3</sup> and they are calculated below. Density and molecular weights are used to convert from volume to molar basis							
<b>Nitrogen flowrate</b>				<b>Physical properties of calibration samples</b>			
cc/min		mol/min		density, g		BPs, oC	
22414		1.00000				Mol Wt	
92		0.00410	Avagadros: molar volume	MeOH	0.79	64.70	32.00
				EtOH	0.79	78.40	46.07
<b>Liquid flowrate</b>				PrOH	0.80	97.10	60.09
cc/min (liquid)		cc/hr		i-PrOH	0.79	82.30	60.09
0.0025		0.15		nBuOH	0.81	117.73	74.12
				tert-BuOH	0.78	82.40	74.12
<b>Calibration standard prepared. Volume % distribution</b>							
	cc	Vol %					
i-PrOH	1	6.578947					
n-PrOH	3	19.73684					
EtOH	4.9	32.24					
MeOH	5.1	33.55					
BuOH	1.2	7.89					
ter-BuOH	0	0.00					
Total cc	15.2						
<b>Calculation of molar concentration to be used in GC calibration</b>							
	cc/min	gm/min	mol/min	mol%	mol/cc	<b>mol/m<sup>3</sup></b>	
i-PrOH	0.00016	0.00013	2.15E-06	0.05184	2.31283E-08	0.023128	
n-PrOH	0.00049	0.00040	6.6E-06	0.158962	7.0921E-08	0.070921	
Ethanol	0.00081	0.00064	1.38E-05	0.332596	1.48388E-07	0.148388	
MeOH	0.00084	0.00066	2.08E-05	0.500252	2.23187E-07	0.223187	
BuOH	0.00020	0.00016	2.16E-06	0.05196	2.31818E-08	0.023182	
ter-BuOH	0	0	0	0	0	0	
Total molar flow (gas+liquid)			0.00415	mol/min			
Adjusted flowrate			93.01913	cc/min			

Appendix 1 – Calculation performed for gas phase calibration of oxygenated compounds

# External Standard Report

Method Name: C:\EZStart\Projects\Default\Method\Alegases conc basis\_operate1.met  
 Data: C:\EZStart\Projects\Default\Data\22ndB\22nd\_d F 3-8-2009 7-48-51 PM.dat  
 User: System  
 Acquired: 3/8/2009 7:50:24 PM  
 Printed: 1/13/2010 4:44:32 PM



DFID Results

Pk #	Name	Retention Time	Area	Conc, mol/m3	Area Percent
2	Methane	0.775	62684638	38.311460	27.718
3	Ethylene	1.938	1828443	0.435668	0.809
4	Ethane	2.500	32728060	11.014952	14.472
5	Methanol	8.003	16096737	0.180417	7.118
6	Propane	8.908	28899745	7.225798	12.779
7	DME	9.798	1700322	1.159111	0.752
9	M formate	11.612	124662	0.000319	0.055
10	Ethanol	11.960	22337339	0.115171	9.877
11	n-Butane	12.420	22069428	4.270390	9.759
	iso-Propanol			0.000000	BDL
13	M Acetate	14.558	406279	0.000680	0.180
14	n-Propanol	15.300	10251630	0.032570	4.533
15	n-Pentane	15.853	14890700	3.793227	6.584
16	n-Butanol	21.383	4623801	0.018686	2.045
17	Hexane	22.830	6962458	0.008607	3.079

Totals			225604242	66.567057	99.758
--------	--	--	-----------	-----------	--------

TCD-L Results

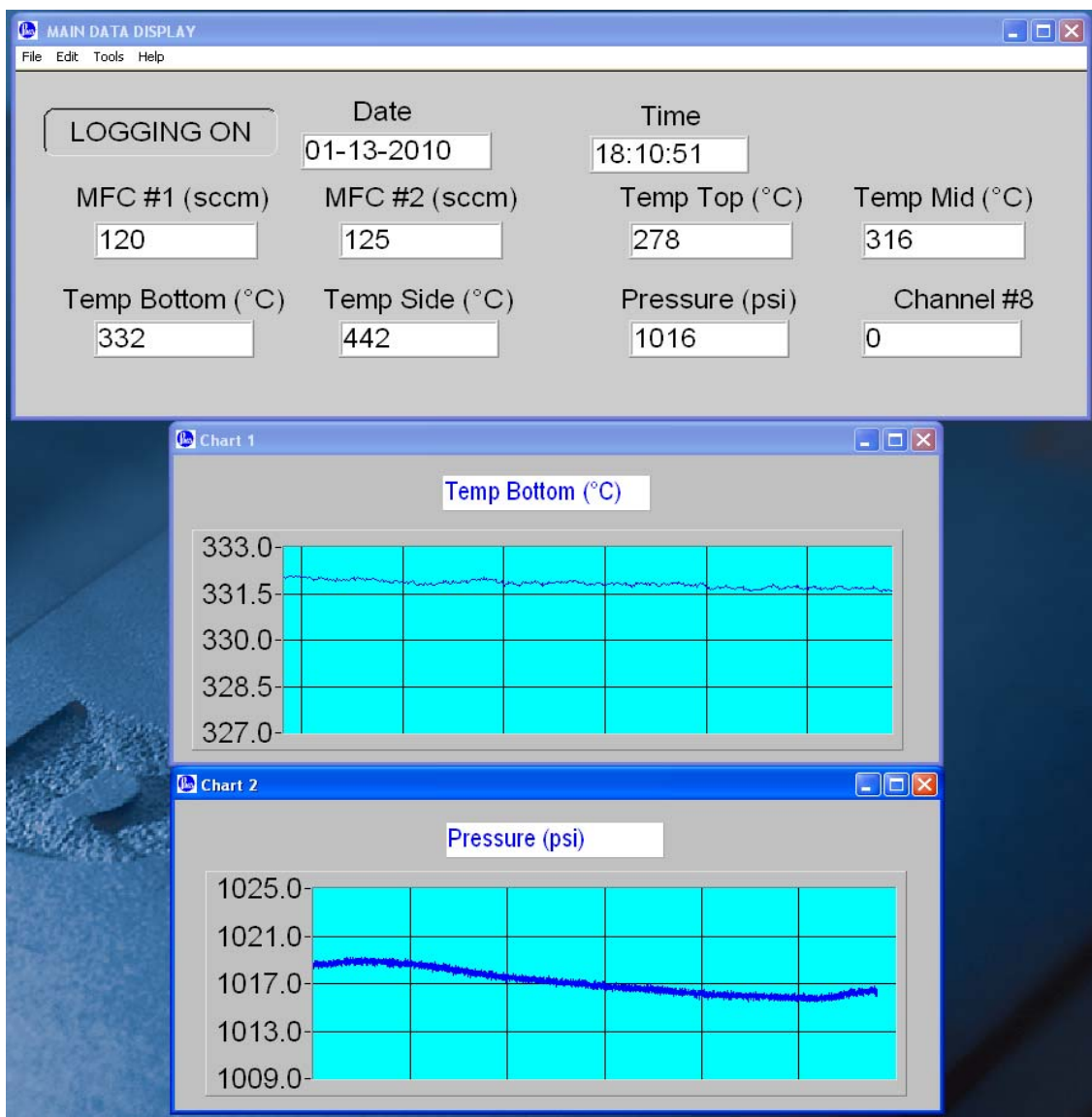
**External Standard Report**

**Method Name:** C:\EZStart\Projects\Default\Method\Alcgases conc basis\_operate1.met  
**Data:** C:\EZStart\Projects\Default\Data\22ndB\22nd\_d F 3-8-2009 7-48-51 PM.dat  
**User:** System  
**Acquired:** 3/8/2009 7:50:24 PM  
**Printed:** 1/13/2010 4:53:55 PM

<i>Pk #</i>	<i>Name</i>	<i>Retention Time</i>	<i>Area</i>	<i>Conc, mol/m3</i>	<i>Area Percent</i>
1	Hydrogen	0.893	35880	9.596234	0.440
2	Nitrogen	1.943	13538	5.456187	0.166
3	Carbon Monoxide	2.242	7486868	3115.892428	91.888
4	Methane	5.228	93794	48.295152	1.151
5	Carbon Dioxide	9.580	485501	177.116502	5.959
	Ethylene			0.000000 BDL	
	Ethane			0.000000 BDL	
6	Methanol	18.883	32234	0.320428	0.396

Totals			8147815	3356.676931	100.000
--------	--	--	---------	-------------	---------

*Appendix 2 – Sample GC output report*



*Appendix 3 – Data acquisition panel for reactor. Reactor pressure and temperature are graphed online*





<b>22nd, 40% K-MoS2 on K-Y zeolite</b>																			
Temp oC	Pressure psi	CO/H2	GHSV/s L/g/hr	hrs	Space time Yield (STY), g/kg.cat/hr				Conversion product	Selectivity, CO2 free basis				Alc Yield g/Kg/hr	Alc Yield C2+/C1				
					MeOH	EtOH	PrOH	DME		Methane	Ethane	MeOH	EtOH			PrOH	T.oxy	T.alcs	alkanes
350	1000	2.0	6,000	21.39	27.95	62.72	37.21	5.56	42.85	49.91	13.61	6.91	10.78	4.90	1.03	26.36	72.60	163.3	4.84
350	1000	2.0	6,000	42.14	28.10	61.63	33.74	8.13	32.86	38.47	11.02	8.33	12.71	5.32	1.77	30.51	67.72	155.9	4.55
301	1000	2.0	6,000	49.81	22.58	34.20	14.91	5.27	7.87	8.20	3.42	19.29	20.33	6.79	3.63	48.71	47.65	77.9	2.45
282	1000	2.0	6,000	65.70	21.93	24.49	9.36	5.75	3.95	3.06	1.93	29.86	23.19	6.78	6.37	61.10	32.53	57.9	1.64
351	1000	2.0	6,000	70.29	31.18	57.22	31.71	8.65	33.10	33.31	10.26	9.97	12.73	5.40	2.07	32.22	65.71	150.0	3.81
349	1000	2.0	3,000	72.57	15.29	48.81	29.74	5.79	27.81	28.21	18.11	5.89	13.07	6.10	1.63	30.56	67.81	126.8	7.29
302	1000	3.0	6,000	90.18	14.36	24.19	10.55	4.19	4.97	5.62	2.29	17.50	20.52	6.85	4.12	44.87	51.01	49.1	2.42
350	1000	3.0	6,000	95.41	22.97	52.76	26.17	5.31	18.53	23.45	6.89	9.49	15.16	5.75	1.68	37.43	60.89	141.3	5.15
350	1000	3.0	10,000	97.76	12.00	50.77	21.09	6.31	14.67	19.38	3.32	6.31	18.57	5.91	2.52	30.79	66.70	83.9	5.99
350	800	2.0	6,000	116.49	24.30	41.86	17.67	5.40	16.65	21.03	6.02	12.67	15.18	4.90	2.06	36.69	61.26	101.3	3.17
350	1300	2.0	6,000	120.48	38.22	78.04	41.52	12.05	30.34	34.61	11.27	10.92	15.51	6.31	2.52	37.67	59.81	197.8	4.17
350	1300	2.0	6,000	124.85	76.74	106.77	47.69	43.47	47.88	37.89	16.44	15.40	14.90	5.09	6.38	40.08	53.54	208.6	
370	1290	2.0	6,000	127.54	37.89	100.57	54.16	9.92	49.23	55.54	16.30	7.93	14.64	6.03	1.52	31.23	67.25	221.8	4.85
370	1290	2.0	4,000	129.36	23.95	93.08	53.51	7.65	45.28	50.88	22.74	5.52	14.92	6.56	1.30	29.94	68.77	199.4	7.32
350	1290	2.0	4,000	130.93	29.90	74.56	45.29	9.35	29.03	34.79	17.56	8.78	15.23	7.08	2.29	34.31	63.40	175.1	4.86
315	1270	2.0	6,000	134.25	35.86	54.51	32.63	6.29	9.32	11.02	4.98	20.95	22.15	10.15	2.98	55.33	41.69	131.3	2.66
315	1270	2.0	3,000	136.38	25.60	41.02	22.97	7.10	10.99	12.82	10.10	16.12	17.96	7.70	3.46	43.88	52.66	97.3	2.80
305	1260	2.0	6,000	139.17	29.71	38.99	18.50	6.52	7.23	7.56	3.49	23.87	21.79	7.91	4.28	55.31	40.41	92.2	2.10
302	1260	0.5	6,000	142.10	21.45	9.77	1.69	10.71	11.83	8.90	2.71	24.37	7.72	1.02	8.85	33.11	58.04	32.9	0.53
350	1260	0.5	6,000	145.61	42.67	45.06	17.56	23.25	62.64	49.27	10.97	11.709	8.601	2.565	4.495	23.74	71.768	112.6	1.64
350	1260	1.0	6,000	148.40	49.44	70.01	34.35	20.11	52.08	48.756	13.11	11.822	11.65	4.374	3.479	30.12	66.398	175.9	2.56

Appendix 8 - Report template displaying operating variables and performance parameters of importance for a particular catalyst.